THE OPTIMAL FULL SETTING SCHEME FOR ADAPTIVE OVERCURRENT RELAY COORDINATION IN MODERN DISTRIBUTION SYSTEM

CHAKIT PLONGKRATHOK

A Thesis Submitted in Partial Fulfillment of the Requirements for the Degree of Master of Engineering in Electrical Engineering

Suranaree University of Technology

Academic Year 2021

แผนการตั้งค่าเต็มรูปแบบที่เหมาะสมที่สุดของการประสานงานรีเลย์ป้องกัน
กระแสเกินแบบปรับตัวในระบบจำหน่ายสมัยใหม่

นายชาคริต ปล้องกระโทก

วิทยานิพนธ์นี้สำหรับการศึกษาตามหลักสูตรปริญญาวิศวกรรมศาสตรมหาบัณฑิต
สาขาวิชาวิศวกรรมไฟฟ้า
มหาวิทยาลัยเทคโนโลยีสุรนารี
ปีการศึกษา 2564

THE OPTIMAL FULL SETTING SCHEME FOR ADAPTIVE OVERCURRENT RELAY COORDINATION IN MODERN DISTRIBUTION SYSTEM

Suranaree University of Technology has approved this thesis submitted in partial fulfillment of the requirements for a Master's Degree.

Thesis Examining Committee

....

(Asst. Prof. Dr. Komsan Daroj)
Chairperson

....

(Assoc. Prof. Dr. Keerati Chayakulkheeree)
Member (Thesis Advisor)

....

(Assoc. Prof. Dr. Thanatchai Kulworawanichpong)
Member

....

(Asst. Prof. Dr. Uthen Leeton)
Member

....

(Assoc. Prof. Dr. Chatchai Jothityangkoon)
Vice Rector for Academic Affairs and Quality Assurance

....

(Assoc. Prof. Dr. Pornsiri Jongkol)
Dean of Institute of Engineering

ชาคริต ปล้องกระโทก : แผนการตั้งค่าเต็มรูปแบบที่เหมาะสมที่สุดของการประสานงานรีเลย์ป้องกันกระแสเกินแบบปรับตัวในระบบจำหน่ายสมัยใหม่ อาจารย์ที่ปรึกษา : รศ. ดร. กีรติ ชยะกุลคีรี, 142 หน้า.

คำสำคัญ : การป้องกันระบบไฟฟ้าแบบปรับตัว/การประสานงานที่เหมาะสมที่สุดของรีเลย์ป้องกันกระแสเกิน/เทคนิคปัญญาประดิษฐ์/ การป้องกันระบบไฟฟ้ากำลัง

วิทยานิพนธ์นี้เสนอแผนการตั้งค่าเต็มรูปแบบที่เหมาะสมที่สุดของการประสานงานรีเลย์ป้องกันกระแสเกินแบบปรับได้ในระบบจำหน่ายที่ทันสมัยซึ่งได้รวมเครื่องกำเนิดไฟฟ้าแบบกระจายและพิจารณาโหมดการทำงานทั้งหมดของระบบ แผนการตั้งค่าเต็มรูปแบบที่เหมาะสมที่สุดจะพิจารณาพารามิเตอร์สามตัวสำหรับรีเลย์แต่ละตัว ประกอบด้วยการตั้งค่าตัวคูณเวลา การตั้งค่ากระแสปรับตั้งและการตั้งค่าเส้นโค้งลักษณะเฉพาะเพื่อเป็นตัวแปรในการตัดสินใจในปัญหาการประสานงานรีเลย์กระแสเกินแบบปรับได้ โดยได้พัฒนาการตั้งค่าเส้นโค้งลักษณะเฉพาะเป็นตัวแปรในการตัดสินใจ แทนที่จะกำหนดประเภทเส้นโค้งไว้ล่วงหน้าตามที่พิจารณาในงานที่มีอยู่ส่วนใหญ่ ผลลัพธ์ของการตั้งค่าเส้นโค้งลักษณะเฉพาะสามารถเป็นได้ทั้งเส้นโค้งลักษณะมาตรฐานของ IEC และ IEEE เทคนิคที่ใช้ในการหาค่าที่เหมาะสมที่สุดคือ การใช้วิธีกลุ่มอนุภาคแบบปัดเศษ เพื่อแสดงประสิทธิภาพของเทคนิคดังกล่าว การทดสอบจะดำเนินการโดยใช้ระบบทดสอบมาตรฐานที่มีการดัดแปลงและเปรียบเทียบกับเทคนิคอื่นๆ ผลลัพธ์ที่ได้แสดงให้เห็นว่าเมื่อเปรียบเทียบกับวิธีอื่นๆพบว่าแผนการตั้งค่าเต็มรูปแบบที่เหมาะสมที่สุดที่เสนอนั้นสามารถลดเวลาการทำงานทั้งหมดของรีเลย์ลงอย่างมากในขณะที่ลำดับการป้องกันยังคงถูกต้องภายใต้ความผิดพร่องและโหมดการทำงานทั้งหมดที่สามารถเกิดขึ้นได้ในระบบ

สาขาวิชาวิศวกรรมไฟฟ้า ลายมือชื่อนักศึกษา ชาคริต.

ปีการศึกษา 2564 ลายมือชื่ออาจารย์ที่ปรึกษา

CHAKIT PLONGKRATHOK : THE OPTIMAL FULL SETTING SCHEME FOR ADAPTIVE OVERCURRENT RELAY COORDINATION IN MODERN DISTRIBUTION SYSTEM. THESIS ADVISOR : ASSOC. PROF. KEERATI CHAYAKULKHEEREE, Ph.D., 142 PP.

Keyword : Adaptive Protection/Optimal Coordination of Overcurrent Relay/Artificial Intelligence/ Power System Protection Optimization

This research proposes the optimal full setting scheme (OFSS) for adaptive overcurrent relays (AOCR) coordination in the modern distribution system. Their system integrates several distributed generator (DG) penetrations with various operational modes of network topologies. The proposed OFSS considers three parameters for each relay including time multiplier setting (TMS), pickup current setting (PS), and characteristic curve setting (CS) to combine in the AOCR coordination problem. As a novelty, the CS of AOCR is considered to be decision variables, instead of predetermining a single type of curve for all relays as considered in most existing works. The proposed approach allows the selection of several IEC and IEEE standard characteristic curves which combination results in the OFSS. The proposed metaheuristic technique implemented for solving the optimal coordination problem is Round-Off Mixed-Integer Particle Swarm Optimization (ROMI-PSO). To show the applicability of the proposed approach. Several tests will be carried out using modified versions of the standard test systems. Therefore, the optimal results have shown that a comparison with other coordination approaches showed that the proposed OFSS approach is absolutely decreased total operation times of adaptive relay while remaining in the protective sequence. At the same time, guarantee the suitable operation of protections under different condition faults and operational modes.

School of Electrical Engineering

Academic Year 2021

Student's Signature ....

Advisor's Signature ....

ACKNOWLEDGEMENT

The authors are particularly grateful to Kittibandit Scholarship at the Suranaree University of Technology for financial support. Specifically, this thesis would not have been as successful without the helpful and supporting contributions of these respectable people, who have always supported me with countless assistance, quality instruction, and encouragement during my studies.

Firstly, I'd like to express my great gratitude towards my parents who gave birth to me. They always support the invaluable assistance and inspiration, constant encouragement, and financial support.

Secondly, I'd like to express my sincere gratitude to Assoc. Prof. Dr. Keerati Chayakulkheeree, my thesis advisor, for his invaluable assistance and continual support during this research. Additionally, I would like to express my gratitude to the committee members, including, Assoc. Prof. Dr. Komsan Daroj from Ubonratchatani University, Assoc. Prof. Dr. Thanatchai Kulworawanichpong, and Dr. Uthen Leeton, for their valuable assistance and advice.

Finally, I'd like to express my appreciation to my lecturers, who have consistently supplied me with knowledge and advice during my studies. Many thanks to my seniors, and comrades for their assistance and motivation throughout this difficult period. I'd also like to thank all of the lecturers, and employees at the university's School of Electrical Engineering for their valuable advice and assistance.

Chakit Plongkrathok

TABLE OF CONTENTS

TABLE OF CONTENTS (Continuous)

PAGE

TABLE OF CONTENTS (Continuous)

PAGE

TABLE OF CONTENTS (Continuous)

PAGE

LIST OF TABLES

TABLE PAGE

LIST OF TABLES (Continuous)

TABLE PAGE

LIST OF TABLES (Continuous)

TABLE PAGE

LIST OF FIGURES

FIGURE PAGE

LIST OF FIGURES (Continuous)

FIGURE PAGE

LIST OF ABBREVIATIONS

DER	=	distributed energy resources
DG	=	distributed synchronous generator
PV	=	photovoltaics
WT	=	wind turbine
AP	=	adaptive protection
AEDP	=	the alternative energy development plan
OCR	=	overcurrent relay
DOCR	=	directional overcurrent relay
AOCR	=	adaptive overcurrent relay
NAOCR	=	non adaptive overcurrent relay
LP	=	linear optimization problem
NLP	=	nonlinear optimization problem
MILP	=	mixed-integer linear optimization problem
MINLP	=	mixed-integer nonlinear optimization problem
CHP	=	the combined heat power
OFSS	=	the optimal full setting scheme
LPP	=	linear programming technique
GA	=	genetic algorithm
ICGA	=	the integer coded genetic algorithm
PSA	=	pattern search algorithm
PSO	=	particle swarm optimization
SA	=	simulated annealing algorithm.
NRPF	=	the newton-raphson power flow

LIST OF ABBREVIATIONS (Continuous)

OF	=	objective function
SRG	=	surrogate optimization
ROMI-PSO	=	rounding-off mixed integer particle swarm optimization
ROMI-GA	=	rounding-off mixed integer genetic algorithm

CHAPTER 1
INTRODUCTION

1.1 General Introduction

Over the past decade, the distribution system has been continuously developed to enhance the reliability, flexibility, and stability of the system to decrease any interruption and smoothly supply to the customer. The high penetration level of DERs might be able to fulfill these requirements. Likewise, the rapid advancement of distributed energy resources (DERs) including distributed synchronous generator (DG), wind turbine (WT) with an induction generator, and a large-scale photovoltaics (PV) play the important roles in the distribution system. Nevertheless, a high penetration level of DERs causes a big problem for conventional distribution system protection. For that reason, adaptive protection (AP) technology is a key role to handle this problem.

1.2 Problem Statement

According to Thailand Power Development Plan 2015-2036 (PDP2015), the total capacity at the end plan (the year 2036) would be 70,335 MW comprising the existing capacity (as of the year 2014) of 37,612 MW, the new capacity added during the year 2015-2036 of 57,459 MW and the capacity of 24,736 MW which would be retired during the year 2015-2036. following the objective of PDP is energy security and environment-friendly society, The target of the Alternative Energy Development Plan (AEDP) is to increase a portion of renewable and alternative energy uses to 30 percent of the total final energy consumption with the target on power generated from renewable energy in the year 2036 of 19,634.4 MW included several types of DERs such as solar, wind, biomass, hydropower and so on. the increasing penetration level of DERs to the Thailand distribution system is the main concern of protection engineers (National Energy Policy Council, 2015). Consequently, the more necessary penetration levels of DERs into the distribution system cause big and various problems to conventional distribution system protection. DERs changed the traditional configuration of unidirectional power flows in distribution systems where there is only a single generation bus. With the presence of DERs, there are multiple generation buses that produce bidirectional power flows. Particularly, a small dispersed synchronous generator type called DG is significantly contributed steady-state fault to the system. It causes a short circuit level of the system change and may cause bidirectional short circuit current flow. The impact of DG on overcurrent relay (OCR) coordination effects on both pickup current setting and the operating time of OCR. The coordination time interval (CTI) associated with primary and backup relay pairs is getting violated due to changes in the fault current level. Furthermore, it led to the loss of coordination of conventional OCR when short circuit current flows in the reverse direction. Likewise, it has several impacts on the conventional OCR such as protection blinding, sympathetic tripping, failed reclosing, Insufficient fault current contribution, and loss-of-mains protection (Vasilis Kleftakis, 2018).

The AP technology result from the application of microprocessors in the area of protective relays and are growing in importance in the electrical power systems. They enable grid operators to have flexible protection schemes in response to changes in the power system. AP schemes, which have been developed and applied so far, are based on the automatic readjustment of relay settings whenever network operational conditions and configuration alter. These schemes require the utilization of numerical or digital DOCRs with several setting groups, which can be parameterized locally or remotely by control signals. Protection element values of the available setting groups are calculated in a central controller by special power engineering software, in an offline manner, and stored in the relays (Vasilis Kleftakis, 2018).

On the other hand, the research on optimal coordination of OCR has been paid attention by protection engineers along the time. Because it can improve the reliability of the protection system by reducing the operating time of OCR when a fault occurs, while the coordination between a primary relay and backup relay is still available. an optimal result of this research is setting parameters scheme of each OCR such as the time multiplier setting (TMS), the plug setting (PS), or the standard characteristic curve setting (CS) within a practical reliable bound.

1.3 Research Objectives

The main objective of this research is to propose an optimal full setting scheme (OFSS) of adaptive overcurrent relay (AOCR) coordination consisting of TMS, PS, and CS of each OCR for distribution system with DG in various operating conditions. To show the capability of the proposed conception clearly, the research objectives are divided into four topics as follows.

1.3.1 To propose the OFSS for optimal AOCR protection scheme.

1.3.2 To implement an effective optimization technique for solving OFSS

1.3.3 To investigate the advantage of AOCR protection scheme over non-AOCR protection scheme.

1.3.4 To implement a novel method for solving the mixed-integer linear optimization problem for AOCR protection scheme by using hybrid particle swarm optimization and mixed-integer linear programming (PSO-MILP)

1.4 Scope and Limitations

The proposed conception was simulated within limitations is shown as follows,

1.4.1 The proposed conception was simulated in a MATLAB environment.

1.4.2 IEEE standard 551^{TM} was used to calculate short circuit analysis.

1.4.3 For short circuit analysis, pre-fault bus voltage is used 1.0 pu., fault impedances are neglected, load currents contribution are neglected.

1.4.4 Only maximum phase fault currents were considered on the objective function for OFSS results.

1.4.5 Ground fault protection scheme is not considered.

1.4.6 A comparative study of the proposed optimization technique with other techniques is used their defaults parameter.

The effectiveness of the OFSS for the AOCR coordination problem was tested and compared with four test systems as follows, 1.4.7 the modified 4-bus radial distribution system to illustrate the advantage of the proposed conception.

1.4.8 The IEC benchmark microgrid system to compare the optimal results with previous existing research.

1.4.9 The modified IEEE 15-bus radial distribution system with recloser and fuse to propose the practical radial system.

To demonstrate the scope of this research clearly, the thesis framework is illustrated in Figure 1.1

1.5 Conception

The AOCR coordination problem formulated as the optimization problem to minimize the total operating time of all relays in the system subjected to the limited boundary of setting variable, the coordination constraint, the plug setting multiplier, and the minimum operating time of the relay. The objective function is mixed-integer nonlinear problem (MINLP) with high nonlinear constraints. The rounding-off mixed-integer particle swarm (ROMI-PSO) technique is proposed to find the OFSS. Hence, an optimal result of this research provided a suitable protection planning scheme recommendation for an adaptive overcurrent relay protection.

1.6 Research Benefits

A benefit of this research is provided a suitable AOCR protection planning scheme recommendation for modern distribution system under different fault allocation and various operating conditions.

1.7 Thesis Outline

The organization of this research are as follows. In Chapter II, the literature review is discussed. Section 2.2 reviews an impact of DG penetration on the radial distribution system. Section 2.3 presents advancement of an AP system on distribution network. An overview of existing researches on an optimal coordination of OCR is presented in Section 2.4. And, Section 2.5 provides a theories background of this research. In Chapter III, A comparative study on scenario-based optimal OCR coordination is discussed in Section 3.2. A comparative study on optimization problem of OCR coordination is illustrated in Section 3.3. In Chapter IV provide the optimal full setting scheme of AOCR within various operating conditions of test system by using ROMI-PSO, and comparative study on effectiveness of several technique was discussed. In Chapter V propose MILP-PSO technique for solving the mixed-integer linear optimization problem (MILP) for AOCR protection scheme. Finally, In Chapter VI provide a conclusion and recommendation.

1.8 Chapter Summary

In this chapter presents the general introduction to the distribution system problems with DER penetration. The impact of DER on distributions system protection, The Thailand power development plan, and AP technology is provided in the problem statement section. Furthermore, the research objective, scope and limitation, conception, and research benefit it also has been presented in this chapter.

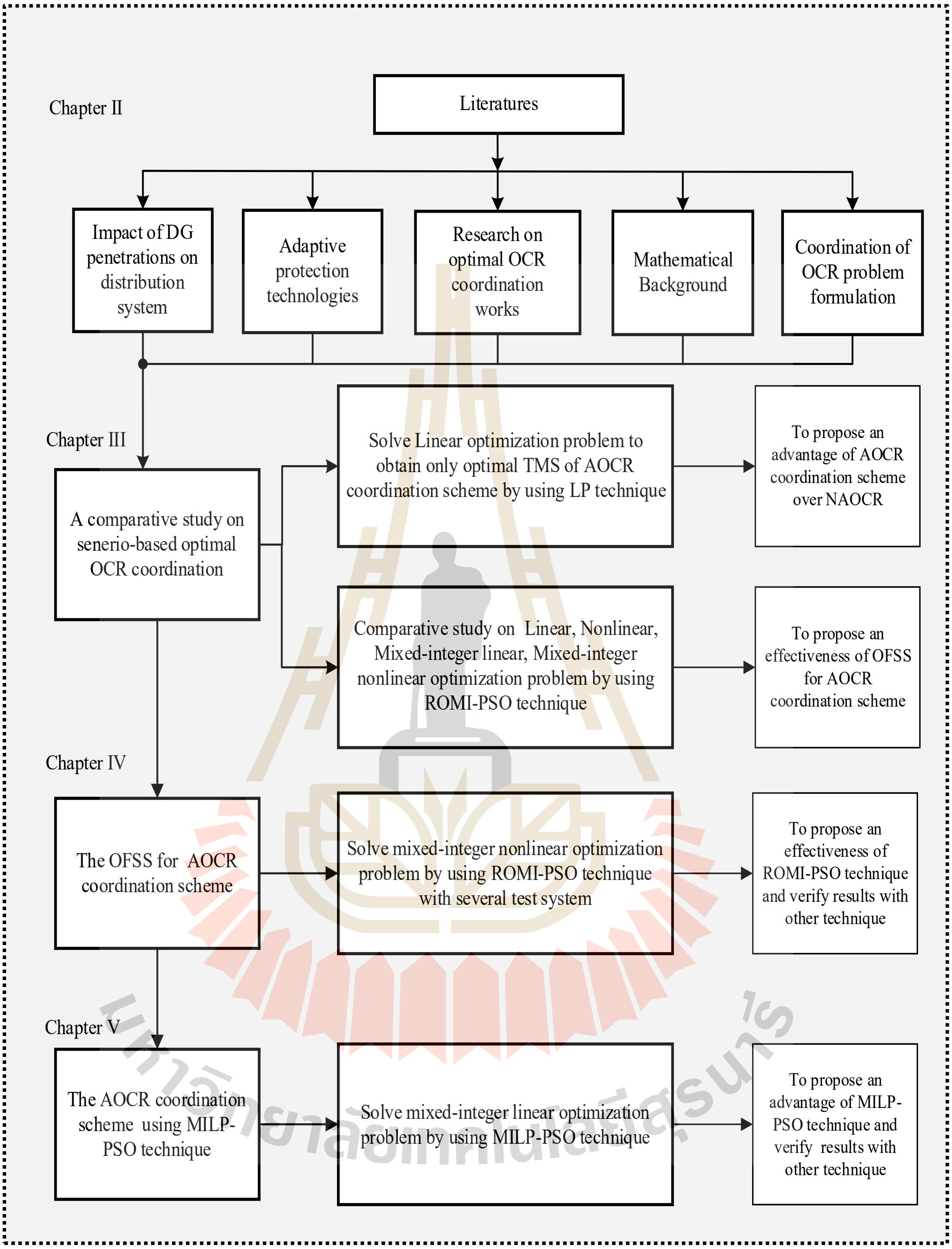

Figure 1.1 The thesis framework

CHAPTER 2

LITERATURE REVIEWS

2.1 Chapter Overview

In this chapter, an impact of DG penetration on distribution system demonstrated in section 2.2. In section 2.3 a construction of AP technology is illustrated. A literature reviews on the optimal coordination of OCR problem are shown in section 2.4 and theories background of this research are presented in section 2.5. In section 2.6 is provided the coordination of OCR in optimize formulation.

2.2 Impact of DG Penetration on Distribution System

Conventional distribution systems are designed to operate without DG on the distribution system or at customer loads. Then, the conventional power flow has unique direction from utility to customer load as shown in Figure 2.1. The impact of generation sources on the distribution system on power flow and voltage conditions at customers and utility equipment can indeed be significant. Depending on the distribution system's operating characteristics and the DG's features, these affects can be beneficial or detrimental. Positive effects are commonly referred to as system support advantages. For instance, support improved voltage and enhanced power quality, feeder cable loss reduction, transmission, distribution capacity release, and utility system dependability has improved. In practice, achieving the following benefits is far more difficult than most realize. The DG sources must be reliable, dispatchable, the proper size, and located in the right locations. They must also satisfy a number of additional operational requirements. There is no certainty that these requirements will be met and that the full system support advantages will be achieved because many DGs will not be owned by utilities or will be variable energy sources like solar and wind. In actuality, if certain basic conditions for control, installation, and location are not satisfied, the penetration of DG might have a negative impact on power system operations. For example, more difficult to control voltage regulation and losses, the potential for observable voltage flicker, the introduction of harmonics, the influence on short circuit levels, and etc. (Nick Jenkins, 2000).

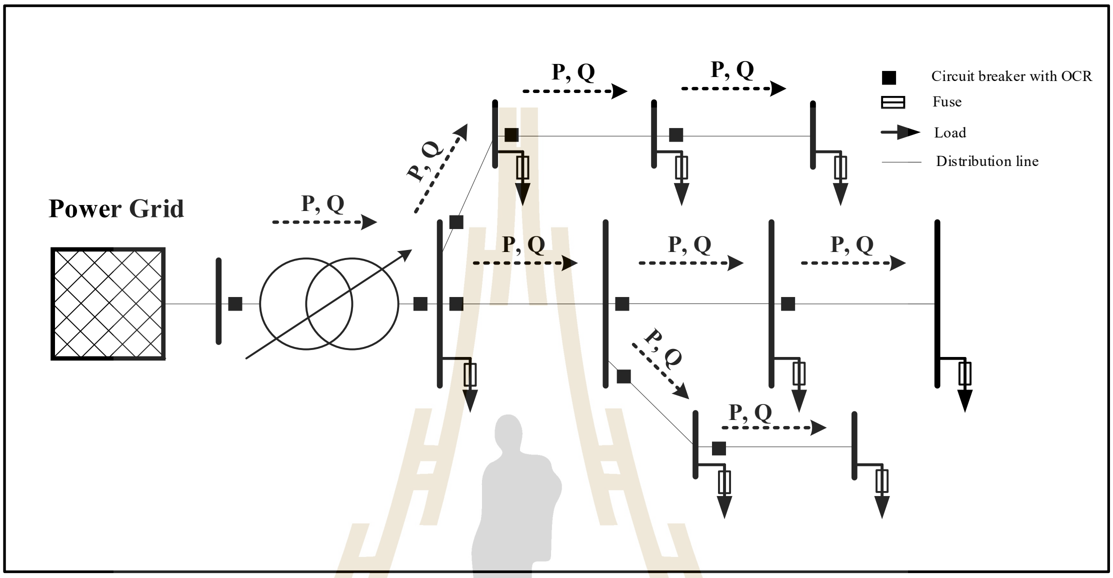

Figure 2.1 The conventional power flow of distribution system

2.2.1 Bidirectional Power Flow

Modern distribution systems were designed to accept bulk power at the bulk supply transformers and to distribute it to customers. Thus, the flow of both real power and reactive power was always from the higher to the lower voltage levels. However, with significant penetration of embedded generation the power flows may become reversed, and the distribution network is no longer a passive circuit supplying loads but an active system with power flows and voltages determined by the generation as well as the loads. For example, the combined heat power (CHP) scheme with the synchronous generator will export real power when the electrical load of the premises falls below the output of the generator but may absorb or export reactive power depending on the setting of the excitation system of the generator. The wind turbine (WT) will export real power but is likely to absorb reactive power as its induction generator requires a source of reactive power to operate. The voltage source convertor of the photovoltaic (PV) system will allow export of real power a set power factor but may introduce harmonic currents.

Thus, the power flows through the circuits may be in either direction depending on the relative magnitudes of the real and reactive network loads compared to the generator outputs and any losses in the network. The change in real and reactive power flows caused by embedded generation has important technical and economic implications for the power system (Nick Jenkins, 2000). The power flow of distribution system with various type of DG as shown in Figure 2.2.

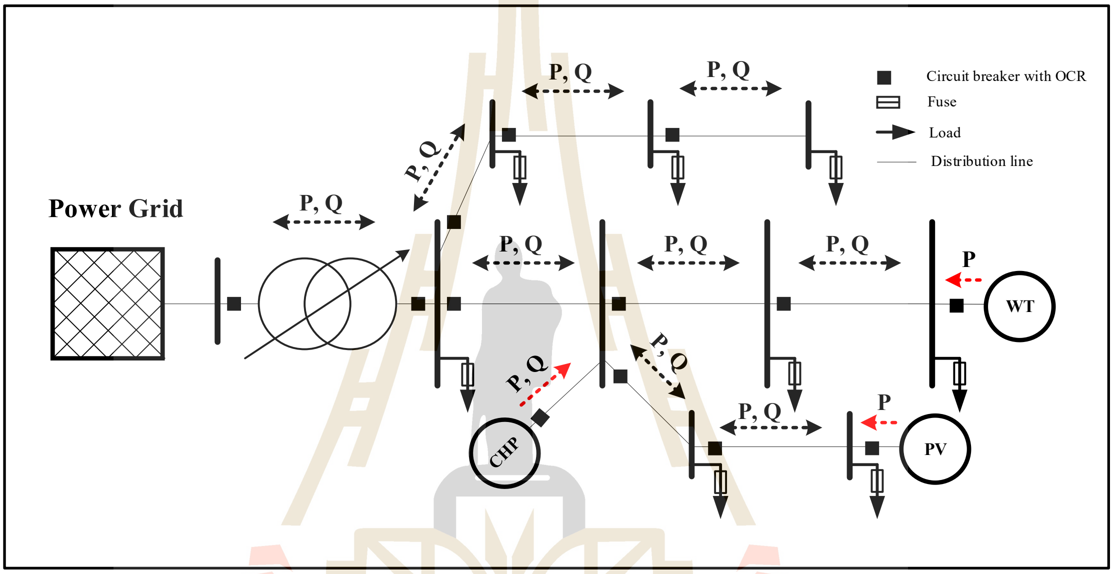

Figure 2.2 The power flow of distribution system with various type of DG

2.2.2 Impact on Short Circuit Levels

Most embedded generation plant uses rotating machines, and these will contribute to the network fault levels. Both induction and synchronous generators will increase the fault level of the distribution system although their behavior under sustained fault conditions differs. In urban areas where the existing fault level approaches the rating of the switchgear, the increase in fault level can be a serious impediment to the development of embedded generation (Nick Jenkins, 2000). The fault contribution from a single small DG unit is not large, however, the aggregate contributions of many small units, or a few large units, can alter the short circuit levels enough to cause fuse-breaker miscoordination. This could affect the reliability and safety of the distribution system. If DG units are added to the system, the fault current may become large enough that the lateral fuse no longer coordinates with the feeder circuit breaker during a fault. This would lead to unnecessary fuse operations and decreased reliability on the lateral (P.P. Barker, 2000). The Figure 2.3 shown that fault contributions due to DG units 1,2 and 3 may increase the short circuit levels to the point where fuse-breaker coordination is no longer achieved. Typical short circuit levels of DG power converters are characterized in Table 2.3 For inverters, the fault contributions will depend on the maximum current level and duration for which the inverter manufacturer’s current limiter is set to respond. On some inverters fault contributions may last for less than a cycle.

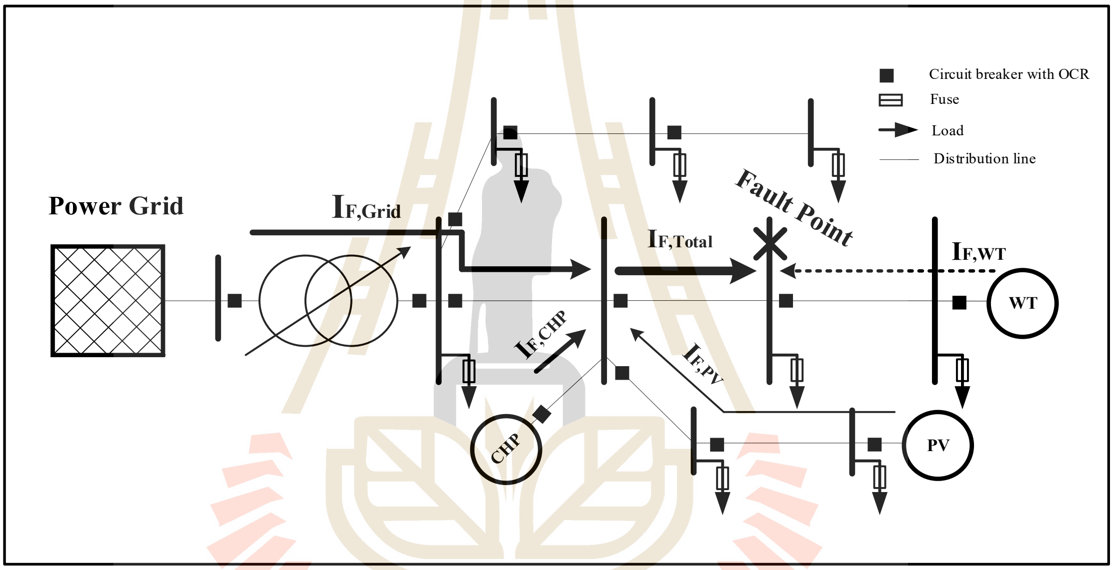

Figure 2.3 The fault contributions from various DG

In other cases, it can be much longer. For synchronous generators, the current contribution depends on the pre-fault voltage, sub-transient and transient reactance of the machine, and exciter characteristics. Induction generators can also contribute to faults as long as they remain excited by any residual voltage on the feeder. For most induction generators, the significant current would only last a few cycles and would be determined by dividing the pre-fault voltage by the transient reactance of the machine. Even though a few cycles are a short time, it is long enough to impact fuse-breaker coordination and breaker duties in some cases. For an example, a 1000 kW synchronous generator would contribute a peak fault current on a 13.2 kV primary feeder of about 218 to 437 Amps to a fault for the first few cycles.

This compares with typical distribution circuits have primary fault currents ranging from about 100 amperes (at remote fringe areas) to more than 10,000 amperes near the substation. Thus, the current contribution from DG units is enough to impact fuse coordination in some cases, especially in weaker parts of the system. Table 2.3 represents the worst-case fault contributions and is only meant as an illustrative guide. For accurate analysis, the generator data should always be obtained from the manufacturer.

Table 2.1 The typical fault level of DG

Type of DG	Fault current into shorted bus terminals as percent of rated output current
Inverter-based	100-400% (duration depend on controller setting and current may even be less than 100% for some inverter).
Separately Excited Synchronous Generator	Starting at 500-1000% for the first few cycles and decaying to 200-400%.
Induction Generator or Self Excited Synchronous Generator	Starting at 500-1000% for the first few cycles and decaying to a negligible amount within 10 cycles.

In addition, Table 2.1 is for faults at the generator terminals. The contributions will decrease the farther the generator is from the fault. The configuration and impedance of the DG site step-up transformer will also play a role. For example, a DG interface configuration that does not provide a zero-sequence path to the utility system will not contribute to ground faults on the primary side. When a single generator is added to the system, a manual calculation of the peak fault currents based on manufacturers data can be performed to screen for a serious impact on the existing short circuit levels. For multiple generation devices scattered throughout the system or large generators, the only accurate approach is to perform a software based short circuit analysis which correctly models the short circuit behavior of the generators. In many cases, the DG units won’t pose a threat to existing coordination, only a relatively few cases may require changes in protection settings (P.P. Barker, 2000).

2.2.3 Impact on Protection System

There are various challenges which are encountered in distributed generation protection. They are discussed below, Protection blinding, this phenomenon occurs when a large-scale conventional DG unit is connected to a distribution feeder between the main grid and the fault location.

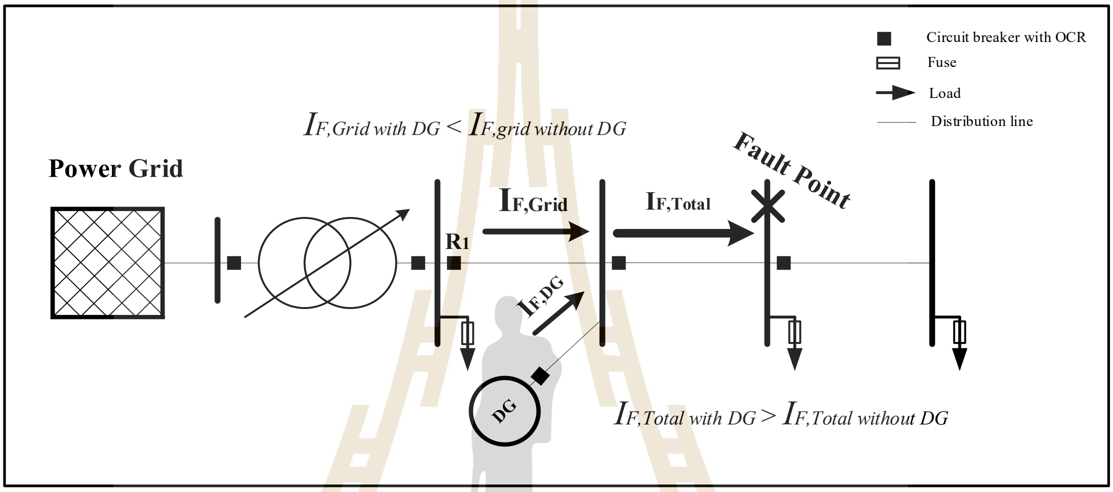

Figure 2.4 Protection blinding

The power grid fault contribution is reduced due to the partial contribution from the DG unit, and the feeder relay R1 senses a lower short-circuit current value. As a consequence, the relay cannot be asserted and clear the fault, suffering from "blinding" as shown in Figure 2.4

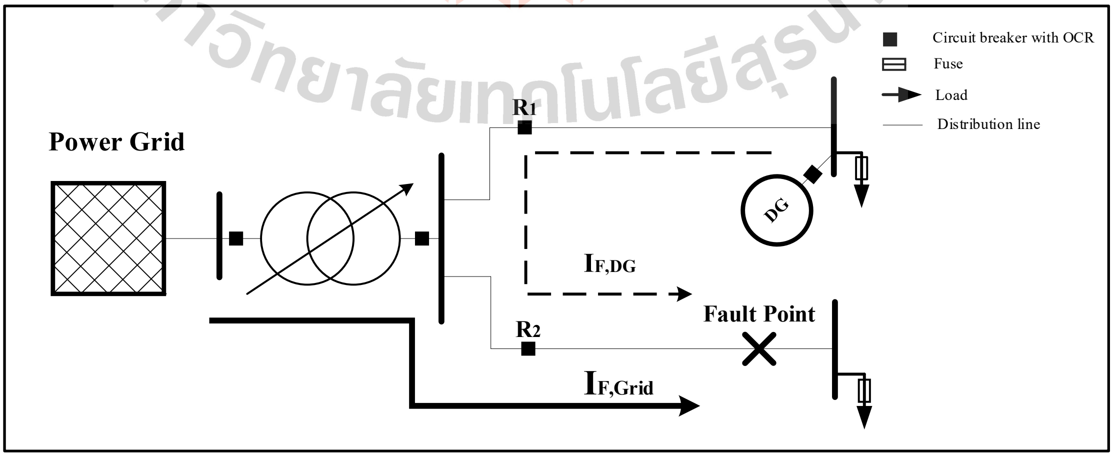

Figure 2.5 Sympathetic tripping

Sympathetic tripping, in grid-connected mode, when a DG unit is connected to a specific feeder and a fault occur on an adjacent one, the fault current contribution from the DG unit might exceed the pickup current setting of feeder's OCR, especially when DG capacity is sufficiently large. Therefore, the relay R1 trips sympathetically to relay R2. and the healthy feeder faces an unexpected outage as shown in Figure 2.5.

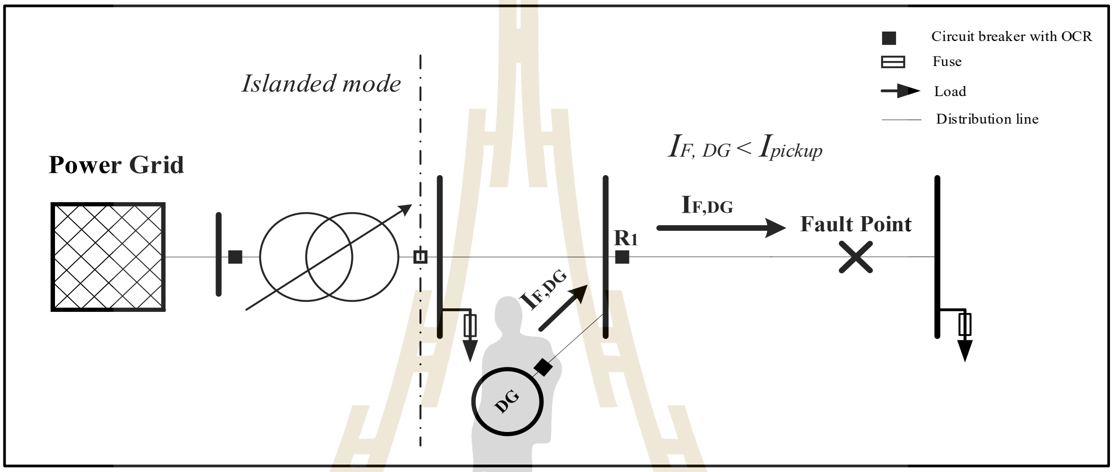

Figure 2.6 Insufficient fault current contribution

Insufficient fault current contribution, in islanded operation mode, the fault current contribution from inverter-interfaced DG units is limited to about twice the rated current of the inverter. Impact to protection is ineffective use of OCR protection. Insufficient fault current contribution could not reach OCR's pickup setting as shown in Figure 2.6.

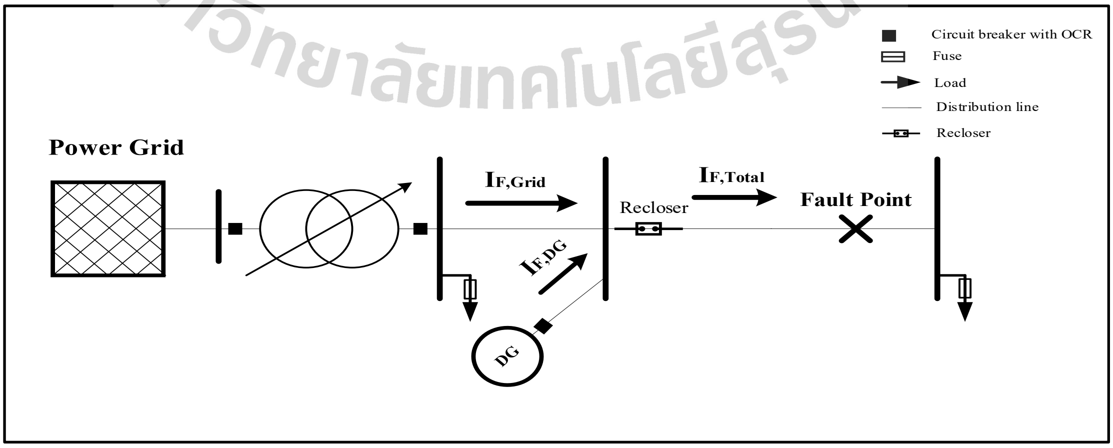

Figure 2.7 Failed reclosing

Loss-of-mains protection, this issue refers to the phenomenon that occurs when the distribution grid disconnects from the main utility grid, but remains connected to part of the load in the utility grid. This can occur for two reasons, a utility grid fault, or a problem in the circuit breaker operating mechanism which is connected to a utility source. During this situation of unintentional islanding, the life of the person attending the fault, is at stake since islanding is not detected. This problem also leads to uncontrolled frequency and voltage and non-synchronized reclosures which, in turn, can damage customers sensitive equipment (Vasilis Kleftakis, 2018).

2.3 Adaptive Protection Technology

Conventional protection system has OCR with fixed setting parameters. With the growing complexity in operating power systems, increasing shares of DER units, a lack of short circuit current injection to correctly detect faults, and increased harmonics that can falsely trigger protection relays, various challenges arise to fulfil the protection requirements in variable operation conditions. The conventional protection system of distribution network as seen in Figure 2.8.

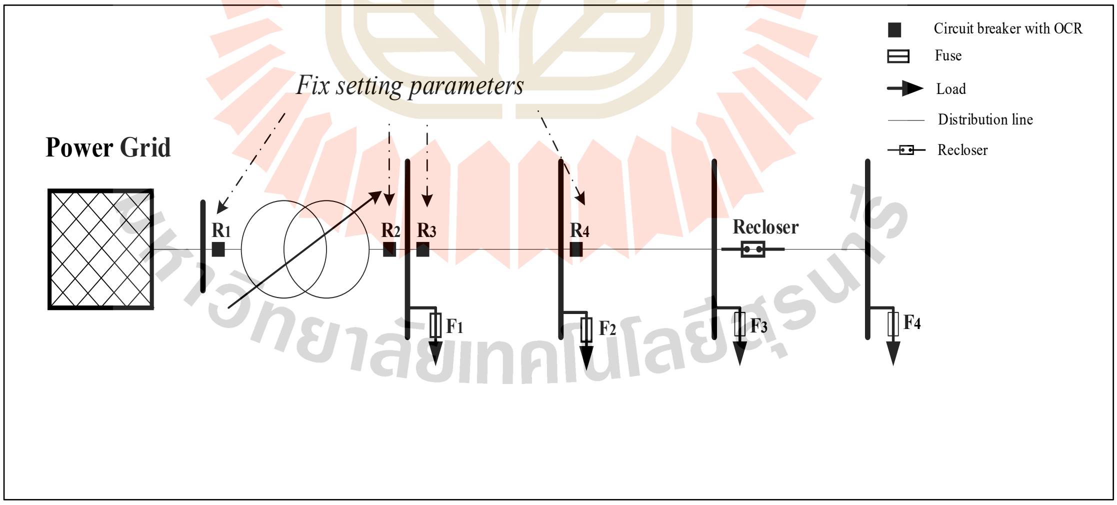

Figure 2.8 The conventional protection system of distribution network

The AP schemes result from the application of microprocessors in the area of protective relays and are growing in importance in the electrical power systems. They enable grid operators to have flexible protection schemes in response to changes in the power system. AP schemes, which have been developed and applied so far, are based on the automatic readjustment of relay settings whenever network operational conditions and configuration alter. These schemes require the utilization of numerical or digital DOCRs with several setting groups, which can be parameterized locally or remotely by control signals. Protection element values of the available setting groups are calculated in a central controller by special power engineering software, in an offline manner, and stored in the relays.

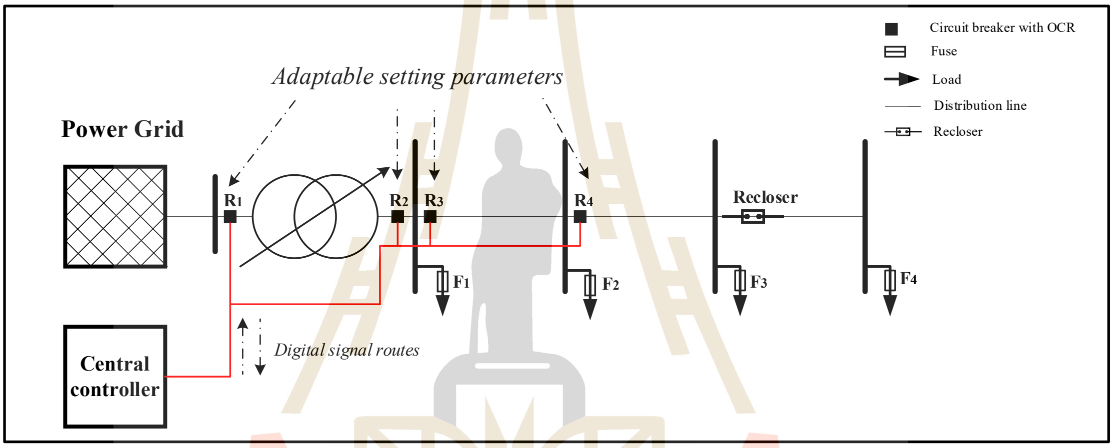

Figure 2.9 The AP system of modern distribution network

To summarize, AP systems are able to monitor and update the relays' settings in accordance with distribution network or microgrid state, based on offline analysis and online operation. The offline analysis is performed by constructing event and action tables for the circuit breaker statuses and relay setting groups respectively, for each possible configuration. During online operation, the central controller monitors the grid operating state and uses the event and action tables to configure the relays properly. Another important aspect of AP schemes regards the capability of data exchange among relays, IEDs, and the central control unit, which can be achieved either by established communication infrastructure or by hardwired control circuits. It is evident that AP systems, which fulfill the previous technical requirements, are characterized by a particularly high investment cost in comparison with conventional protection systems based on non-DOCRs and fuses. However, a cost-benefit analysis would show that benefits offered by AP systems to end-customers, which correspond to reduced outage time and improved power quality, outweigh the investment and operating costs (Vasilis Kleftakis, 2018).

The AP system components include a central control unit to receive the network configuration (topology, DG connection status, circuit breaker status, loading status) changes, by using signals from local sensors or others shown on the red line in Figure 2.9. Then, select the optimal scheme and forward the optimal setting to each relay by the red line in Figure 2.9. microprocessor-based digital relay with various technique requirement such as the DOCRs element due to the bi-directional flow of short-circuit currents, several setting groups must be encapsulated, and establishment of communication infrastructure and use of industrial communication protocols, e.g., Modbus, IEC 61850, DNP3 (necessity of communication between adjacent relays and individual relays with the central control system) (Vasilis Kleftakis, 2018).

2.4 The Optimal Coordination of OCR Research

Previous research studies have shown that the objective function is used in the same direction to find the minimum total operating time of all relays in the system with any fault that can occur in the system. Each article discusses the different forms of objective functions, tested systems, and problem-solving methods. The problem types can be divided into two categories as follow.

2.4.1 Linear Optimization Problem

In the general form, the objective function of OCR coordination is a non-linear optimization problem (NLP). to optimize both TMS and PS. However, solving nonlinear optimization problem methods are complex as well as time-consuming. To avert complexity, this problem commonly formulated as a linear optimization problem (LP) by predetermined PS based on minimum fault current or maximum load current passing through relay. This approach was applied in the various articles to handle coordination problems using different algorithms, respectively.

Chattopahyay et al (1996) present two phase simplex methods were used to find the optimal value of TMS for each AOCR using several cases from the ‘City of Saskatoon' distribution test network, such as maximum system load and maximum system generation with line 1-20 closed, minimum system load and maximum system generation with line 1-20 open, etc., and compared the results with the non-adaptive overcurrent relay (NAOCR) (Bijoy Chattopahyay, 1996).

Bedekar et al (2009) used the dual simplex method handled the coordination of NAOCR for ring main feeder and parallel feeders, single-end-fed system. optimal of TMS value founded (Prashant P. Bedekar, 2009).

Gupta et al (2015) used the big-m method to compare the optimal value of an objective function with the dual simplex method in a three-bus radial test system. Found that the big-m method provided a more optimal solution than the dual simplex method, but it taken more time-consuming (Anjali Gupta, 2015).

Deepak et al (2017) used the revised simplex method to compare the optimal value of an objective function with the big-m method in a two-bus radial test system. Found that the revised simplex method gives same optimal solution as big-m method. But the total time taken by the revised simplex method to find the optimum solution is less than that of the big-m method as calculation time decreases (A.M.S. Deepak, 2017).

In the other hand, the several stochastic search and meta-heuristic search was applied in many articles as following. Bedekar et al (2009) proposed genetic algorithm (GA) handling the coordination of NAOCR for ring main feeder and parallel feeders, single-end multi-loop system. Found that the results for the same problem are obtained using the revised simplex method and dual simplex method also and are found to be the same. Thus, the optimality of the result is confirmed (Prashant P. Bedekar, 2009).

Adhishree et al (2014) used several the heuristic searches to find the optimal value of TMS of AOCR for distribution system with DG penetration consists of linear programming (LPP), GA, pattern search algorithm (PSA), particle swarm optimization (PSO), and simulated annealing (SA). It is observed that GA and PSO are superior methods than that of LPP, PS, and SA. They are giving better optimal solutions (Adhishree, 2014).

Ibrahim et al (2015) presented an artificial bee colony (ABC) to dealing the optimal value of TMS of AOCR for 30 bus distribution test system with DG penetration and considering DG loading effect (A.M. Ibrahima, 2015).

Bedekar et al (2017) used the modified jaya algorithm (MJA) to handle this problem of NAOCR for two bus radial and parallel, single-end-feeder system. it is found that MJA always converges to the same and optimum value different from GA sometimes converges at values that are not the optimum solution (P. P. Bedekar, 2017).

Chaitanya et al (2017) proposed the differential evolution (DE) was used to find the optimum value of TMS of NAOCR for radial four bus test system and was compared to the dual simplex approach. The DE and dual simplex methods were found to produce the closest optimum value. However, as compared to the dual simplex approach, it takes less time to calculate. These algorithms can likewise be applied to larger distribution networks with proficiency (A. V. K. Chaitanya, 2017).

Tharakan et al (2017) used the firefly algorithm (FF) to identify the optimum value of TMS of NAOCR in a radial two bus system and was compared to ant colony optimization (ACO). the FF, rather than the ACO algorithm, appears to produce a better optimal solution. These algorithms can also be conveniently extended to larger distribution networks (Kevin Isaac Tharakan, 2017).

Saad et al (2018) presented the GA to find the optimal value of TMS of AOCR for Benghazi distribution network with DG penetration. considering different operation modes such as without DG, with DG, and islanding mode (Saad. M. Saad, 2018). The conclude of the related research on OCR coordination in LP form as shown in Table 2.2.

Table 2.2 The related research on OCR coordination in LP formulation

Reference	Objective	Constraints	Solver	Test case	Significant finding and extra detail
B. Chattopahyay et al.,1996	- The total operating time of primary relay for a near-end fault.	- The coordination constraints. - limit boundary of TMS.	- The two-phase simplex method.	- City of Saskatoon distribution network.	- Considering various system conditions. - Implemented overload and Instantaneous OCR. - Using AOCR. - Found that satisfactory results in all the cases.
P. P. Bedekar et al.,2009	- The total operating time of primary relay for a near-end fault.	- The coordination constraints. - limit boundary of TMS. -The minimum operating time constraint of OCR.	- The dual simplex method	- Ring main feeder. -Parallel feeders. -Single-end-fed system.	- Considering various test system. - Using NAOCR. - Found that satisfactory results in all the cases.
A. Gupta et al.,2015	- The total operating time of primary relay for a near-end fault.	- The coordination constraints. - limit boundary of TMS. -The minimum operating time constraint of OCR.	-The big-m technique and dual simplex method.	- Three bus radial test system.	- Using NAOCR. - Found that the big-m method provided a more optimal solution than the dual simplex method but it taken more time-consuming.
A.M.S. Deepak et al.,2017	- The total operating time of primary relay for a near-end fault.	- The coordination constraints. - limit boundary of TMS. -The minimum operating time constraint of OCR.	- The revised simplex method and the big-m technique.	- Radial two bus system.	- Using NAOCR. - Found that the Revised simplex method gives same optimal solution as big-b method. But the total time taken by the revised simplex method is less than that of the big-m method as calculation time decreases.

Table 2.2 The related research on OCR coordination in LP formulation (continuous)

Reference	Objective	Constraints	Solver	Test case	Significant finding and extra detail
P. P. Bedekar et al.,2009	- The total operating time of primary relay for a near-end fault.	- The coordination constraints. - limit boundary of TMS. -The minimum operating time constraint of OCR.	- The GA	- Ring main feeder. -Parallel feeders. -Single-end-fed multi loop system.	- Using NAOCR. - Found that satisfactory results in all the cases.
Adhishree et al.,2014	- The total operating time of primary relay for a near-end fault.	- The coordination constraints. - limit boundary of TMS. -The minimum operating time constraint of OCR.	-The LPP, GA, PS, PSO, and SA.	-Single source three bus radial system with DG.	- Using AOCR. - Found that GA and PSO are superior methods than that of LPP, PS, and SA. They are giving better optimal solutions.
A.M. Ibrahim et al.,2015	- The total operating time of primary relay when fault take place.	- The coordination constraints. - limit boundary of TMS. -The minimum operating time constraint of OCR.	-The ABC	-IEEE 30 bus system with DG.	- Using AOCR. - Considering various system conditions and DG loading effect. - Found that satisfactory results in all the cases.
P. P. Bedekar et al.,2017	- The total operating time of all relays when fault take place.	- The coordination constraints. - limit boundary of TMS. -The minimum operating time constraint of OCR.	-The MJA	- Two bus radial system -Parallel, Single-end feeder system.	- Using NAOCR. - Found that MJA always converges to the same and optimum value different from GA sometimes converges at values that are not the optimum solution.

Table 2.2 The related research on OCR coordination in LP formulation (continuous)

Reference	Objective	Constraints	Solver	Test case	Significant finding and extra detail
A V K. Chaitanya et al.,2017	- The total operating time of primary relay for a near-end fault.	- The coordination constraints. - limit boundary of TMS. -The minimum operating time constraint of OCR.	- The DE and dual simplex methods.	- Radial four bus test system.	- Using NAOCR. - Found that the algorithm produces the closest optimum value. But, as compared to the Dual simplex approach, it takes less time to calculate.
K. I. Tharakan et al.,2017	- The total operating time of primary relay for a near-end fault.	- The coordination constraints. - limit boundary of TMS. -The minimum operating time constraint of OCR.	- The FF and ACO	- Radial two bus system.	- Using NAOCR. - Found that FF provides better optimal solution rather than ACO algorithm.
Saad. M. Saad et al.,2018	- The total operating time of all relays when fault take place.	- The coordination constraints. - limit boundary of TMS. -The minimum operating time constraint of OCR.	- The GA	- 'Benghazi' distribution network with DG penetration	- Using AOCR. - Considering various system conditions. - Found that satisfactory results in all the cases.

2.4.2 Nonlinear Optimization Problem

In this approach, both TMS and PS are decision variables of each relay. But the main objective function and other constraints are the same as LP. several existing research are addressed this OCR problem as follow,

Vijayakumar et al (2008) proposed the modified particle swarm optimization (MPSO) was utilized to find the optimal TMS and PS for NAOCR in a six-bus multi-generator power system network. MPSO modifies the standard PSO is initial step of randomly generating PS just to ensure that the constraint is satisfied. As a result, the issue is converted to LP, and the optimal TMS is found using traditional PSO. The result is compared to the generalized algebraic modeling system (GAMS) commercial software for solving nonlinear programming. It was discovered that MPSO gave nearly optimal value when compared with GAMS (D. Vijayakumar, 2008).

Bedekar et al (2011) founded that the GA has the disadvantage of sometimes convergent to values that aren't optimal, while NLP approaches have the disadvantage of convergent to local optimum values if the initial decision is close to the local optimum. As a result, the authors offer GA-NLP approaches to solve the NAOCR coordination problem for a nine-bus loop distribution system and a single-end-fed distribution system. The GA-NLP technique entails first finding the initial answer with GA and then utilizing NLP to discover the final optimal answer. The proposed strategy outperforms the other techniques, according to the findings (Prashant Prabhakar Bedekar, 2011).

Singh et al (2012) used the covariance matrix adaptation evolution strategy (CMA-ES) was in IEEE 30 bus mesh distribution network for optimal coordination of NAOCR. The far vector of the LINK NET structure is used to select a combination of primary and backup relays to avoid relay miscoordination. The objective function is to minimize the operating time between backup and primary relays. The results are compared to the TMS and PS optimized values from the modified DE. The proposed algorithm outperforms the DE algorithm, according to the results (Manohar Singh, 2012).

Amraee (2012) proposed that PS is a discrete variable ranging from 1.5 to 5 in steps of 0.5, but TMS remains a continuous value. As a result, the coordination of DOCR is formulated as a mixed-integer nonlinear programming problem (MINLP), which is then solved using a new seeker optimization approach (SOA) for multiloop sub-transmission or mesh distribution test cases with low to high DG penetration. It was discovered that the proposed technique's efficiency was validated for both continuous and discrete variables. The findings indicated that both linear and nonlinear models, The result shows that the proposed technique is capable of finding superior TMS and PS than MINLP with standard branch-and-bound algorithm (SBB) solvers already supported by GAMS (Amraee, 2012).

Singh (2013) developed the gravitational search algorithm (GSA) to solve the coordination of AOCR for a three-bus radial microgrid with three DG source penetrations to find the optimum value of TMS and PS for each operation mode, such as all DG linked to the grid, DG1and DG2 linked to the grid, and no DG connected to the grid. Expert-based AOCR coordination was discovered to be a very effective method for restoring relay coordination in such microgrid operational modes. The circuit breakers are used to assess system conditions, and AOCR settings are communicated to the relay via effective communication routes. AOCR settings are optimized with the help of a fast and robust of GSA (Singh, 2013).

Papaspiliotopoulos et al (2014) using a hybrid PSO-LP method to handle the problem of DOCR coordination in a five-bus radial distribution network with high DG penetration is solved. The proposed methodology's task is to find the TMS and PS settings for each DOCR that minimize the sum of relay operation times under certain constraints. In addition, the suggested method may address protection issues that arise as a result of DG infeed and network topology changes, and it may be integrated into future AP schemes (V.A. Papaspiliotopoulos, 2014).

Tripathi et al (2014) used the GSA was used to handle AOCR coordination for a four-bus radial system with DG and compare the optimal answer with PSO. The mal operation of relays caused by the presence of DG is carefully explained, and the findings are compared. This shows that GSA provides an amazing strategy for relay coordination problems (Jyant Mani Tripathi, 2014).

Papaspiliotopoulos et al (2015) used hybrids PSO-LP to find optimal setting value of AOCR for five-bus radial distribution network with high DG. and verify answer with KNITRO commercial solve. Furthermore, a hardware-in-the-loop (HIL) testbed, developed at the electric energy systems laboratory of the national technical university of Athens (NTUA), was employed to evaluate the performance of the proposed AP scheme. It is actually a closed-loop topology consisting of a real-time digital simulator (RTDS), multifunction digital relays, and a programmable logic controller (PLC). Finally, the efficacy of the proposed methods was evaluated on two DG penetrated distribution grids, and the AP enhancement was verified utilizing a HIL testbed (Vasileios A. Papaspiliotopoulos, 2015).

Saha et al (2015) developed the symbiotic organism search optimization methodology (SOS), a newly published nature-inspired metaheuristic optimization methodology, to compute the optimal DOR coordination settings. IEEE 6-bus and WSCC 9-bus test systems are used to test relay coordination. The results show that the SOS algorithm outperforms PSO and the learning-based optimization (TLBO) methodology in calculating the best relay settings in interconnected power networks. SOS also has the advantages of fast convergence and initial value independence. It can be predicted that the SOS would help protection engineers to incorporate other types of relays and to solve relay coordination problem in more complicated networks such as renewable energy sources-based distributed generation systems (Debasree Saha, 2015).

Kheshti et al (2016) investigated PSO for NAOCR coordination problems. IEEE 15 node radial network was considered as a case study. The obtained optimum values of PS and TMS come to confirm that this useful optimization technique carefully implemented in MATLAB software is feasible for OCR protection coordination in radial networks. However, the calculation time of the PSO algorithm is still an issue, especially in very large-scale networks (Mostafa Kheshti, 2016).

Chakor et al (2016) used GA to find the optimal of an AOCR setting for a single-end three-bus multi-loop system with interconnected DG to solve the coordination problem. In every case of the test system, the outcome has proved that GA can solve optimum results (Sahebrao V. Chakor, 2016).

Pujiantara et al (2016) developed GA to deal AOCR coordination and find the optimal value of TMS and PS in a five-bus radial network with DG. Based on the DG's operation modes, the best results for each scenario have been shown. The simulation results show that the proposed algorithm's TMS and PS values are lower than the conventional technique (trial and error technique), reducing the coordinated protection of OCR's operating time (Margo Pujiantara, 2016).

Bedekar et al (2016) proposes a small and simple change to the MJA. The algorithm was used to find the optimal PS and TMS values for NAOCRs. The algorithm's usefulness was tested using a variety of systems, including a large number of OCRs. It is demonstrated that the problem can be decomposed in some circumstances, considerably reducing the complexity of the problem without sacrificing accuracy. The outcomes are compared to those achieved with GA. MJA has been proven to outperform the GA. It is also demonstrated that the problem can be divided into components to reduce complexity while maintaining accuracy (P. P. Bedekar, 2016).

Korde et al (2016) This study presents a sequential quadratic programming method (SQP) for determining the optimal PS and TMS values for a three-bus multi-loop distribution system. The program has been successfully tested for a variety of systems, including different types of OCRs and all inverse definite minimum time (IDMT) relays, which are presented in this paper. When compared to GA, it was revealed that SQP is the superior method. It is also discovered that, when compared to all IDMT relays, the overall time of operation of all relays lowers with different OCRs in the system. As a result, the proposed strategy for optimum relay coordination appears to be promising (P. N. Korde, 2016).

Pathade et al (2017) proposed the coordination of NAOCR for a nine-bus mesh distribution system was solved using GA in this research. TMS and PS of the relay were found to be optimal. The algorithm was put to the test and found to be capable of producing satisfactory results in all scenarios (Sumit U Pathade, 2017).

Bhatiya et al (2017) present the amalgam of GA-NLP method for determination of optimum values of TMS and PS for nine-bus mesh distribution system as an optimization problem presented in this paper. The initial solution of GA has been applied to NLP method to obtain optimum values. Thereby making both GA and NLP advantageous and at the same time it overcomes shortcomings of these methods (Pushpa Bhatiya, 2017).

Atteya et al (2017) presented the modified particle swarm algorithm (MPSO) to solve the relay coordination problem The modification added to the typical PSO technique helped to hold all particles in feasible solution by applying the interior-point method to select the initial positions. To confirm the concepts of adaptive protection, the 14 IEEE bus loop distribution network was tested for various power system topologies. The effect of DGs penetration and disconnection, as well as the occurrence of line outages on distribution networks, were discussed in the selected case studies. The obtained results show that the proposed methodology is effective in achieving optimal relay setting groups for each network topology while minimizing total operation time and satisfying selectivity constraints among all protective devices (Ayatte. I. Atteya, 2017).

Tjahjono et al (2017) presented an adaptive modified firefly algorithm (AMFA) for the optimal coordination of AOCR with DG in a radial system, The suggested approach uses TMS and PS parameters to minimize the operation times for the main and backup OCRs. The results show that the suggested methodology improves the performance of the FA with self-adaptive parameter tuning of the random movement factor when applied to five conditions to evaluate its performance. In radial systems with DG, the results also show that the proposed algorithm is superior to the standard approach, FA, MFA, and PSO for protection coordination. In comparison to FA and MFA, the proposed algorithm has a faster convergence rate. For all test cases, the operation time reduction is at least 40.446 percent greater than the conventional approach FA (Anang Tjahjono, 2017).

Hatata et al (2018) presented the ant lion optimizer (ALO) to find the optimal setting of AOCRs such as PS and TMS for IEEE 30-bus mesh distribution network and 11-Bus radial distribution system with DG in various cases such as 30% of DG1, 30% of DG2, etc. The main objective is to maintain the primary-backup relays coordinated while minimizing the total operating time of the primary relays, which is dependent on the system's far-end and near-end fault currents. The constraint of transient stability is taken into consideration. The results confirmed ALO's visibility and effectiveness. ALO is capable of achieving the lowest operating time. The proposed ALO has the maximum accuracy, according to the comparison results. Furthermore, among PSO, Artificial immune systems (AIS), DE, and GA, it has the shortest computing time and the best stability (A. Y. Hatata, 2018).

Khurshaid et al (2018) proposed the PS is a discreate value, but TMS is a continuous value. As a result, NAOCR relay coordination has become a MINLP problem. To address this issue, the author proposed the modified seeker algorithm (MSA). The proposed idea's main accomplishment is that it is too familiar with the concept of robust coordination for determining the optimal total operating time for the coordination problem in a power system. On an IEEE 8 bus power system, the proposed technique has been successfully implemented. When compared to LP, NLP, GA, GA-LP, and SOA, the results reveal that the suggested algorithm outperforms them all (Tahir Khurshaid, 2018).

Khurshaid et al (2019) presented the DOCR optimum coordination problem is modeled as an MINLP. The hybrid metaheuristic algorithms based on the whale optimization algorithm (WOA) were proposed in this research. The proposed methods combine the SA algorithm with WOA's global search. After each cycle of WOA, SA was employed as a local search operator around the selected search agents in order to search the neighborhood of the best solution. the proposed hybrids whale optimization algorithm (HWOA) has been tested on five different systems, including the IEEE 3-bus 8-bus, 9-bus, 15-bus, and 30-bus loop multi-generator test systems, in order to assess its performance. The observed results demonstrate that the suggested HWOA is a useful and reliable tool for coordinating DOCR. Furthermore, the results obtained with HWOA are superior to those achieved with a native WOA and a number of well-known and current algorithms described in the literature (Tahir Khurshaid, 2019).

In the other hand, Alam (2019) proposed the optimum settings of AOCR considering different characteristic curves for the protection of AC microgrids with islanded and grid-connected modes of operation is presented. In this work, all the relays are considered to be associated with three variables which are TMS, PS, and CS to obtain their correct operating times. Here, TMS, PS, and CS are associated with time scaling, pickup current value and characteristic curve selection, respectively, of an AOCR. The proposed protection coordination problem has been formulated as a MINLP and solved using the genetic algorithm in MATLAB environment. The effectiveness and suitability of the proposed approach have been demonstrated on 7 and 18 bus microgrids. founded those satisfactory results in all the cases and the optimum settings obtained using GA are better than PSO and DE for both the test systems (7 and 18 bus microgrids). The best values of the objective function (i.e., the sum of operating times of all the relays) for the 7 and 18 bus microgrids obtained using GA are always less than those obtained using PSO and DE (Alam, 2019).

Consequently, Sorrentino and Rodríguez (2020) proposed the effect of curve type of OCR functions and the location of analyzed faults on the optimal coordination of DOCR protections in several complex loop power system. the problem formulates as MILP to find TMS and CS of each OCR. The result founded extremely inverse curves were between 7 and 16 times faster than results with normal inverse curves. The curve type can determine the feasibility of having solutions, especially due to the upper limits for time multiplier settings. however, the optimal solutions without considering these limits are useful because some technically feasible solutions can be hidden in mathematically unfeasible solutions.

On the other hand, the selection of very inverse curves might be considered a better solution in some cases for the compromise between obtaining fast operating times for faults very near to main relays and reasonably low times for the backup action for faults near to the remote line end. Thus, the selection of curve type has an influence on feasibility of obtaining solutions and reasonably low trip times. The effect of fault location was analyzed using solid faults at two locations (near to the main relay, and near to the remote line end).

The numerical results of two examples demonstrated that including only faults near to the main relay does not guarantee selectivity in other cases. Therefore, other fault locations must be included in the problem formulation in order to obtain certainty about selectivity in diverse cases. This article also showed the analytical way of knowing a priori if the constraint related to only one fault location is sufficient for the proper problem formulation (Elmer Sorrentino, 2020).

And the recent, S. D. Saldarriaga-Zuluaga et al (2020) proposes an approach for the optimal coordination of OCRs in microgrids that integrate renewable DG and feature several operational modes. As a main contribution, the characteristic curves of OCRs are considered to be decision variables, instead of fixing a single type of curve for all relays as considered in previous works. The proposed approach allows for the selection of several IEC and IEEE curves which combination results in the best protection coordination. Several tests were carried out on an IEC benchmark microgrid in order to show the applicability of the proposed approach. all operational modes, the proposed approach presented better operational times (Saldarriaga-Zuluaga, 2020).

The conclude of the related research on OCR coordination in NLP form as shown in Table 2.3.

Table 2.3 The related research on OCR coordination in NLP formulation

Reference	Objective	Constraints	Solver	Test case	Significant finding and extra detail
D. Vijayakumar et al.,2008	- The total operating time of all relays when fault take place.	- The coordination constraints. - limit boundary of TMS and PS.	- The MPSO	-The six-bus power system network.	- Using NAOCR. - Found that that MPSO gave nearly optimal value when compared with GAMS
P. P. Bedekar et al.,2011	- The total operating time of all relays when fault take place.	- The coordination constraints. - limit boundary of TMS and PS. -The minimum operating time.	-The GA-NLP	-The nine-bus loop distribution system -single-end-fed distribution system.	- Using NAOCR. - Found that satisfactory results in all the cases -The strategy outperforms than GA, Hybrid GA-LP.
M. Singh et al.,2012	- The total operating time of all relays when fault take place.	- The coordination constraints. - limit boundary of TMS and PS. -The minimum operating time.	-The CMA-ES	- IEEE 30 bus distribution system.	- Using NAOCR. - Found that the proposed algorithm outperforms the DE algorithm.
T. Amraee 2012	- The total operating time of all relays when fault take place.	- The coordination constraints. - limit boundary of TMS and PS. -The minimum operating time.	- The SOA technique.	- The three-bus loop multi-gen system. - The eight-bus loop multi-gen system. - The 15-bus network.	- Using NAOCR. - Considering PS is step/discreate value - Found that the proposed algorithm covers the weakness of the previously proposed evolutionary Techniques.

Table 2.3 The related research on OCR coordination in NLP formulation (continuous)

Reference	Objective	Constraints	Solver	Test case	Significant finding and extra detail
M. Singh 2013	- The total operating time of primary relay for near end faults and for far bus end faults	- The coordination constraints. - limit boundary of TMS and PS. -The minimum operating time.	- The GSA	- The three-bus radial microgrid with three DG source penetrations.	- Using AOCR. - Considering various system conditions. - Found that satisfactory results in all the cases.
V.A. Papaspili otopoulos et al.,2014	- The total operating time of primary relay for fault inside its protection zone.	- The coordination constraints. - limit boundary of TMS and PS. -The minimum operating time.	-The PSO-LP	- The five-bus radial distribution network with high DG penetration. - The 8-bus power system. - The 15-bus distribution network.	- Using NAOCR. - Found that satisfactory results in all the cases and verified that this hybrid technique provides satisfactory results in combination with high rate of convergence.
J. M. Tripathi et al.,2014	- The total operating time of all relays when fault take place.	- The coordination constraints. - limit boundary of TMS and PS. -The minimum operating time.	- The GSA	- The single source four bus radial system with DG.	- Using AOCR. - Found that the proposed algorithm outperforms the PSO algorithm for all system conditions.
V.A.Papaspili otopoulos et al.,2015	- The total operating time of primary and backup relays when fault take place.	- The coordination constraints. - limit boundary of TMS and PS. -The minimum operating time.	-The PSO-LP	- The five-bus radial distribution network with high DG penetration. - The 15-bus distribution network.	- Using AOCR. -Found that the proposed algorithm provides the optimal solution close to KNITRO.

Table 2.3 The related research on OCR coordination in NLP formulation (continuous)

Reference	Objective	Constraints	Solver	Test case	Significant finding and extra detail
D. Saha et al.,2015	- The total operating time of primary and backup relays when fault take place.	- The coordination constraints. - limit boundary of TMS and PS. -The minimum operating time.	- The SOS	- IEEE 6-bus power system. -WSCC 9-bus test system.	- Using NAOCR. - Found that satisfactory results in all the cases and the obtained results prove that the SOS algorithm is more effective than PSO TLBO.
M. Kheshti et al.,2016	- The total operating time of all relays when fault take place.	- The coordination constraints. - limit boundary of TMS and PS. -The minimum operating time.	-The PSO	- IEEE 15 node distribution system.	- Using NAOCR. - Found that satisfactory results in all the cases.
S. V. Chakor et al.,2016	- The total operating time of primary relay for a near-end fault.	- The coordination constraints. - limit boundary of TMS and PS. -The minimum operating time.	- The GA	- The single-end three-bus multi-loop system with interconnected DG.	- Using AOCR. - Found that satisfactory results in all the cases.
M. Pujiantara et al.,2016	- The total operating time of all relay when fault take place.	- The coordination constraints. - limit boundary of TMS and PS. -The minimum operating time.	-The GA	- The five-bus radial network with DG.	- Using AOCR. - Found that satisfactory results in all the cases and the proposed algorithm's TMS and PS values are lower than trial and error technique.

Table 2.3 The related research on OCR coordination in NLP formulation (continuous)

Reference	Objective	Constraints	Solver	Test case	Significant finding and extra detail
P. P. Bedekar et al.,2016	- The total operating time of all relays when fault take place.	- The coordination constraints. - limit boundary of TMS and PS. -The minimum operating time.	- The MJA	-The two-bus radial system. - The single-end three-bus multi-loop system.	- Using NAOCR. - Found that satisfactory results in all the cases and the proposed algorithms have been proven to outperform the GA.
P. N. Korde et al.,2016	- The total operating time of all relays when fault take place.	- The coordination constraints. - limit boundary of TMS and PS. -The minimum operating time.	-The NLP	- Two bus system with parallel feeders. -Three bus multi-loop distribution system.	- Using NAOCR. - Considering different curve type. - Found that satisfactory results in all the cases and the proposed algorithms have been proven to outperform the GA.
S. U. Pathade et al.,2017	- The total operating time of primary relay for a near-end fault.	- The coordination constraints. - limit boundary of TMS and PS. -The minimum operating time.	- The GA	- The nine- bus loop distribution system.	- Using NAOCR. - Found that satisfactory results in all the cases.
P. Bhatiya et al.,2017.	- The total operating time of all relays when fault take place.	- The coordination constraints. - limit boundary of TMS and PS. -The minimum operating time.	-The GA-NLP	- The nine- bus loop distribution system.	- Using AOCR. - Found that satisfactory results in all the cases and the proposed algorithm have been proven to outperform the GA.

Table 2.3 The related research on OCR coordination in NLP formulation (continuous)

Reference	Objective	Constraints	Solver	Test case	Significant finding and extra detail
A. I. Atteya et al.,2017	- The total operating time of all relays when fault take place.	- The coordination constraints. - limit boundary of TMS and PS. -The minimum operating time.	- The MPSO	- The IEEE 14 bus test system.	- Using AOCR. - Considering various system condition. - Found that satisfactory results in all the cases.
A. Tjahjono et al.,2017	- The total operating time of all relays when fault take place.	- The coordination constraints. - limit boundary of TMS and PS. -The minimum operating time.	-The AMFA	- The five-bus radial system with several DER.	- Using AOCR. - Considering various system condition. - Found that the proposed algorithm is superior to the standard approach, FA, MFA, and PSO.
A. Y. Hatata et al.,2018	- The total operating time of primary relay for a near-end fault and for far-end fault.	- The coordination constraints for near end and far end faults, limit boundary of TMS and PS, the minimum operating time, the transient stability.	- The ALO and AIS	- The IEEE 30-bus distribution section - The 11-Bus distribution system with DG.	- Using AOCR. - Considering the transient stability. - Considering penetration level of DG. - Found that ALO is effectiveness to provide the lowest operating time than PSO, AIS, DE, and GA.
T. Khurshaid et al.,2018	- The total operating time of all relays when fault take place.	- The coordination constraints. - limit boundary of TMS and PS. -The minimum operating time.	-The MSA	- The eight-bus loop multi gen system.	- Using NAOCR. - Considering PS is step/discreate value. - Found that the proposed algorithm outperforms LP, NLP, GA, GA-LP, and SOA.

Table 2.3 The related research on OCR coordination in NLP formulation (continuous)

Reference	Objective	Constraints	Solver	Test case	Significant finding and extra detail
T. Khurshaid et al.,2019	- The total operating time of primary relay for primary zone fault.	- The coordination constraints. - limit boundary of TMS and PS. -The minimum operating time.	- The HWOA	-IEEE 3-bus 8-bus, 9-bus, 15-bus, and 30-bus loop multi-generator test systems,	- Using NAOCR. - Considering PS is step/discreate value. - Found that the results obtained with HWOA are superior to achieved with a native WOA and well-known current algorithms.
M. N. Alam.,2019	- The total operating time of primary relay when fault take place.	- The coordination constraints. - limit boundary of TMS, PS, and CS. -The minimum operating time.	-The GA	- The 7-bus loop system with DER. - The 18-bus loop system with DER.	- Using AOCR. - Considering various system condition. - Found that the proposed algorithm has effectiveness and suitability to satisfactory results in all the cases and the optimum settings obtained using GA are better than PSO and DE for both the test systems
E. Sorrentino and J. V. Rodríguez.,2020	- The total operating time of relay for faults very near to this relay.	- The coordination constraints. - limit boundary of TMS and CS. -The minimum operating time.	- The MILP	- The IEEE 3-bus, 6-bus, and 9-bus loop multi-gen system.	- Using NAOCR. - Found that all extremely inverse types provided the best solution of all curve types, but the mixed-curve type obtained a better solution than all extremely inverse types.
S. D. Saldarriaga-Zuluaga et al.,2020.	- The total operating time of primary relay when fault take place.	- The coordination constraints. - limit boundary of TMS and CS. - limit boundary of PSM. -The minimum operating time.	-The GA	-The benchmark IEC micro-grid with DER.	- Using AOCR. - Considering various system condition. - Integrate IEEE and IEC curve type on the selection of CS.

2.5 Theories Background

The theories background of this research includes three subsections, power flow calculation with DG, short circuit analysis with DG, and OCR theories on mathematical formulation, respectively. The theories background of this research is illustrated as follows.

2.5.1 Power Flow Calculation with DG

The Newton-Raphson Power Flow (NRPF) technique is used to find the power flow solution of the system such as bus voltage, angle of bus voltage, the line flow current and etc. The DG is formulated as a PQ bus to inject an active power (P_{DG}) and reactive power (Q_{DG}) to the bus (Nick Jenkins, 2000). as shown in Figure 2.10.

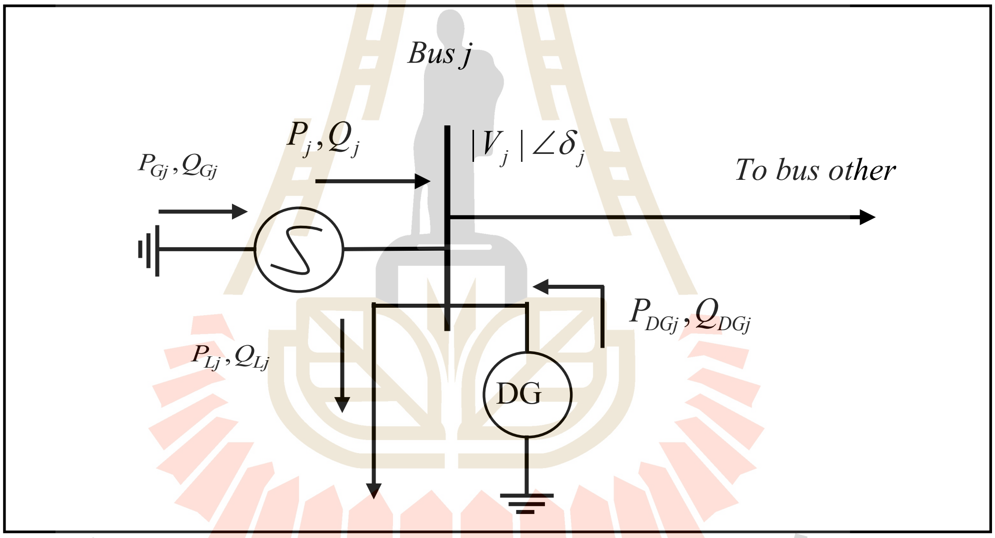

Figure 2.10 The NRPF calculation with DG

Therefore, the formulation DG in NRPF and the line flow current from bus j to k of the system for setting PS of each AOCR to detected line overload and line short circuit are computed as below,

$$P_j + P_{DGj} = \sum_{k=1}^{NB} |V_j||V_k||y_{jk}|\cos(\theta_{jk} - \delta_{jk}),\ \ P_j = P_{Gj} - P_{Lj},\ \ j = 1,\ldots,NB\ , \tag{2.1}$$

$$Q_j + Q_{DGj} = -\sum_{k=1}^{NB} |V_j||V_k||y_{jk}|\sin(\theta_{jk} - \delta_{jk}),\ \ Q_j = Q_{Gj} - Q_{Lj},\ \ j = 1,\ldots,NB\ , \tag{2.2}$$

$$I_{jk} = y_{jk}(V_j - V_k) + y_{j0}V_j\ \ ,\ j = 1,\ldots,NB,\ k = 1,\ldots,NB\ . \tag{2.3}$$

Where, P_j is the total active power injected at bus j, PG_j is the active power of generator at bus j, P_{Lj} is the total active power of load at bus j, P_{DGj} is the active power of DG at bus j, Q_j is the reactive power injected at bus j, Q_{Gj} is the reactive power of generator at bus j, Q_{Lj} is the reactive power of generator at bus j, Q_{DGj} is the reactive power of DG at bus j, NB is total number of bus of system, $|V_j|$ is the voltage at bus j, $|V_k|$ is the voltage at bus k, θ_{jk} is the angle of the y_{jk} element of bus admittance matrix (Ybus) , δ_{jk} is the voltage angle difference between bus j and k. the model for line flow current shown in Figure 2.11.

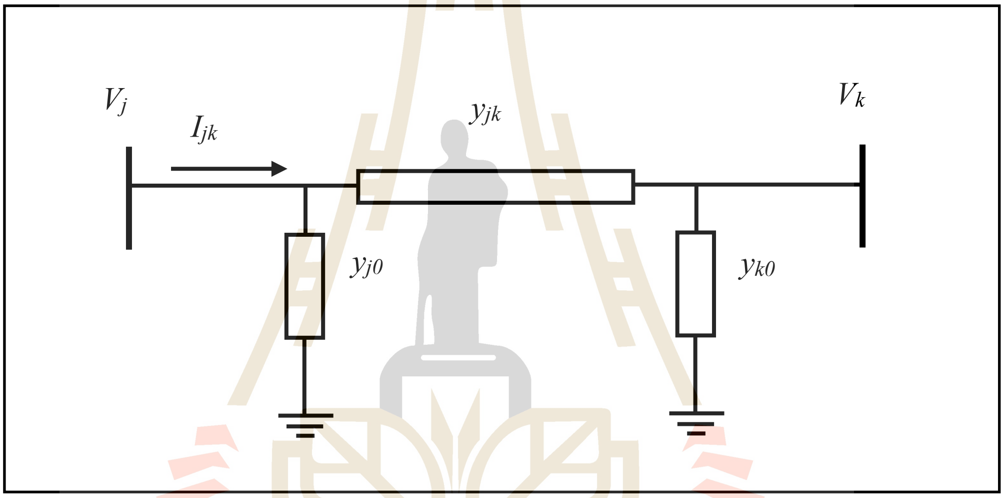

Figure 2.11 The line flow current calculation

2.5.2 Short Circuit Analysis with DG

In the duration of the short circuit, DG can be formulated as a Thevenin's equivalent circuit as voltage source and series impedance joined to the bus. Thus, Ybus of system has updated by including the admittance of DG (y_{DGi}) and admittance of another generator (y_{Gi}) in the system. In this research, only steady-state faults are considered for AOCR setting. Therefore, a series impedance of DG is steady-state synchronous reactance (X_d). Then, the bus voltage during fault and fault flow current (line flow current during fault) can be calculated by using the symmetrical component and bus impedance matrix (Nick Jenkins, 2000), (Saadat, 1999). The included admittance of DG calculation in short circuit analysis, the bus voltage during fault, and fault flow current in short circuit analysis can be expressed as,

$$Y_{ii}^{new} = Y_{ii}^{old} + y_{DGi} \ , \ for\ i \in \ bus\ connected\ with\ DG, \tag{2.4}$$

$$Vf_i^0 = 0 - Z_{ik}^0 If_k^0 \ , \tag{2.5}$$

$$Vf_i^1 = Vp_i^1 - Z_{ik}^1 If_k^1 \ , \tag{2.6}$$

$$Vf_i^2 = 0 - Z_{ik}^2 If_k^2 \ , \tag{2.7}$$

$$I_{ij}^0 = \frac{Vf_i^0 - Vf_j^0}{z_{ij}^0} \ , \tag{2.8}$$

$$I_{ij}^1 = \frac{Vf_i^1 - Vf_j^1}{z_{ij}^1} \ , \tag{2.9}$$

$$I_{ij}^2 = \frac{Vf_i^2 - Vf_j^2}{z_{ij}^2} \ , \tag{2.10}$$

$$V_i^{abc} = \mathrm{A} V_i^{012} \ , \tag{2.11}$$

$$I_{ij}^{abc} = \mathrm{A} I_{ij}^{012} \ . \tag{2.12}$$

Where,

Y_{ii}^{new} is the new diagonal element of Y_{bus} of the system for short circuit analysis,

Y_{ii}^{old} is the original diagonal element of Y_{bus} of the system for NRPF,

y_{DGi} is admittance of DG number *i*,

Vf_i^0 is the zero-sequence component (ZSC) of bus voltage during fault at bus *i*,

Vf_i^1 is the positive-sequence component (PSC) of bus voltage during fault at bus *i*,

Vf_i^2 is the negative-sequence component (NSC) of bus voltage during fault at bus *i*,

Vp_i^1 is pre-fault voltage at bus *i*,

If_k^0, is the ZSC of short circuit level at bus *k*,

If_k^1 is the PSC of short circuit level at bus *k*,

If_k^2 is the NSC of short circuit level at bus *k*,

Z_{ik}^0 is the ZSC of Z_{bus} matrix in row *i* and columns *k*,

Z_{ik}^{1} is the PSC of Z_{bus} matrix in row *i* and columns *k*,

Z_{ik}^{2} is the NSC of Z_{bus} matrix in row *i* and columns *k*,

I_{ij}^{0} is the ZSC of fault flow current from bus *i* to bus *j*,

I_{ij}^{1} is the PSC of fault flow current from bus *i* to bus *j*,

I_{ij}^{2} is the NSC of fault flow current from bus *i* to bus *j*,

z_{ij}^{0} is the ZSC of the actual line impedance from bus *i* to *j*,

z_{ij}^{1} is the PSC of the actual line impedance from bus *i* to *j*,

z_{ij}^{2} is the NSC of the actual line impedance from bus *i* to *j*,

A is the A-operator matrix,

V_{i}^{abc} is the phase voltage during fault of bus *i*,

I_{ij}^{abc} is the phase fault current in line *i* to *j*.

2.6 Coordination of OCR's Formulation

The OCR coordination problem is always formulated as an optimization formulation with the objective function and set of constraints. Nowadays, the formulation of the OCR coordination problem is expressed as follows.

2.6.1 Objective Function

The objective function *(OF)* of this problem is to minimize the total operating time of all the AOCRs present in the system (Elmer Sorrentino, 2020). The function is to be minimized so that each relay operates in minimum time and the reliability of the system is maintained by the constraints. The objective function can be expressed as,

$$OF = Minimize \sum_{k=1}^{NF} \sum_{j=1}^{NR} t_{j,k} \, , \tag{2.13}$$

where, $t_{j,k}$ is the operating time of relay *j* when fault at *k* has occurred, *NF* is a number of faults can occur in the system in the system, *NR* is a number of all required relays when fault at *k* occurs.

2.6.2 OCR Characteristics

The standard OCR with inverse time-current characteristic can be categorized into two well-known standard characteristic curves, which are the IEC and IEEE standards. The OCR operating time characteristic depends on short circuit current and setting parameters. The short circuit current flow magnitude and direction are uncontrollable and depend on network topologies and system operating conditions. Meanwhile, the setting parameters are *TMS*, *PS*, and *CS* of each AOCR, which can be considered as decision variables in these problems. The standard characteristics of AOCR in general form can be expressed as follows,

$$t_{j,k} = \frac{A_{csj} TMS_j}{\left(PSM_{jk}\right)^{B_{csj}} - 1} + E_{csj}, \tag{2.14}$$

$$PSM_{jk} = \frac{I_{jk}}{\left(PS_j CTR_j\right)}, \tag{2.15}$$

where, TMS_j is the time multiplier setting of relays j, PSM_j is the plug setting multiplier of relay j, it can be calculated from Eq 2.15. where, I_{jk} is the short-circuit current flowing through relay j when fault at k is occurred (A), PS_j is the pickup setting of relay j (A), CTR_j is the CT ratio of relay j, A_{csj}, B_{csj}, and E_{csj} are the OCR characteristics.

2.6.3 Boundary of Setting Parameters

AOCR is the multiple setting group microprocessor-based OCR. The setting parameters of each OCR is *TMS*, *PS*, and *CS*. Hence, it can define as decision variables (Saldarriaga-Zuluaga, 2020). The limit of variables can be express as,

$$TMS_j^{\min} \le TMS_j \le TMS_j^{\max}, \ j = 1,\ldots,NR \ , \tag{2.16}$$

$$PS_j^{\min} \le PS_j \le PS_j^{\max}, \ j = 1,\ldots,NR \ , \tag{2.17}$$

$$CS_j^{\min} \le CS_j \le CS_j^{\max}, \ j = 1,\ldots,NR \ , \tag{2.18}$$

where, TMS_j^{max} is the maximum time multiplier of relay j, TMS_j^{min} is the minimum time multiplier of relay j, PS_j^{max} is the maximum pickup setting of relays j (A), PS_j^{min} is the minimum pickup setting of relay *j* (A), CS_j^{max} is the maximum characteristic curve type of relays *j*, CS_j^{min} is the minimum characteristic curve type of relays *j*.

2.6.4 The Operating Time Constraints

In theory, the OCR closest to the fault and must respond to the fault as fast as possible. Nevertheless, the operating time of the OCR, in practice, has a minimum limit, to avoid unnecessary tripping. The minimum operating time of the OCR must be greater than the duration time of the temporary fault and abnormal but un-fault condition. Meanwhile, the OCR's maximum operating time is crucial to maintain the system stability. The operating time constraint of each OCR can be expressed as,

$$t_{j,k}^{max} \geq t_{j,k} \geq t_{j,k}^{min}, \; j = 1,\ldots,NR \;, \tag{2.19}$$

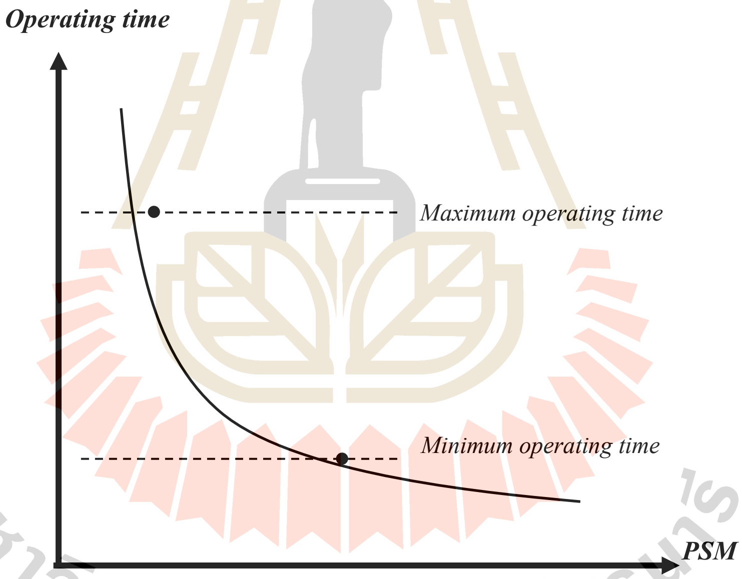

Figure 2.12 The operating time constraint

where, $t_{j,k}^{min}$ is the minimum operating of each relay *j* when fault k occurs, $t_{j,k}^{max}$ is the maximum operating of each relay *j* when fault *k* occurs as shown in Figure 2.12

2.6.5 Coordination Constraints

A primary relay that is located closest to the fault and must respond as rapidly as feasible to the fault. Backup relays are devices that are activated within a certain amount of time after the main relay fails to break the fault in order to achieve a reliable protection system. the relation between primary and backup relay can be expressed as,

$$t_{b,k} - t_{p,k} \geq CTI,\ k = 1,\ldots,NF\ , \tag{2.20}$$

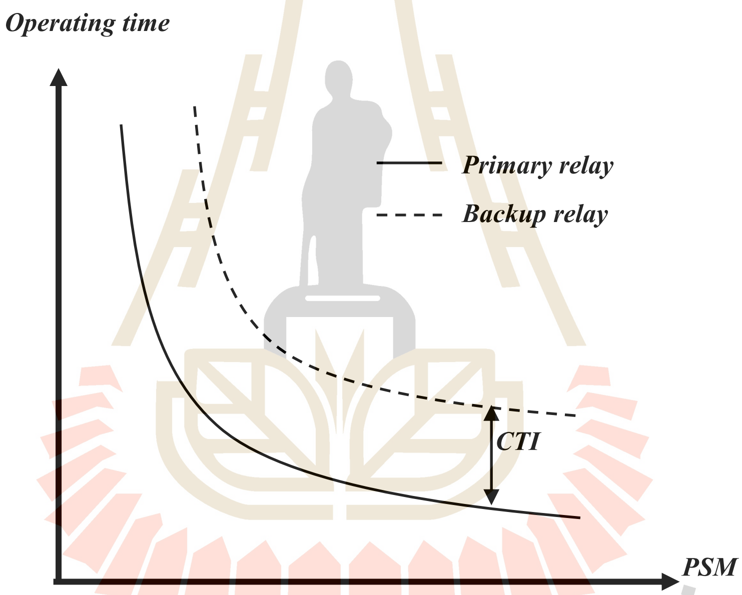

Figure 2.13 The coordination of OCR

where, $t_{b,k}$ is the operation time of the backup relay b when fault k occurs, and $t_{p,k}$ is the operation time of the primary relay p, for the same fault, *CTI* is the coordination time interval as shown in Figure 2.13.

2.6.6 Plug Setting Multiplier Constraints

In practice, the plug setting multiplier of industrial AOCRs has inverse definite minimum time (IDMT) characteristic. The limit of *PSM* depends on the sizing of current transformer, short circuit level, and the technology of industrial AOCRs, the plug setting multiplier constraint can be express as Eq. 2.21 and can be seen in Figure 2.14,

$$PSM_j^{\min} \le PSM_j \le PSM_j^{\max},\ j = 1,\ldots,NR\ , \tag{2.21}$$

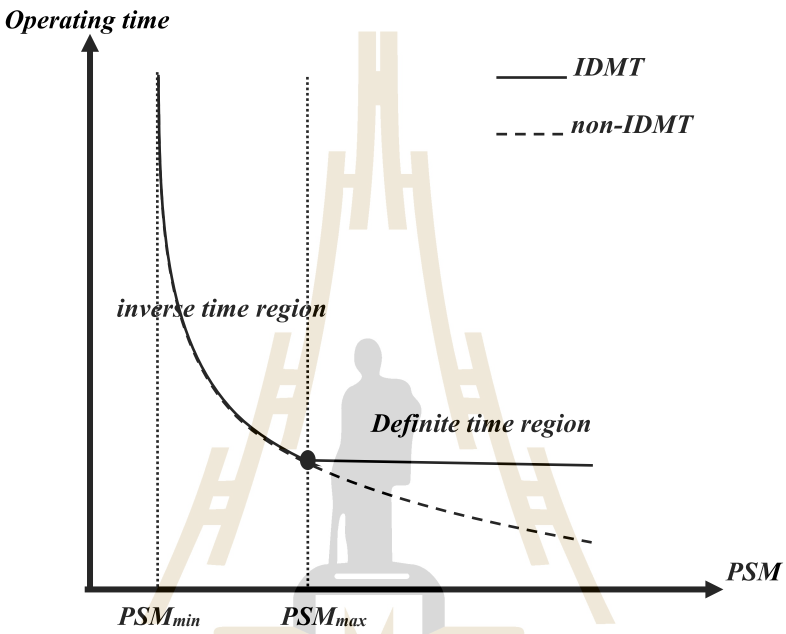

Figure 2.14 The plug setting multiplier limit

where, PSM_j^{max} is the maximum plug setting multiplier of relay *j*, PSM_j^{min} is the minimum plug setting multiplier of relay *j*.

2.6.7 The Characteristic Curve Setting

The operating time characteristics of OCRs, can be expressed by the constant parameters *A*, *B*, and *E*. Consequently, the operating time of the OCR will be different if it has a different *CS* at the same *PSM*. Hence, the operating time of each OCR might be decreased at the optimal characteristic curve selection. Moreover, a modern microprocessor OCR can be set in accordance to both IEC and IEEE standard characteristic curves. Thus, the *CS* of OCRs can be defined in mathematic form as an integer decision variable as shown in Eq 2.22. Figures 2.15 show the operating time of OCR in the different standards curve, and Table 2.4 shown the constant values of standard relay characteristic curve settings.

$$CS_j \in \{1,2,3,\ldots,11\},\ j = 1,\ldots,NR. \tag{2.22}$$

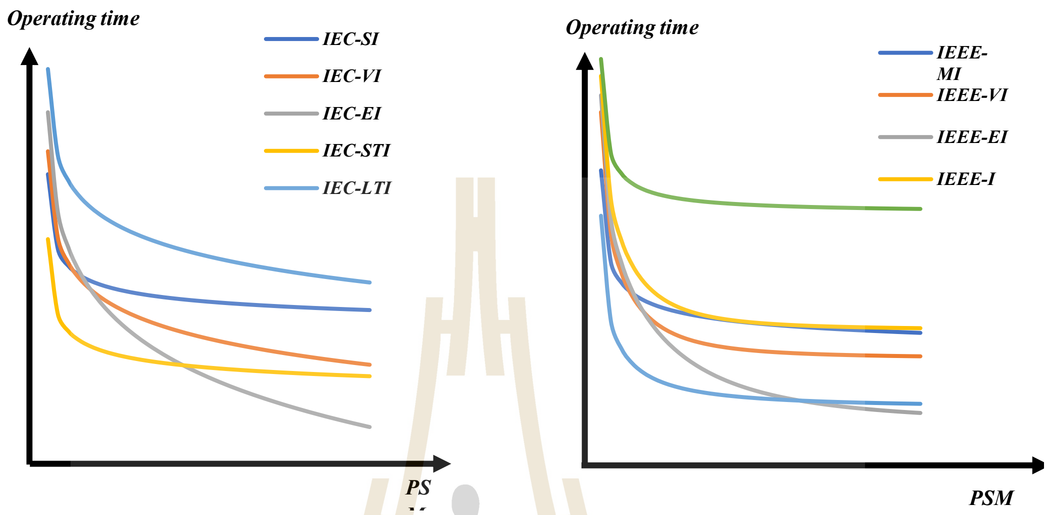

(a) IEC characteristic curve (b) IEEE characteristic curve

Figure 2.15 The standard characteristic curve

Table 2.4 The standard OCR characteristic curves setting

Characteristic curves type	CS_j	A_{csj}	B_{csj}	E_{csj}
Standard inverse (IEC SI)	1	0.14	0.02	0
Very inverse (IEC VI)	2	13.5	1	0
Extremely inverse (IEC EI)	3	80	2	0
Longtime inverse (IEC LTI)	4	120	1	0
Shot time inverse (IEC STI)	5	0.05	0.04	0
Moderately inverse (IEEE MI)	6	0.0515	0.02	0.114
Very inverse (IEEE VI)	7	19.61	2	0.4910
Extremely inverse (IEEE EI)	8	28.2	2	0.1217
Inverse (IEEE I)	9	44.6705	2.0938	0.8983
Shot inverse (IEEE-STI)	10	1.3315	1.2969	0.16965
Long inverse (IEEE LTI)	11	28.0715	1	10.9296

2.6.8 The Characteristic of Fuse and Recloser

Fuses also have such an inverse-time overcurrent characteristic. The minimum melting (MM) and total clearing times (TC) for fuses are usually expressed by the straight-line log–log plot. To be used in the protection setting, the fuse characteristic on the log–log curve is better to be mathematically approximated by the second-order polynomial function. However, the interested range of the curve approaches a straight line. Moreover, a linear equation can substantially simplify the calculation task. Consequently, the general equation describing the fuse characteristic curve can be expressed as in Eq 2.23.

$$\log(t_{j,k}^{fuse}) = F\log(I_{j,k}) + G \tag{2.23}$$

where, $t_{j,k}^{fuse}$ is the operating time of fuse j when fault k occurred, F and G is the fuse coefficients are calculated from curve fitting.

Recloser has an inverse current-time characteristic as the same as OCR characteristic. Typically, traditional reclosers use IEEE-EI characteristic curve for their overcurrent element to provide good coordination with fuses. The operating time of recloser with extremely inverse time-current characteristic can be expressed as Eq. 2.4-2.5 substitute CS_j=9.

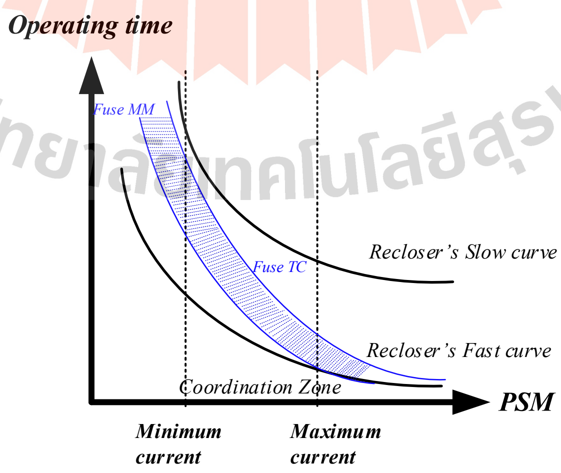

Figure 2.16 Fuse recloser coordination curve

The principle of recloser–fuse coordination is extended in this section. When a fault occurs at the lateral feeder, the recloser in fast mode should operate first to discriminate for temporary faults. If the fault still exists, the lateral fuse will blow up and cause a permanent electricity interruption. However, if the fuse fails to operate in this stage, the recloser in slow mode can act as backup protection later as shown in Figure 2.16. In this paper, the operating time of fuse was considered only TC curve (MM curve is neglected). The coordination between fuse -recloser are expressed as follow,

$$t_{j,k}^{fuse} - t_{j,k}^{Recfast} \geq CTI,\ k = 1,\ldots,NF\ , \tag{2.24}$$

$$t_{j,k}^{Recslow} - t_{j,k}^{fuse} \geq CTI,\ k = 1,\ldots,NF\ , \tag{2.25}$$

where, $t_{j,k}^{Recfast}$ is the operating time of recloser's fast curve *j* when fault *k* occurred and $t_{j,k}^{Recslow}$ is the operating time of recloser's slow curve *j* when fault *k* occurred.

CHAPTER 3

A COMPARATIVE STUDY ON OCR COORDIINATION[1]

3.1 Chapter Overview

This chapter is categorized into two sections. In section 3.2, A comparative study on scheme type of OCR proposes an advantage of AOCR over the NAOCR coordination scheme. In section 3.3, compare several OCR coordination formulation types, and compare optimal results of the OFSS with other partial scheme, that can effectively decrease total operating time

3.2 The Advantage of AOCR Coordination Scheme

In the NAOCR scheme or Traditional scheme, the relay will be set a setting parameter only once a time for all the system operating conditions and must be set to cover all of the fault cases that can occur in the system. In the AOCR scheme, the relay can be set a setting parameter multiple times depending on the system operating conditions. So, a setting parameter can be predetermined appropriately in each case.

3.2.1 Problem Formulation

To avert complexity and simplify the problem, this section formulated as a LP by predetermined *PS* based on minimum fault current flowing through relay and characteristic curve setting is used IEC-SI for all relay. In this case study, LPP technique is adapted to find optimal *TMS* only. The objective function will be minimized subjected to limit boundary of *TMS*, the coordination constraint, and the minimum operating time constraint.

---

[1]*Part of this chapter was presented at the 43rd electrical engineering conference (EECON-43), 2020*

The formulation of this problem is,

Minimize: Eq. 2.13

Subjected to: Eq. 2.16, Eq. 2.19, Eq. 2.20

Decision variable: *TMS*.

In this section, a decision variable is *TMS* of each relay, limit boundary of *TMS* is used within range 0.1-1, the minimum operating time is used 0.1 sec., and the *CTI* is used 0.3 sec. The *CTR* is 1.

3.2.2 Study Cases

A single source four bus radial system with the presence of DG at bus 1. In order to prevent faults in all areas of the system, use five OCR (R_{Gr}, R_{DG}, R_1, R_2 and R_3) installed at the upstream of each transmission line.

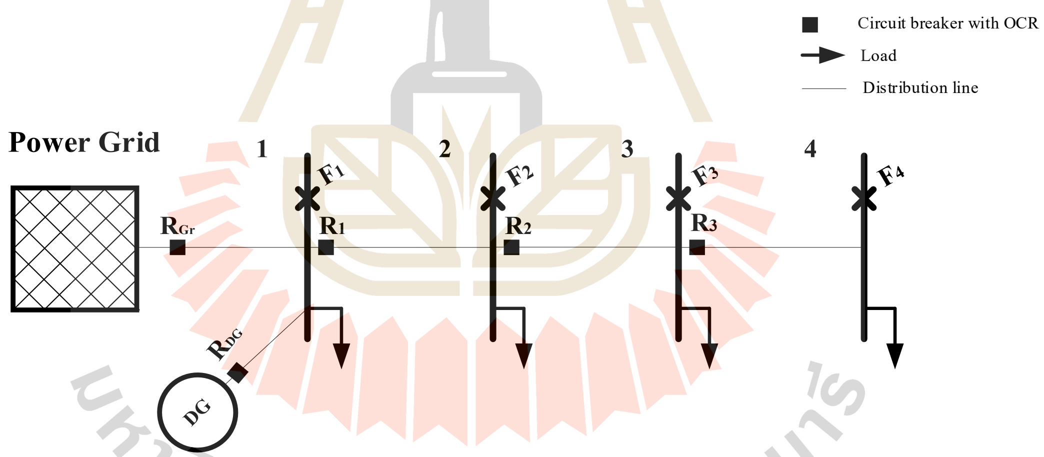

Figure 3.1 The modified four bus radial distribution system

The operating condition of the test system is categorized into; Case I: Grid connected without DG, Case II: Grid connected with DG, Case III: Islanding mode with DG. As shown in Figure 3.1. The fault is occurred at each bus and fault current is found by relay. Table 3.1, 3.2, and 3.3 gives the fault current seen by each relay for all case. The *PS* setting of each relay show in Table 3.4, The primary-backup coordination scheme is shown in Table 3.5. The optimal results shown in Table 3.6.

Table 3.1 Fault current of case I

Fault Point	Fault Current (A)	R_{Gr}	R_{DG}	R_1	R_2	R_3
Bus1	Max	2624.3	-	-	-	-
	Min	2272.7	-	-	-	-
Bus2	Max	1290.8	-	1290.8	-	-
	Min	1117.9	-	1117.9	-	-
Bus3	Max	855.9	-	855.9	855.9	-
	Min	741.2	-	741.2	741.2	-
Bus4	Max	640.2	-	640.2	640.2	640.2
	Min	554.4	-	554.4	554.4	554.4

Table 3.2 Fault current of case II

Fault Point	Fault Current (A)	R_{Gr}	R_{DG}	R_1	R_2	R_3
Bus1	Max	2624.3	2186.9	-	-	-
	Min	2272.7	1893.9	-	-	-
Bus2	Max	906.8	755.7	1662.5	-	-
	Min	785.3	654.4	1439.8	-	-
Bus3	Max	548.1	456.8	1004.9	1004.9	-
	Min	474.6	395.6	870.2	870.2	-
Bus4	Max	392.7	327.3	720.0	720.0	720.0
	Min	340.1	283.4	623.5	623.5	623.5

From the simulation results, the DG penetration at bus 1 when considering the system operation (Cases I-III). However, the short circuit current of the three cases will flow in the same direction as shown in Figure 3.1. The primary and backup relay assignments for coordination are still similar in all three cases as shown in Table 3.5. In case II, the level of short circuit current is significantly increased. but still, it is possible to use a

NAOCR coordination scheme and find the optimal TMS to decrease the total relay operating time as in the Table 3.5.

Table 3.3 Fault current of case III

Fault Point	Fault Current (A)	R_{Gr}	R_{DG}	R_1	R_2	R_3
Bus1	Max	-	2186.9	-	-	-
	Min	-	1893.9	-	-	-
Bus2	Max	-	1175.2	1175.2	-	-
	Min	-	1017.8	1017.8	-	-
Bus3	Max	-	803.5	803.5	803.5	-
	Min	-	695.8	695.8	695.8	-
Bus4	Max	-	610.4	610.4	610.4	610.4
	Min	-	528.6	528.6	528.6	528.6

Table 3.4 The PS of each relay

Relay	*PS* (A)			
	NAOCR	AOCR		
	All Case	Case I	Case II	Case III
R_{Gr}	261.76	372.63	261.76	-
R_{DG}	218.13	-	218.13	339.26
R_1	231.93	247.06	290.06	231.93
R_2	176.20	184.8	207.83	176.2
R_3	176.20	184.8	207.83	176.2

Table 3.5 Primary and backup scheme

Fault Point	NAOCR		AOCR					
	All Case		Case I		Case II		Case III	
	Primary	Backup	Primary	Backup	Primary	Backup	Primary	Backup
Bus1	R_{Gr},R_{DG}	-	R_{Gr}	-	R_{Gr},R_{DG}	-	R_{DG}	-
Bus2	R_1	R_{Gr},R_{DG}	R_1	R_{Gr}	R_1	R_{Gr},R_{DG}	R_1	R_{DG}
Bus3	R_2	R_1	R_2	R_1	R_2	R_1	R_2	R_1
Bus4	R_3	R_2	R_3	R_2	R_3	R_2	R_3	R_2

From Table 3.5 can be seen that the NAOCR setting scheme there will be only one optimal *TMS* scenario which is used to protect all of the system operations. However, comparing to the AOCR setting scheme, it can be seen that the optimal *TMS* is appropriate for each system operation. Resulting in the total relay operating time of the system is significantly reduced, as shown in the Table 3.6. The reduction of fault clearing time is leading to system reliability enhancement.

Table 3.6 Optimal results

	Case I		Case II		Case III	
	NAOCR	AOCR	NAOCR	AOCR	NAOCR	AOCR
TMS_{Gr}	0.2544	0.1874	0.2544	0.1777	0.2544	-
TMS_{DG}	0.2802	-	0.2802	0.1777	0.2802	0.1909
TMS_1	0.1991	0.1783	0.1991	0.1749	0.1991	0.1796
TMS_2	0.1612	0.1539	0.1612	0.1539	0.1612	0.1539
TMS_3	0.1	0.1	0.1	0.1	0.1	0.1
OF (sec.)	2.791	2.6501	3.4068	2.9726	2.9652	2.722

3.3 A Comparative Study on AOCR Optimization Problem Types

This chapter describes, discusses, and compares the advantages and disadvantages of several types of AOCR coordination problem formulations of previous research. by comparing the simulation results generated by the authors. and describes the simulation results of the proposed technique.

3.3.1 Non-linear Optimization Problem

As a matter of realized, the *PS* can be a decision variable of AOCR coordination problem with in limit boundary of the maximum load current flowing through relay and the minimum fault current flowing through relay. But the *CS* setting still used IEC-SI for all relays in this study. The objective function of the problem is the total operating time of all the relays present in the system. The function is to be minimized so that each relay operates in minimum time and the reliability of the system is maintained by coordination constraints. The PSO was used to handle this problem. Then, the optimal result was compared with the LP approach in section 3.2. The formulation of this problem is,

Minimize: Eq. 2.13

Subjected to: Eq. 2.16, Eq. 2.17, Eq. 2.19, Eq. 2.20

Decision variable: *TMS*, *PS*.

In this section, a decision variable is *TMS* and *PS* of each relay, limit boundary of *TMS* is used within range 0.1-1, limit boundary of *PS* within range of PS^{max} and PS^{min} as shown in Table 3.7, the minimum operating time is used 0.1 sec., and the *CTI* is used 0.3 sec. The *CTR* is 1. Then, the optimal result was compared with the LP in section 3.2 for the same study case.

Table 3.7 The optimal results of Case I with NLP approach

	LP approach		LP approach		NLP approach	
	TMS	PS^{max}	*TMS*	PS^{min}	*TMS*	*PS*
R_{Gr}	0.1874	372.63	0.3450	114.21	0.1539	372.61
R_{DG}	-	-	-	-	-	-
R_1	0.1783	247.06	0.2791	76.4891	0.1352	242.12
R_2	0.1539	184.8	0.2241	38.35	0.1	178.72
R_3	0.1	184.8	0.1	38.35	0.1	38.35
OF (sec.)	2.6501		2.1500		1.7788	

Table 3.8 The optimal results of Case II with NLP approach

	LP approach		LP approach		NLP approach	
	TMS	PS^{max}	*TMS*	*TMS*	PS^{max}	*TMS*
R_{Gr}	0.1777	261.76	0.2858	114.21	0.1483	261.71
R_{DG}	0.1777	218.13	0.4197	37.12	0.3662	37.12
R_1	0.1749	290.06	0.2929	76.49	0.1333	290.07
R_2	0.1539	207.83	0.2294	38.35	0.1288	135.85
R_3	0.1	207.83	0.1	38.35	0.1	38.35
OF (sec.)	2.9726		2.6635		2.2422	

The scenario-based optimal OCR coordination is seen in Table 3.7, 3.8 and 3.9. The PSO technique was compared an effectiveness with other technique shown in Table 3.10.

Table 3.9 The optimal results of Case III with NLP approach

	LP approach		LP approach		NLP approach	
	TMS	PS^{max}	*TMS*	PS^{min}	*TMS*	PS^{max}
R_{Gr}	-	-	-	-	-	-
R_{DG}	0.1909	339.25	0.3450	114.21	0.1565	338.99
R_1	0.1796	231.94	0.2791	76.4891	0.1343	231.94
R_2	0.1539	176.21	0.2241	38.35	0.1	172.14
R_3	0.1	176.21	0.1	38.35	0.1	38.35
OF (sec.)	2.722		2.1939		1.8401	

From the simulation results, the LP approach with PS^{min} provided a better solution than the LP approach with PS^{max}. But for all approaches, the optimal results of the NLP approach offered the best optimal solution for all cases of the test system. However, the NLP approach was solved in the PSO algorithm only. Therefore, we resolve that problem with several stochastic search algorithms such as GA, pattern search (PTS), SA, and surrogate optimization (SRG) to verify the optimal results and find better solutions more than the PSO algorithm. The comparative study of various techniques is addressed in Table 3.10 and the discussion on the advantage of each algorithm can be seen as follow. From Table 4.5, the strength of PTS is offered the closely optimal results of each trial. but the converge rate is just 73.34 percent. Then, the *OF* best of SA is greater than PTS and confirms converge rate of all trials. However, it has weakness is the high standard deviation *(STD)* and the *OF* average. The biggest problem of both techniques is requirement the populations of starting point. Consequently, the later three techniques do not require the starting point of populations. The SRG technique provided the worst solution of all techniques decided from the worst value of *OF best*, *OF average*, highly *STD*, and high Range. While, the GA technique offered the *OF best*, *OF average*, and *STD* greater than the SRG technique and the most advantage of the GA technique is provided the lowest STD of all techniques. Meanwhile, PSO has obtained the best solution of all techniques decided from given the best optimal answers (1.7751 sec.), the best *OF average* (1.8537 sec.), low *STD* (0.0775), and confirm converge rate of all trials. From Table 3.10, we can see that PSO algorithm is the most powerful technique for the OCR coordination problem, and the next are GA, SA, PTS and SRG, respectively.

Table 3.10 The NLP approach with various optimization techniques

	PTS		SA		SRG		GA		PSO	
	TMS	*PS*	*TMS*	*PS*	*TMS*	*PS*	*TMS*	*PS*	*TMS*	*PS*
R_{Gr}	0.345	114.2	0.196	328.1	0.356	247.5	0.328	114.2	0.153	372.6
R_{DG}	-	-	-	-	-	-	-	-	-	-
R_1	0.2791	76.49	0.2432	93.45	0.3753	95.96	0.1958	149.90	0.1330	247.07
R_2	0.2241	38.35	0.1021	177.99	0.1	183.81	0.1613	83.09	0.1	178.76
R_3	0.1	38.35	0.1	42.56	0.1	39.04	0.1	38.35	0.1	38.35
*OF (best) **	2.1501		1.9777		2.7064		2.0427		1.7751	
*OF (avg.) **	2.1501		2.4235		3.9914		2.1071		1.8537	
*STD**	0.00		0.2822		0.8023		0.0326		0.0775	
*Range**	0.00		1.0717		3.6401		0.1046		0.2423	
*Converge rate (%) **	73.34		100		100		100		100	

**The 30-trial test raw data are provided in https://drive.google.com/drive/folders/1ilbjHjng2TQb2Mw3t21qsxHfWte7Pn7c?usp=shari*

3.3.2 Mixed Integer Linear Optimization Problem

In this topic, we predetermined the *PS* and vary *CS* of each relay for standard inverse, very inverse types, extremely inverse types, and long-time inverse types for all relay and use LPP technique to find the optimal *TMS* of each OCR, to studies the effect of various curve types on the operating time of the OCR. The characteristic of various curve on operating time of OCR are shown in Figure 3.2. Therefore, we predetermined *PS* and the *CS* of OCR as decision variables, instead of fixing a single type of curve for all relays. The problem become the mixed-integer linear problem (MILP) to find the optimal TMS with mixed *CS* of OCR. The formulation of this problem is,

Minimize: Eq. 2.13

Subjected to: Eq. 2.16, Eq. 2.18, Eq. 2.19, Eq. 2.20, Eq. 2.22,

Decision variable: *TMS*, *CS*.

In this section, a decision variable is *TMS* and *CS* of each relay, limit boundary of *TMS* is used within range 0.1-1, the minimum operating time is used 0.1 sec,

Table 3.11 The effect of several curves type and MILP approach for Case I

		LP approach								MILP approach	
	PS^{min}	*TMS*	*CS*	*TMS*	*CS*	*TMS*	*CS*	*TMS*	*CS*	*TMS*	*CS*
R_{Gr}	114.2	0.3450	SI	0.520	VI	0.8875	EI	0.1	LI	0.8875	EI
R_{DG}	-	-	-	-	-	-	-	-	-	-	-
R_1	76.49	0.2791	SI	0.448	VI	0.9256	EI	0.1	LI	0.9230	EI
R_2	38.35	0.2241	SI	0.465	VI	0.7332	EI	0.1392	LI	0.4650	VI
R_3	38.35	0.1	SI	0.116	VI	0.3485	EI	0.1	LI	0.3471	EI
OF (s)		2.1500		1.0955		0.8025		146.85		0.7894	

and the *CTI* is used 0.3 sec. The *CTR* is 1. And, limit boundary of *CS* is used within range 2-5. From the simulation results in Table 3.12, we can discuss that *CS* is greatly affecting the total operating time of OCR.

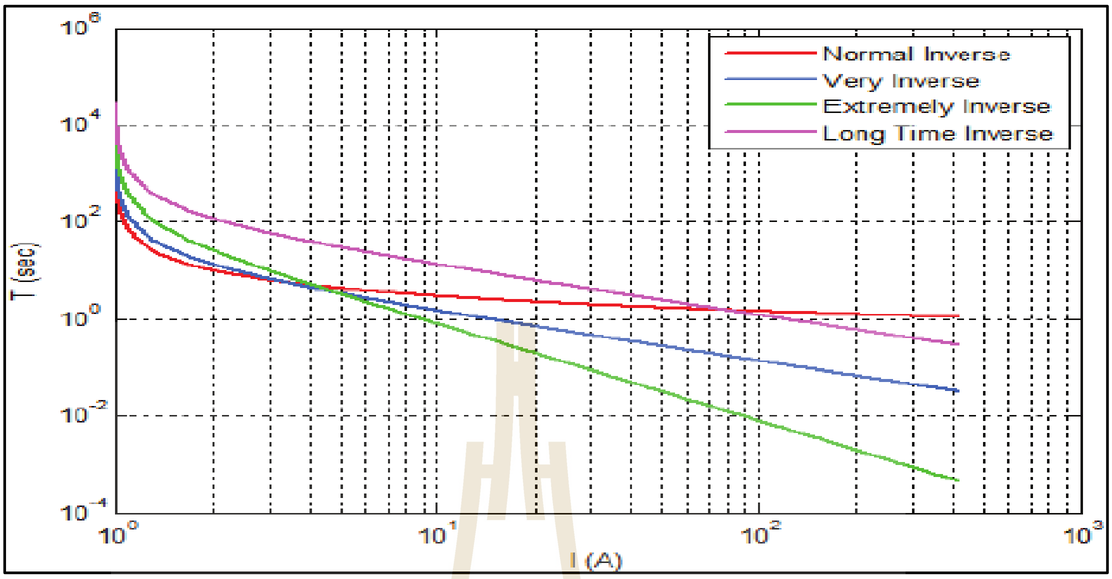

Figure 3.2 The characteristic of various curve of OCR

All extremely inverse *CS* provides the greatest optimal results. The *CS* that provides the better *OF* to the worst *OF* are all very inverse *CS*, all standard inverse *CS*, and all long-time inverse, respectively. The results showed that this approach offered the best solution for all cases. The optimal results of each case as shown in Table 3.11.

3.3.3 Mixed Integer Nonlinear Optimization Problem

To verify the effect of curve type, the *PS* and *TMS* of each OCR are considered to be decision variables and vary *CS* of each relay such as standard inverse, very inverse types, extremely inverse types, and long-time inverse types for all relay and use PSO technique to find the optimal *TMS* and *PS* of each OCR. From the simulation results in Table 3.12, we can discuss that *CS* is so greatly affecting the total operating time of OCR. All extremely inverse *CS* is provided the greatest optimal results. The *CS* that provides the better *OF* to worst *OF* are all very inverse *CS*, all standard inverse *CS*, and all long-time inverse respectively. The effect of curve type on NLP approach provided the solution in the same way as LP approach.

Table 3.12 The comparative on approaches of OCR coordination problem

	LP approach	NLP approach	MILP approach	MINLP approach
OF best (s)	2.15	1.7788	0.7894	0.6632

Accordingly, the MINLP approach is interesting issue to improve the OCR coordination. the *PS*, *TMS*, and *CS* are decision variables of each relay is called OFSS in this research. ROMI-PSO technique is used to handle this problem. The formulation of this problem is,

Minimize: Eq. 3.13

Subjected to: Eq. 3.16- 3.20, Eq. 3.22,

Decision variable: *TMS*, *PS*, and *CS*.

In this section, a decision variable is *TMS*, *PS*, and *CS* of each relay, limit boundary of *TMS* is used within range 0.1-1, the limit boundary of *PS* are shown in Table 3.7, the limit boundary of *CS* is illustrated in Eq.3.22, the minimum operating time is used 0.1 sec., and the *CTI* is used 0.3 sec. The *CTR* is 1.

Table 3.13 The effect of several curves type and MINLP approach

	NLP approach								MINLP approach		
	IEC-SI		IEC-VI		IEC-EI		IEC-LI		Mixed CS		
	TMS	*PS*	*TMS*	*PS*	*TMS*	*PS*	*TMS*	*PS*	*TMS*	*PS*	*CS*
R_{Gr}	0.154	372.6	0.122	372.6	0.824	114.2	0.1	114	0.205	226.7	EI
R_{DG}	-	-	-	-	-	-	-	-	-	-	-
R_1	0.135	242.1	0.369	89.06	0.1	211.3	0.1	76.5	0.1	211.4	EI
R_2	0.1	178.7	0.1	146.3	0.1	139.7	0.1	52.2	0.120	127.8	EI
R_3	0.1	38.3	0.116	38.35	0.347	38.4	0.1	38.4	0.100	44.1	VI
OF (s)	1.779		1.020		0.664		146.8		0.663		

The optimal results show that the MINLP approach is powerful and effective to improve the OCR coordination problem, as shown in Table 3.12 and 3.13. However, the simulation results of the MINLP approach in Table 3.12 and 3.13 used the ROMI-PSO algorithm only. To verify and find a better solution than ROMI-PSO, several techniques such as ROMI-GA, SRG, were used and compared with ROMI-PSO. A comparative study of the various optimization techniques can see in Table 3.14.

The simulation results in Table 3.15 can discuss that the SRG technique obtained the worst solution, considering by the worst *OF best*, the worst *OF average*, high *STD*, and high *Range*. the next is the ROMI-GA technique given a better solution than SRG technique for all factors. Then, the integer coded genetic algorithm (ICGA) provided a better solution than ROMI-GA and SRG for all factor and the strengths of ICGA is the lowest *STD* of all technique. Meanwhile, the ROMI-PSO technique offered the best solutions considered from *OF best* (0.6592 sec.), *OF average* (0.6840 sec.), *STD* (0.03355), and *Range* (0.1296 sec.). Consequently, we can conclude that the ROMI-PSO technique is so effective to handle the MINLP approach of OCR coordination problem.

3.4 Chapter Summary

From the simulation results in the previous section, we can conclude that the AOCR coordination scheme has more effectiveness than the NAOCR scheme, as discussed in section 3.2. The OFSS of the AOCR coordination can absolutely decrease the total operating time of relay over other partial schemes of the AOCR coordination and the ROMI-PSO is the most powerful method to solve the MINLP problem as illustrated in section 3.3.

Table 3.14 The MINLP approach with various optimization techniques

	ROMI-PSO			ROMI-GA			SRG			ICGA		
	TMS	*PS*	*CS*	*TMS*	*PS*	*CS*	*TMS*	*PS*	*CS*	*TMS*	*PS*	*CS*
R_{Gr}	0.1018	316.32	EI	0.3624	172.22	EI	0.3559	247.47	EI	0.3280	114.21	EI
R_{DG}	-	-	-	-	-	-	-	-	-	-	-	-
R_1	0.1	211.25	EI	0.2832	128.14	EI	0.3753	95.96	EI	0.1958	149.90	EI
R_2	0.1	139.70	EI	0.1111	132.87	EI	0.1	183.81	EI	0.1613	83.09	EI
R_3	0.1071	68.77	EI	0.3126	40.40	EI	0.1	39.04	EI	0.1	38.35	VI
*OF (best) **	0.6592			0.6703			0.6928			0.6670		
*OF (avg.) **	0.6840			0.6891			1.1802			0.6774		
*STD **	0.0335			0.0478			0.3453			0.0199		
*Range **	0.1296			0.2172			1.3963			0.1147		
*Converge rate (%) **	100			100			100			100		

**The 30-trial test raw data are provided in https://drive.google.com/drive/folders/1ilbjHjng2TQb2Mw3t21qsxHfWte7Pn7c?usp=sharing*

CHAPTER 4

THE OPTIMAL FULL SETTING SCHEME FOR AOCR COORDINATION[2]

4.1 Chapter Overview

This chapter contribute the OFSS of AOCR coordination in various test system. Section 4.2 explains the problem formulation of OFSS, ROMI-PSO technique procedure explain in section 4.3. Section 4.4 obtain the optimal result of OFSS for AOCR coordination scheme in several test system.

4.2 Mathematical Formulation

The OFSS is a method was considering all of setting parameter of each AOCR to decision variables including *TMS*, *PS*, and *CS*. The plug setting multiplier constraint is considering in this section The formulation of the OFSS for AOCR coordination are illustrated as bellow,

Minimize: Eq. 2.13

Subjected to: Eq. 2.16- 2.22

Decision variable: *TMS*, *PS*, and *CS*.

4.3 ROMI-PSO Technique

Traditional PSO can only solve problems with continuous variables and unconstrainted. The *CS* variable is set to an integer value in this paper, and the coordination constraint introduces many nonlinear inequalities constrained to this problem.

---

[2]Part of this chapter was under review at the electric power systems research journal (EPSR), 2021.

As a result, the problem has been changed into a mixed-integer nonlinear constrained problem. To address this problem, for every iteration, integer variables are treated similarly to continuous variables during the optimization process, but they are rounded off to the nearest integer value at the end. And then, nonlinear constraints are then handled using the penalty function. In this algorithm is the most commonly used approach for tackling discrete/integer variables in electrical power system search fields. The working process of this algorithm is following step by step as below, and in Figure 4.1.

Step 1: Random initial position of the population matrix (X) within the limited boundary.

$$\mathrm{TMS} = [TMS_i,\ldots,TMS_{NR}] = rand(TMS_i^{\min},TMS_i^{\max}),\ i = 1,\ldots.,NR, \tag{4.1}$$

$$\mathrm{PS} = [PS_i,\ldots,PS_{NR}] = rand(PS_i^{\min},PS_i^{\max}),\ i = 1,\ldots.,NR, \tag{4.2}$$

$$\mathrm{CS} = [CS_i,\ldots,CS_{NR}] = rand(CS_i^{\min},CS_i^{\max}),\ i = 1,\ldots.,NR, \tag{4.3}$$

$$\mathrm{X} = \left[\mathrm{TMS},\mathrm{PS},\mathrm{CS}\right]^{\mathrm{T}}. \tag{4.4}$$

Step 2: Round-off CS_i to the nearest integer position value within the limited boundary.

$$CS_i = \begin{cases} CS_i^u \ \text{ if } \ CS_i + 0.5 \geq CS_i^u, \\ CS_i^l \ \text{ if } \ CS_i - 0.5 < CS_i^l, \end{cases} \quad i = 1,\ldots.,NR, \text{ where } CS_i^u, CS_i^l \in \{\text{integer}\}. \tag{4.5}$$

Step 3: Calculate *OF* value and find the *pbest* and *gbest* of each population from Eq. 3.13 -3.15.

Step 4: Update velocity and position of a particle from Eq. 4.6 -4.8.

$$\mathrm{V}^{k+1} = w\mathrm{V}^{k} + c_1 r_1\left(pbest_i^{\,k} - \mathrm{X}^{k}\right) + c_2 r_2 (gbest_k - \mathrm{X}^{k}), \tag{4.6}$$

$$V_i^k = [V_1^k, \ldots, V_{3NR}^k], \tag{4.7}$$

$$X_i^{k+1} = X^k + V^{k+1}, \tag{4.8}$$

where, k indicates the iteration, w is the inertia weight, v_i^k is the i particle's velocity vector, x_i^k is the i particle's vector, $gbest^k$ is the historically best position of the entire swarm, $pbest_i^k$ is the historically best position of particle i, $c_1$and c_2 are the personal and global learning coefficients, respectively, while r_1 and r_2 are uniformly distributed random numbers in the range [0,1].

Step 5: Check constraint violation and handle by penalty function from Eq. 3.16- 3.22.

if *feasible answer pass all constraints*
$OF = OF;$
else
$OF = OF + (C \times PNF);$

where, PNF is penalty factor, C is a number of violated constraints.

Step 6: Repeat step (2), (3), (4), (5) until the maximum iteration.

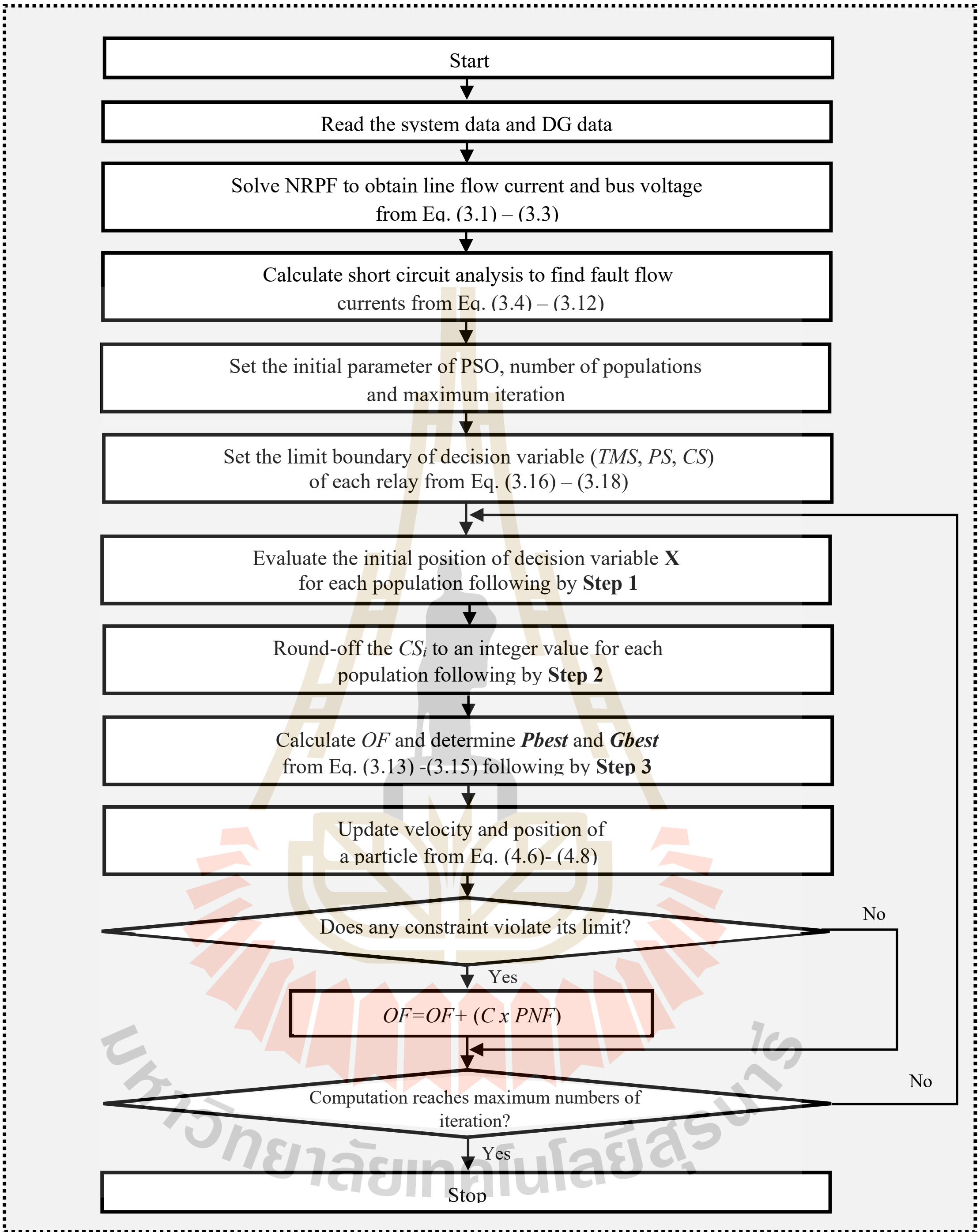

Figure 4.1 The procedure of this research

4.4 Test Case

4.4.1 IEC-Benchmark Microgrid

The proposed strategy was tested on the IEC-benchmark microgrid with various operating conditions (Saldarriaga-Zuluaga, 2020). In the test system, the operating conditions can be categorized into four conditions depend on the status of the circuit breaker as seen in Table 4.1. The test system includes main six buses, six loads, two distributed synchronous generators (DG1 and DG3), two doubly-fed induction generator (DFIG), wind turbines (DG-2 and DG-4), and five distribution lines (DL-1, DL-2,..., DL-5). The three-phase faults arise in the middle of each distribution line (F1-F5).

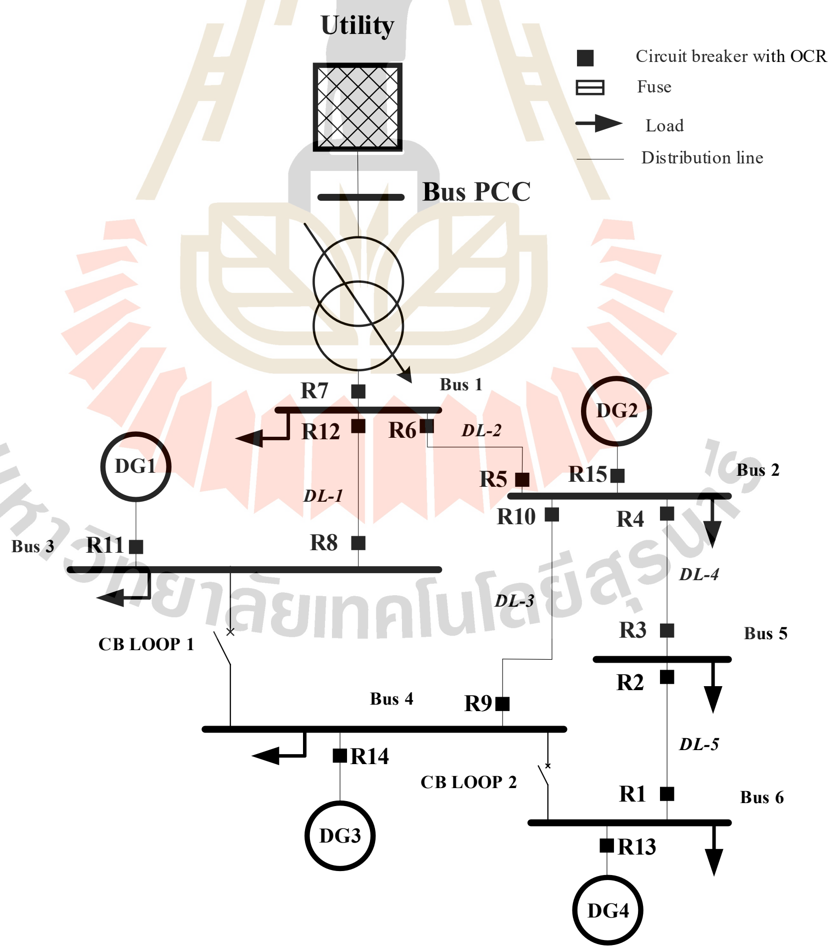

Figure 4.2 IEC benchmark microgrid

Therefore, F1 represents the fault on distribution line DL-5. F2, F3, and F4 denote the fault on distribution lines DL-4, DL-2, and DL-1, respectively. F5 indicates the fault on lines DL-3. The fault level on each distribution line within various operating conditions can be seen in Figure 4.3. To handle these faults that can be occurred in this system, an AOCR was installed at every end of the distribution line and the point of common coupling of each DG (R1-R15). The parameters of the system and fault levels are referred from (Saldarriaga-Zuluaga, 2020), (Kar, 2017). To avoid the complexity of the system, CB LOOP 1 and CB LOOP 2 are considered in open circuit status on any operating conditions.

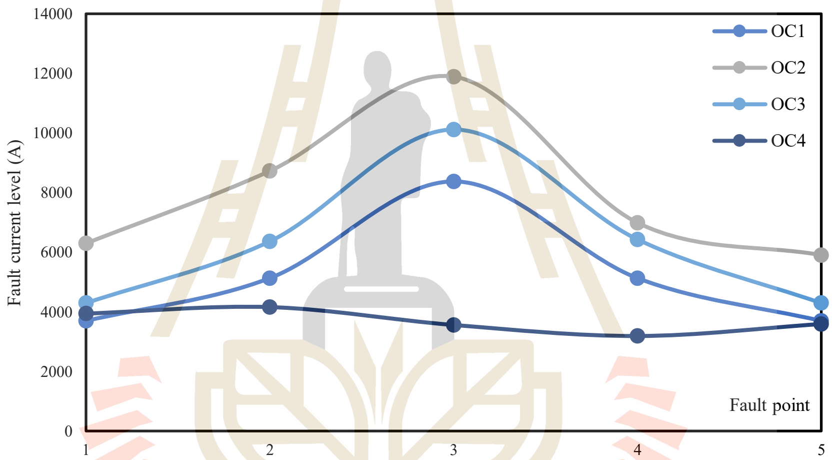

Figure 4.3 Fault current level of IEC microgrid

Table 4.1 The circuit breaker status

The operating conditions (OC)	Utility	DG1	DG2	DG3	DG4
OC1	on	off	off	off	off
OC2	on	on	on	on	on
OC3	on	on	on	off	off
OC4	off	on	on	on	on

To verify the proposed method and comparing to the previous existing method (Saldarriaga-Zuluaga S.D, 2021), the limit boundary of decision variables and the constant parameters of any constraints used are the same as in the previous existing papers (Saldarriaga-Zuluaga S.D, 2021). Hence, the limit of TMS_j used within a range of TMS_j^{min} at 0.05 to TMS_j^{max} at 15. The limit of PS_j used is within a range of PS_j^{min} depending on CT ratio and load current flowing through the relay to PS_j^{max} at 120 percent on PS_j^{min}, as shown in Table 4.2. The limit of PSM_j is within the range 1.1 PSM to 100 PSM. The limit of $t_{j,k}$ is between 0.01 and 2 sec, and the *CTI* used is 0.3 sec. As a result, the manifold optimal answers are available. To encounter the nearest global optimum solution and decrease the variance, 2000 population sizes are utilized. c_1 and c_2 are 1.49, and the 30 trials test are utilized.

Table 4.2 The CT ratio and PS boundary of each OCR

Relay	*CT ratio*	PS^{min}	PS^{max}	Relay	*CT ratio*	PS^{min}	PS^{max}
R1	400	0.50	0.60	R8	400	0.50	0.60
R2	400	0.50	0.60	R9	400	0.50	0.60
R3	400	0.50	0.60	R10	400	0.50	0.60
R4	400	0.50	0.60	R11	400	0.65	0.78
R5	400	0.50	0.60	R12	400	0.50	0.60
R6	400	0.50	0.60	R13	400	0.88	1.05
R7	1200	1.00	1.20	R14	400	0.65	0.78

Table 4.3 The coordination schemes of OC1

Fault Point	Primary	Backup		Primary	Backup
	RP	RB	RB	RP	RB
F1	R2	R4	-	R1	R13
	3695	3695		-	-
F2	R4	R6	R15	R3	R1
	5130	5130	-	-	-
F3	R6	R7	R8	R5	R15
	8375	8375	-	-	-
F4	R12	R7	R5	R8	R11
	5130	5130	-	-	-
F5	R10	R6	R15	R9	R14
	3695	3695	-	-	-

Results for OC1: In the OC1, the test system is connected to the utility and all of DG are not operated. Accordingly, the power flow and the short circuit flow have in one direction and similarly. the direction of current flow is from utility to load point or fault point. Consequently, only six relays are desire to detect in this operating condition (R2, R4, R6, R7, R10, R12). The coordination schemes and short circuit current flowing through each relay of this operating condition are shown in Table 4.3. The OFSS for each relay are shown in Table 4.4. The improvement of objective function value with up-to-date previous research is shown in Table 4.5. The operating time of each relay when fault occur is shown in Table 4.6.

Table 4.4 The OFSS for OC1

Relay	(Saldarriaga-Zuluaga S.D, 2021)			OFSS of AOCR		
	TMS_i	PS_i	CS_i	TMS_i	PS_i	CS_i
R1	-	-	-	-	-	-
R2	0.05	0.69	IEC-EI	0.05	0.50	IEC-EI
R3	-	-	-	-	-	-
R4	4.58	0.68	IEEE-STI	0.964	0.586	IEC-EI
R5	-	-	-	-	-	-
R6	2.16	0.67	IEEE-VI	3.789	0.51	IEC-EI
R7	0.05	1.15	IEEE-EI	0.05	1.0	IEEE-VI
R8	-	-	-	-	-	-
R9	-	-	-	-	-	-
R10	0.05	0.64	IEC-EI	0.05	0.50	IEC-EI
R11	-	-	-	-	-	-
R12	0.05	0.71	IEC-EI	0.0616	0.577	IEC-EI
R13	-	-	-	-	-	-
R14	-	-	-	-	-	-
R15	-	-	-	-	-	-
OF (sec.)	4.4			3.09		

From Table 4.3, it can be seen that the primary and backup relay can see the same magnitude fault current because this operating condition has a radial topology and a one fault source. And then, the fault current level is increase when the fault point near the fault source and decrease when fault point far from fault source. From the optimal results in Table 4.4, we can observe that the *CS* put to decision variable can absolutely decrease the minimum operating time than fixed *CS* in (A. Y. Hatata, 2018), (Anang Tjahjono, 2017). The proposed algorithm provides the results with several types of *CSs*, not the single type of curve. Meanwhile, in many existing researches, the optimal result of the single characteristic curve is IEC EI because it provides the minimum operating time than other curves.

Table 4.5 The comparison with previous research for OC1

Previous paper	*OF (sec.)*
(Saad, 2019)	7.53
(El-Naily N, 2019)	6.64
(Muñoz-Galeano N, 2020)	4.99
(Saldarriaga-Zuluaga S.D, 2021)	4.4
(Saldarriaga-Zuluaga, 2020)	4.19
(López-Lezama J.M, 2021)	3.86
Proposed	3.09

Table 4.6 The operating times of AOCRs for OC1

Fault Point	(Saldarriaga-Zuluaga S.D, 2021)			OFSS of AOCR		
	RP1	RB1	CTI	RP1	RB1	CTI
F1	R2	R4		R2	R4	
	0.0118	0.3118	0.300	0.0118	0.3118	0.300
F2	R4	R6		R4	R6	
	0.2967	0.5976	0.300	0.1614	0.4614	0.300
F3	R6	R7		R6	R7	
	0.5976	0.9372	0.340	0.1730	0.5115	0.3386
F4	R12	R7		R12	R7	
	0.01	1.01	1.000	0.01	0.5477	0.5377
F5	R10	R6		R10	R6	
	0.0118	0.6159	0.6041	0.0118	0.8906	0.8789
Total CTI	2.544			2.355		

Therefore, the trend of *TMS* will converge to the lower bound but it can slightly increase to avoid the constraint violation and the advantage of considering the *PS* as the decision variable, rather than fixed *PS*, result in the decrement the operating time and provide the algorithm to choose better the *CS* while remaining the coordination constrained.

The proposed method improves the objective function by around 46% from the previous paper (Saldarriaga-Zuluaga S.D, 2021), slightly decrease form (López-Lezama J.M, 2021), (Saldarriaga-Zuluaga, 2020) and more than 65% when compare with (Saad, 2019), (El-Naily N, 2019), and (Muñoz-Galeano N, 2020), as shown in Table 4.5. Table 4.6 presents the comparative study on the operating of primary and backup relays for each fault. For all cases, the proposed method can enhance the total *CTI* of the system when compared with (Saldarriaga-Zuluaga S.D, 2021) that superior improved system reliability. The typical of coordination curves for the proposed strategy can be seen in Figure 4.4.

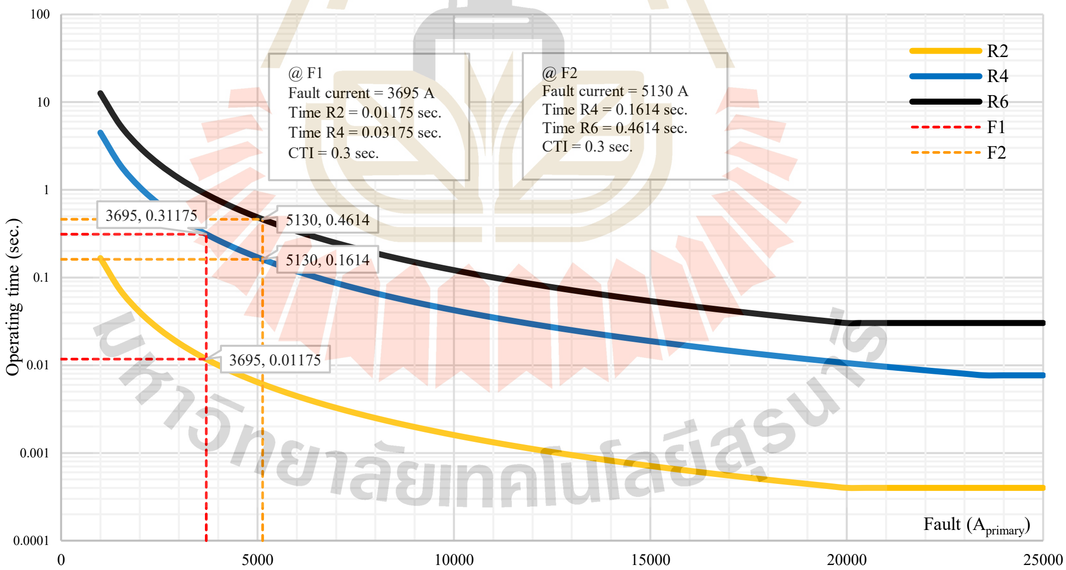

Figure 4.4 The coordination curve for OC1 of the proposed method

Results for OC2: In the OC2, the test system is connected to the utility and all of DG are operated. The power flow and the short circuit current flow can be in bi-direction and complex. The direction of current flow is from utility and DGs to load point or fault point. All relays are required to protect the system under this operating condition. The coordination schemes and short circuit current flowing through each relay of this operating condition are shown in Table 4.7. The OFSS for each relay are shown in Table 4.8. The comparison of objective function value of the proposed method with previous research is shown in Table 4.9. The operating time of each relay when fault occur is shown in Table 4.10.

Table 4.7 The coordination schemes of OC2

Fault Point	Primary	Backup		Primary	Backup
	RP1.1	RB1.1	RB1.2	RP2.1	RB2.1
F1	R2	R4	-	R1	R13
	4648	4648		1648	1648
F2	R4	R6	R15	R3	R1
	7260	5443	920	1465	1465
F3	R6	R7	R8	R5	R15
	9256	8375	923	2635	737
F4	R12	R7	R5	R8	R11
	5998	4572	1439	991	991
F5	R10	R6	R15	R9	R14
	4913	3416	578	991	991

From Table 4.7, when F1 take place, the fault flows current from DG4 is seen by relay R1 and R13. The fault current is also flow in another way from the utility and the upstream DGs (DG1, DG2, DG3). These fault current flows are seen by relay R2 and R4. Similarly, as when F2 take place, the R3 and R1 are required to operate to clear this fault from DG4. Meanwhile R4, R6, and R15 are required to operate with this fault flows current from the utility and upstream DGs. Therefore, when F3 take place R5 and R15 require to operate for this fault from downstream DG (DG2, DG3, DG4). R6, R7, and R8 are required to operate for this fault from the utility and DG1.Consequently, when fault F4 take place R8 and R11 are required to operate for this fault from DG1.On another hand, R12, R7 and R5 are required to operate for this fault from the utility and downstream DGs. When F5 take place, R9 and R14 are required to operate for this fault from DG3. Meanwhile, R10, R6, and R15 are required to operate for this fault from another fault source. Hence, when fault source increases the coordination schemes will be more complexity to maintain the system reliability.

Table 4.8 The OFSS for OC2

Relay	(Saldarriaga-Zuluaga S.D, 2021)			OFSS of AOCR		
	TMS_i	PS_i	CS_i	TMS_i	PS_i	CS_i
R1	0.217	0.58	IEC-EI	1.838	0.542	IEC-EI
R2	0.05	0.58	IEC-EI	0.05	0.5	IEC-STI
R3	0.05	0.73	IEC-STI	0.05	0.5	IEC-STI
R4	0.235	0.62	IEEE-MI	2.124	0.5027	IEC-EI
R5	0.197	0.7	IEC-EI	1.321	0.5	IEEE-STI
R6	1.55	0.62	IEC-STI	3.647	0.5223	IEC-EI
R7	0.05	1.12	IEEE-EI	0.724	1.004	IEC-STI
R8	0.567	0.62	IEEE-EI	1.313	0.5002	IEEE-STI
R9	0.05	0.7	IEC-STI	0.05	0.5	IEC-STI
R10	0.05	0.6	IEC-EI	0.05	0.5	IEC-STI
R11	0.469	0.7	IEEE-EI	1.931	0.6503	IEEE-STI
R12	0.05	0.73	IEC-EI	0.05	0.5	IEC-STI
R13	0.325	0.88	IEEE-EI	1.875	0.8804	IEEE-STI
R14	0.104	0.8	IEEE-EI	0.35	0.7004	IEC-STI
R15	0.2796	0.71	IEEE-MI	0.05	0.55	IEEE-VI
OF (sec.)		11.6			8.77	

From Table 4.8, the *CS* provided by the proposed algorithm are STI and EI similar with OC1, that absolutely confirmed these curve setting obtained the most effective to decrease the operating time of OCR. The *PS* of most relay converged to lower bound but the *PS* of some relay *PS* moved up form lower bound for adapted to another better curve and maintain the constraint violation. The trend of *TMS* still converged to lower bound as close as possible. The proposed algorithm results to the best *OF* value, slightly lower than (López-Lezama J.M, 2021), around 40% lower than (Saldarriaga-Zuluaga S.D, 2021), (Saldarriaga-Zuluaga, 2020), around 50% lower than those of (Saad, 2019) , (El-Naily N, 2019), (Muñoz-Galeano N, 2020) as shown in Table 4.9. Table 4.10 show that the proposed algorithm is effectively improved the system reliability than (Saldarriaga-Zuluaga S.D, 2021). Figure 4.5 shown the coordination curve for OC2 of the proposed method.

Table 4.9 The comparison with previous research for OC2

Previous paper	*OF (sec.)*
(Saad, 2019)	19.18
(El-Naily N, 2019)	17.48
(Muñoz-Galeano N, 2020)	13.66
(Saldarriaga-Zuluaga S.D, 2021)	11.6
(Saldarriaga-Zuluaga, 2020)	12.48
(López-Lezama J.M, 2021)	8.58
Proposed	8.77

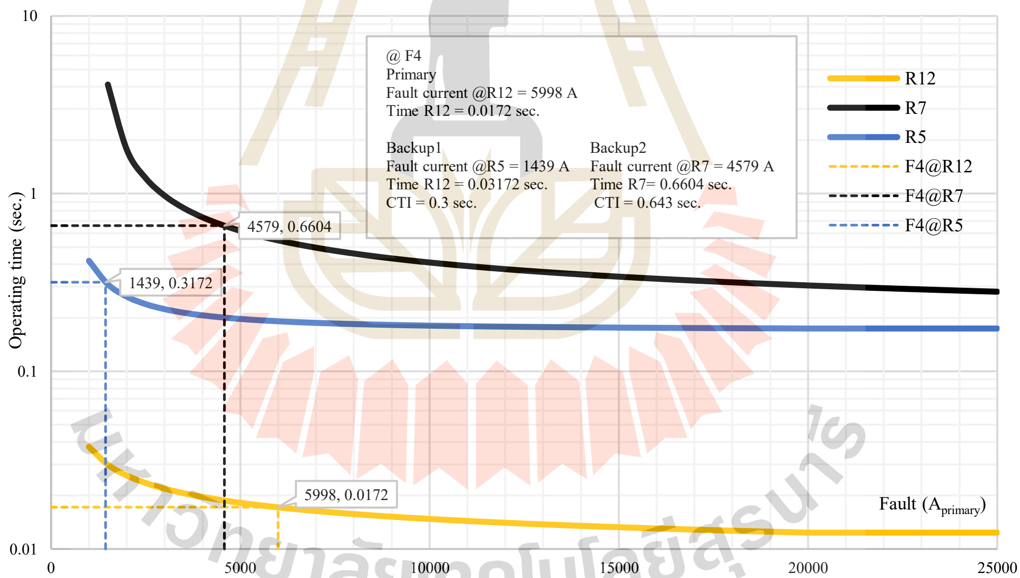

Figure 4.5 The coordination curve for OC2 of the proposed method

Table 4.10 The operating times of AOCRs for OC2

Fault Point	(Saldarriaga-Zuluaga S.D, 2021)				
	Primary	Backup		Primary	Backup
	RP1.1	RB1.1	RB1.2	RP2.1	RB2.1
F1	R2	R4	-	R1	R13
	0.01	0.31		-	-
F2	R4	R6	R15	R3	R1
	0.31	0.61	0.61	-	-
F3	R6	R7	R8	R5	R15
	0.61	0.9372	0.91	0.2023	0.6411
F4	R12	R7	R5	R8	R11
	0.01	1.02	0.3197	0.91	1.152
F5	R10	R6	R15	R9	R14
	0.01	0.625	0.8347	-	-
Total CTI	4.9674				
Fault Point	**OFSS for AOCR**				
	Primary	Backup		Primary	Backup
	RP1.1	RB1.1	RB1.2	RP2.1	RB2.1
F1	R2	R4	-	R1	R13
	0.0186	0.3186		0.2567	0.5597
F2	R4	R6	R15	R3	R1
	0.1305	0.4305	0.5505	0.0302	0.3302
F3	R6	R7	R8	R5	R15
	0.1487	0.4487	0.4487	0.234	0.587
F4	R12	R7	R5	R8	R11
	0.0172	0.6604	0.3172	0.4206	0.7206
F5	R10	R6	R15	R9	R14
	0.0183	1.0954	0.6571	0.0378	0.3378
Total CTI	5.83				

Results for OC3: In the OC3, the test system is connected to the utility and the upstream DGs (DG1, DG2) are in operation while the downstream DGs (DG3, DG4) are not operated. The fault current level is still higher than OC1 but slightly decrease from OC2. Attributable, the fault current contributed from downstream DG are disappear, so the relay that detects these faults is not required. The ten relays are required to detect faults in this operating condition, consist of (R2, R4, R5, R6, R7, R8, R10, R11, R12, and R15).

Table 4.11 The coordination schemes of OC3

Fault Point	Primary	Backup		Primary	Backup
	RP1.1	**RB1.1**	**RB1.2**	**RP2.1**	**RB2.1**
F1	R2	R4	-	R1	R13
	4293	4293		-	-
F2	R4	R6	R15	R3	R1
	6363	5443	920	-	-
F3	R6	R7	R8	R5	R15
	9256	8375	923	860	860
F4	R12	R7	R5	R8	R11
	5437	4933	570	991	991
F5	R10	R6	R15	R9	R14
	4293	3673	631	-	-

The coordination schemes and short circuit current flowing through each relay of this operating condition are shown in Table 4.11. The OFSS for each relay are shown in Table 4.12. The comparison of objective function values with up-to-date previous researches is shown in Table 4.13. The operating time of each relay when fault occur is shown in Table 4.14. From Table 4.11, the relay R1, R3, and R13 are not seen any fault current, because DG4 is not operated in this operating condition, similarly to R9 and R14 effected by DG3. Thus, the coordination scheme is less complicated than OC2. Meanwhile, the other relays are still operated in this operating condition. From Table 4.12, the total operating time of relay in this operating condition is lower than OC2 and the optimal results obtained by the proposed algorithm are extremely improved when compare with (Saldarriaga-Zuluaga S.D, 2021).

Table 4.12 The OFSS for OC3

Relay	(Saldarriaga-Zuluaga S.D, 2021)			OFSS of AOCR		
	TMS_i	PS_i	CS_i	TMS_i	PS_i	CS_i
R1	-	-	-	-	-	-
R2	0.05	0.61	IEC-EI	0.05	0.5	IEC-STI
R3	-	-	-	-	-	-
R4	2.66	0.71	IEC-EI	1.5698	0.5404	IEC-EI
R5	0.05	0.56	IEC-EI	0.05	0.5	IEEE-EI
R6	0.5947	0.51	IEEE-MI	3.2369	0.5637	IEC-EI
R7	0.05	1.38	IEEE-EI	0.05	1	IEEE-VI
R8	0.4337	0.6	IEEE-VI	1.264	0.519	IEEE-STI
R9	-	-	-	-	-	-
R10	0.05	0.57	IEC-EI	0.0509	0.5315	IEC-EI
R11	0.2399	0.71	IEC-VI	0.137	0.671	IEC-SI
R12	0.05	0.72	IEC-EI	0.05	0.5	IEC-STI
R13	-	-	-	-	-	-
R14	-	-	-	-	-	-
R15	0.7186	0.8	IEC-STI	0.563	0.55	IEC-STI
OF (sec.)	9.97			6.913		

Table 4.13 The comparison with previous research for OC3

Previous paper	*OF (sec.)*
(Saad, 2019)	14.04
(El-Naily N, 2019)	12.67
(Muñoz-Galeano N, 2020)	10.71
(Saldarriaga-Zuluaga S.D, 2021)	9.97
(Saldarriaga-Zuluaga, 2020)	10.49
(López-Lezama J.M, 2021)	8.39
Proposed	6.913

Table 4.14 The operating times of AOCRs for OC3

Fault Point	(Saldarriaga-Zuluaga S.D, 2021)				
	Primary	Backup		Primary	Backup
	RP1.1	RB1.1	RB1.2	RP2.1	RB2.1
F1	R2	R4	-	R1	R13
	0.01	0.31		-	-
F2	R4	R6	R15	R3	R1
	0.31	0.61	0.61	-	-
F3	R6	R7	R8	R5	R15
	0.61	0.9372	0.91	0.2023	0.6411
F4	R12	R7	R5	R8	R11
	0.01	1.02	0.3197	0.91	1.152
F5	R10	R6	R15	R9	R14
	0.01	0.625	0.8347	-	-
Total CTI	4.9674				
Fault Point	**OFSS for AOCR**				
	Primary	Backup		Primary	Backup
	RP1.1	RB1.1	RB1.2	RP2.1	RB2.1
F1	R2	R4	-	R1	R13
	0.0192	0.3192		-	-
F2	R4	R6	R15	R3	R1
	0.1451	0.4451	0.478	-	-
F3	R6	R7	R8	R5	R15
	0.1537	0.5116	0.4537	0.2023	0.5023
F4	R12	R7	R5	R8	R11
	0.0177	0.5527	0.3197	0.4249	0.7249
F5	R10	R6	R15	R9	R14
	0.01	0.9794	0.654	-	-
Total CTI	4.6411				

The most *CS* obtained from the proposed algorithm are EI and STI respectively. The total operating time is improved around 45% when compare with (Saldarriaga-Zuluaga S.D, 2021), slightly decrease for (López-Lezama J.M, 2021), and extremely decreased more than 50% when compare with (Saad, 2019), (El-Naily N, 2019), (Muñoz-Galeano N, 2020) and (Saldarriaga-Zuluaga, 2020) as shown in Table 4.13. Table 4.14 shown that the operating time of each relay when fault take place of the proposed strategy has more advantage in the system reliability than the previous paper. The coordination curve for OC3 of the proposed method can see in Figure 4.6.

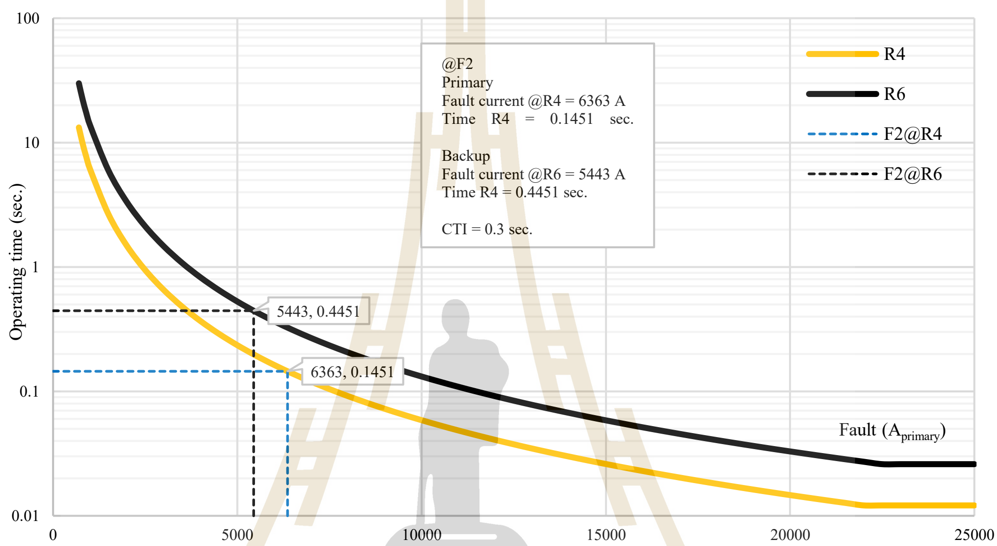

Figure 4.6 The coordination curve for OC3 of the proposed method

Results for OC4: In the OC4, the test system is disconnected form the utility while all of DG are in operation. This condition is called islanded mode. This operating condition provided the lowest fault current level from other operating conditions. All relays are required to detect the fault except the relay R7, because this relay cannot see any fault current in this operating condition. The coordination schemes and short circuit current flowing through each relay of this operating condition are shown in Table 4.15. The OFSS for each relay is shown in Table 4.16. The improvement of objective function value with up-to-date previous research is shown in Table 4.17. The operating time of each relay when fault occur is shown in Table 4.18. From Table 4.15, we can see that all relays are operate except relay R7 then the coordination scheme is more complicated than OC3 but simpler than OC2 in this operating condition. Consequently, the total operating time of relay is greater than OC3 and less than OC2.

Table 4.15 The coordination schemes of OC4

Fault Point	Primary	Backup		Primary	Backup
	RP1.1	RB1.1	RB1.2	RP2.1	RB2.1
F1	R2	R4	-	R1	R13
	2293	2293		1648	1648
F2	R4	R6	R15	R3	R1
	2693	864	920	1465	1465
F3	R6	R7	R8	R5	R15
	923	-	923	2635	737
F4	R12	R7	R5	R8	R11
	2197	-	2197	991	991
F5	R10	R6	R15	R9	R14
	2599	664	631	991	991

Table 4.16 The OFSS for OC4

Relay	(Saldarriaga-Zuluaga S.D, 2021)			OFSS of AOCR		
	TMS_i	PS_i	CS_i	TMS_i	PS_i	CS_i
R1	0.5475	0.5	IEC-STI	1.388	0.522	IEEE-STI
R2	0.05	0.5	IEC-STI	0.05	0.5	IEC-STI
R3	0.05	0.62	IEC-STI	0.05	0.5	IEC-STI
R4	0.9376	0.63	IEEE-EI	0.439	0.5488	IEC-EI
R5	0.8621	0.5	IEEE-EI	2.474	0.5027	IEEE-STI
R6	0.6852	0.5	IEC-STI	0.2175	0.5802	IEEE-MI
R7	-	-	-	-	-	-
R8	0.5192	0.51	IEEE-EI	0.91	0.5926	IEC-STI
R9	0.05	0.66	IEC-STI	0.05	0.5	IEC-STI
R10	0.05	0.58	IEC-STI	0.05	0.5	IEC-STI
R11	0.4895	0.87	IEEE-MI	1.1691	0.6575	IEC-STI
R12	0.05	0.58	IEC-STI	0.05	0.5	IEC-STI
R13	0.7783	1.09	IEC-STI	2.07	0.888	IEEE-STI
R14	0.3715	0.79	IEC-STI	0.5897	0.65	IEEE-STI
R15	0.6695	0.55	IEC-STI	0.237	0.5502	IEEE-MI
OF (sec.)	9.99			9.08		

Table 4.17 The comparison with previous research for OC4

Previous paper	*OF (sec.)*
(Saad, 2019)	15.56
(El-Naily N, 2019)	15.56
(Muñoz-Galeano N, 2020)	12.63
(Saldarriaga-Zuluaga S.D, 2021)	9.99
(Saldarriaga-Zuluaga, 2020)	8.96
(López-Lezama J.M, 2021)	8.83
Proposed	9.08

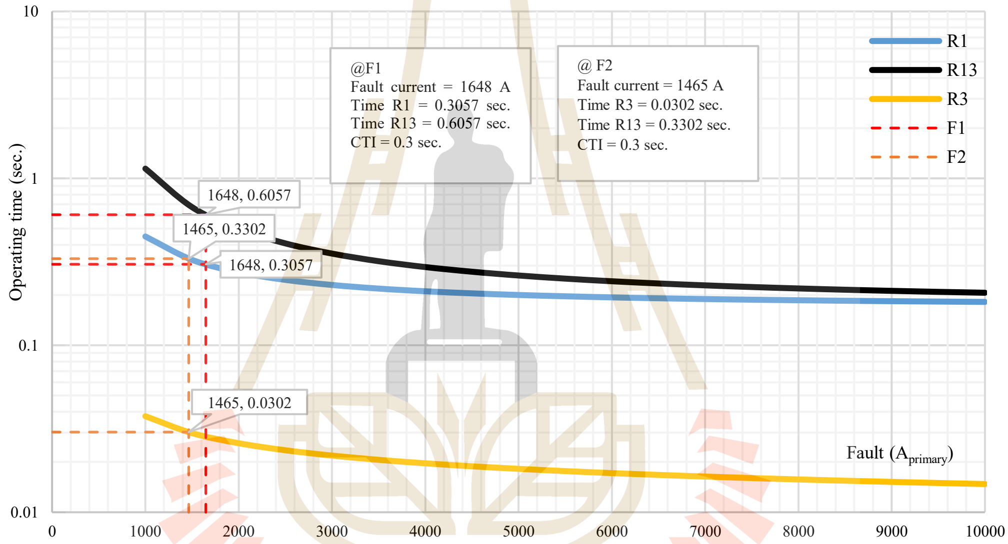

Figure 4.7 The coordination curve for OC4 of the proposed method

Anyway, the fault current seen by each relay are the lowest when compare with other operating conditions. Thus, the main CS resulted from the proposed algorithm are IEEE-STI and IEC-STI as shown in Table 4.16. Table 4.17 shown that the total operating time of the proposed algorithm improved around 10% from (Saldarriaga-Zuluaga S.D, 2021), slightly increase when compare with (López-Lezama J.M, 2021), (Saldarriaga-Zuluaga, 2020) and significantly decrease from (Saad, 2019) , (El-Naily N, 2019), (Muñoz-Galeano N, 2020). Table 4.18 shown that the total CTI provided by the proposed algorithm is as close as the previous paper. The coordination curve for this operating condition can see in Figure 4.7.

Table 4.18 The operating times of AOCRs for OC4

Fault Point	(Saldarriaga-Zuluaga S.D, 2021)				
	Primary	Backup		Primary	Backup
	RP1.1	**RB1.1**	**RB1.2**	**RP2.1**	**RB2.1**
F1	R2	R4	-	R1	R13
	0.0244	0.3244		0.4063	0.7063
F2	R4	R6	R15	R3	R1
	0.2683	0.5683	0.5684	0.1485	0.4485
F3	R6	R7	R8	R5	R15
	0.5484	-	0.8484	0.2253	0.6529
F4	R12	R7	R5	R8	R11
	0.0248	-	0.3249	0.8096	1.109
F5	R10	R6	R15	R9	R14
	0.1301	0.6695	0.7733	0.0378	0.3379
Total CTI	4.3105				
Fault Point	OFSS for AOCR				
	Primary	Backup		Primary	Backup
	RP1.1	**RB1.1**	**RB1.2**	**RP2.1**	**RB2.1**
F1	R2	R4	-	R1	R13
	0.0244	0.3244		0.3057	0.6057
F2	R4	R6	R15	R3	R1
	0.2345	0.5345	0.5345	0.0302	0.3302
F3	R6	R7	R8	R5	R15
	0.5142	-	0.8142	0.2911	0.6128
F4	R12	R7	R5	R8	R11
	0.0249	-	0.3249	0.7726	1.0726
F5	R10	R6	R15	R9	R14
	0.0231	0.6413	0.6873	0.0378	0.3378
Total CTI	4.304				

Overview of the proposed algorithm: From Table 4.19, the total operating time of the AOCR protection for the IEC benchmark microgrid has improved over the time, augmenting the constraint, proffer the effectiveness of the proposed strategy on the AOCR setting. The proposed strategy provided the lower total operating time and the total *CTI* of the AOCR than those existing works. The proposed algorithm has been tested with 30 trials to verify the optimal results. Table 4.20 shown the best, mean, worst, range, and standard deviation (STD) of the optimal results.

Table 4.19 The total operating time of each OC

Operating mode	OC1	OC2	OC3	OC4	*Total time*	*Total CTI*
(Saad, 2019)	7.53	19.18	14.04	15.56	56.31	19.04
(El-Naily N, 2019)	6.64	17.48	12.67	15.56	52.35	18.44
(Muñoz-Galeano N, 2020)	4.99	13.66	10.71	12.63	41.99	18.12
(Saldarriaga-Zuluaga S.D, 2021)	4.4	11.6	9.97	9.99	35.96	17.88
(Saldarriaga-Zuluaga, 2020)	4.19	12.48	10.49	8.96	36.12	17.62
(Saldarriaga-Zuluaga, 2020)	3.86	8.58	8.39	8.83	29.66	16.09
Proposed	3.09	8.77	6.913	9.079	27.85	17.13

Table 4.20 The statistic optimal results with 30 trials test

Operating mode	OC1	OC2	OC3	OC4
best	3.091	8.777	6.913	9.08
mean	3.261	10.67	8.078	9.968
worst	3.818	15.47	10.13	12.08
STD	0.208	1.66	0.715	0.613
range	0.727	6.693	2.625	2.997

**The 30-trial test raw data are provided in*
https://drive.google.com/drive/folders/1ilbjHjng2TQb2Mw3t21qsxHfWte7Pn7c?usp=sharing

From Table 4.21, we can observe that the lowest of the best value on total operating time of relay are OC1, OC3, OC2, and OC4, respectively. Meanwhile, the lowest of the mean value on the total operating time are OC1, OC3, OC4, and OC2, respectively. The high STD is due to high complexity operating conditions as in OC2 and OC4, because these operating conditions are required more relays to operate and more coordination constraints than other operating conditions.

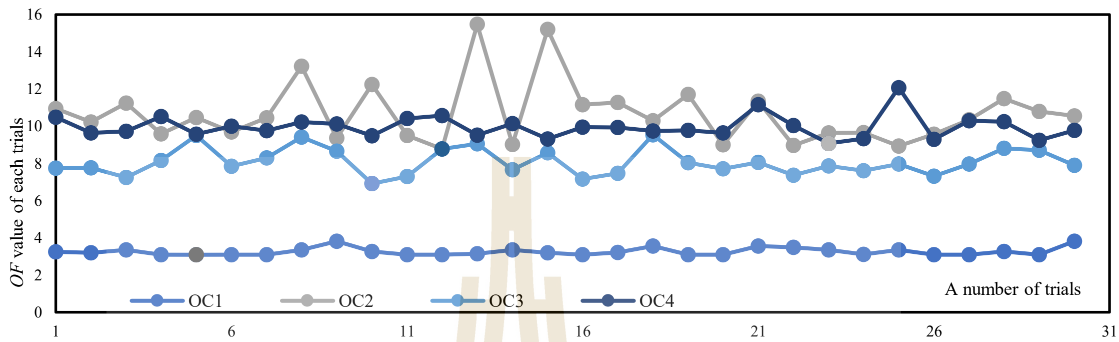

Figure 4.8 The operating time of each trial

we can decrease the STD on these operating condition by increasing population size of the proposed algorithm.

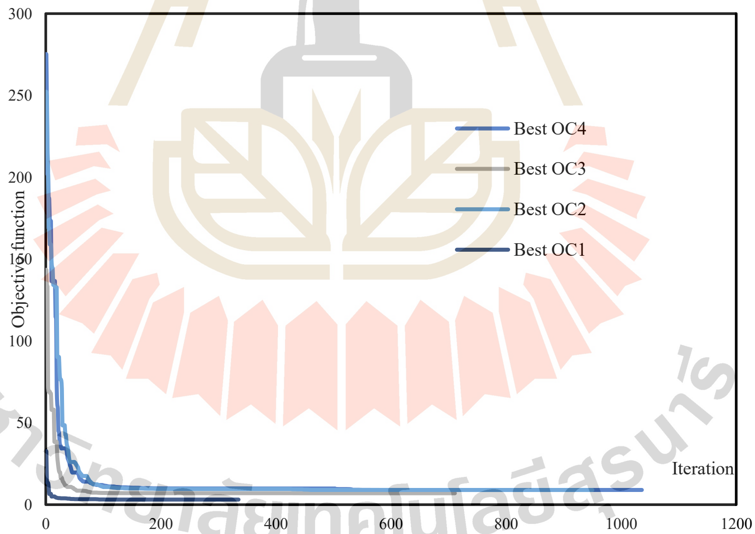

Figure 4.9 The convergence plot of the proposed method

Nevertheless, it is increasing the computational time. The operating time for each trial is shown in Figure 4.8. The convergence plot of the proposed method shown in Figure 4.9.

4.4.2 The Modified IEEE-15 BUS Radial System

To demonstrate a practical test system, the OFSS of AOCR was repeatedly tested on the modified IEEE 15 bus radial system, that combination with several protective device. In the test system, the operating conditions can be categorized into two conditions depend on the status of the circuit breaker. In OC1, the utility is energized without DG, and OC2 both utility and DG are energized. The test system includes main fifteen buses, fourteen loads, DG connected to bus three, eight a lateral fuse, three reclosers, and four AOCRs. The configuration of the system has shown in Figure 4.10, Fault current level of the system are illustrated in Figure 4.11, the other parameter of the system can be seen in Appendix A.

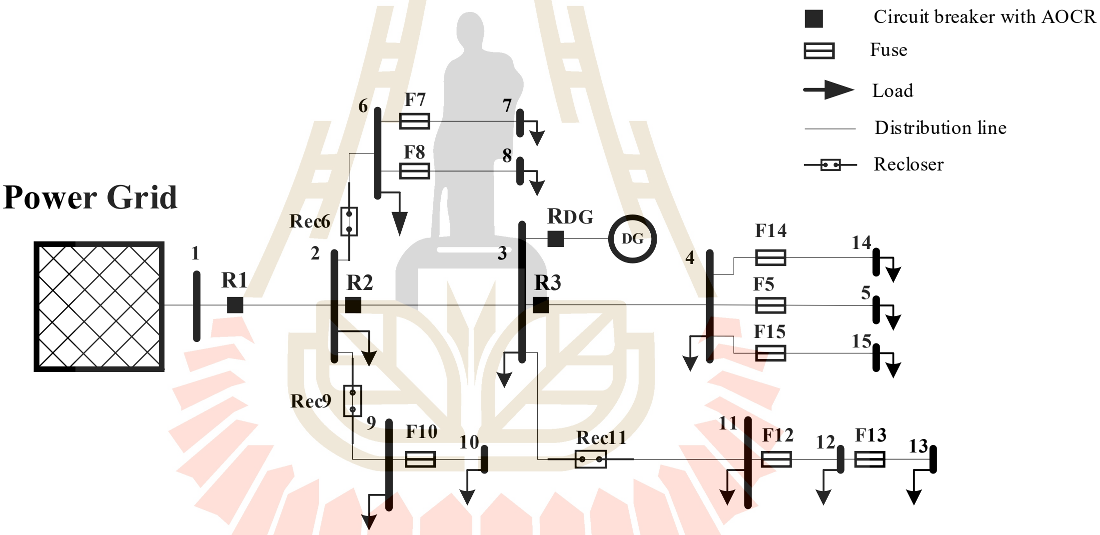

Figure 4.10 The modified IEEE 15 bus

Table 4.21 and Table 4.22 show that the limit boundaries of AOCR's *PS* were used within a range of 150 percent to 200 percent of load currents while the *PS* of the reclosers is set as 200 percent of load current. The fuse setting implies the determination of the fuse constants "F" and "G" as shown in Eq. 2.23 The constant "F" represents the slope of the straight-line log-log plot and is fixed at a specified value equal to -1.8 for all fuses in the system. This condition is practically acceptable because all fuses in the system should be of the same type. The constant G is calculated using the value of F and the coordinates of one operating point of the fuse.

Hence, we are designing the fuse to handle the fault with 0.5 sec (except LF13 is uses 0.8 sec for coordination with LF12). in OC1. Then, the calculated parameter G of each fuse is shown in Table 4.23.

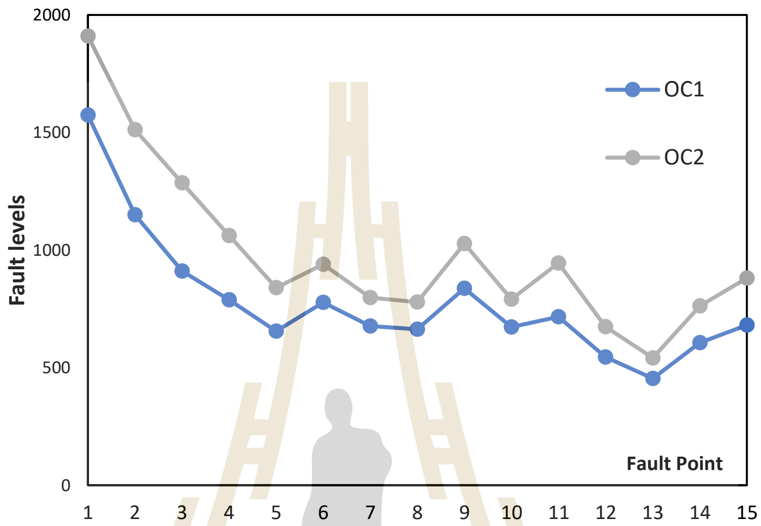

Figure 4. 11 The fault levels of IEEE 15 bus system

Table 4.21 The *PS* of Protective device in OC1

Protective device	***Maximum Load Current (A)***	***PS^{min} 1.5 Load (A)***	***PS^{max} 2 Load (A)***
R1	96.4	144.5	192.7
R2	56.7	85.1	113.4
R3	31.1	46.7	62.2
RDG	-	-	-
Rec6	27.9	-	55.7
Rec9	9	-	18.1
Rec11	19.9	-	39.8

The coordination schemes of the system are show in Table 4.24, 4.25. we can observe that in the OC2 fault current can be bidirectional flow. Due to the coordination scheme is more complex in OC2. For the simulation, the limit of TMS_j used within a range of TMS_j^{min} at 0.05 to TMS_j^{max} at 15. The limit of PSM_j is within the range 1.1 PSM to 20

PSM. The limit of $t_{j,k}$ is between 0.05 and 50 sec, and the *CTI* used is 0.3 sec. The *CTR* is 1 for all AOCR and recloser. The *PNF* is 1000 sec. The swarm size is use to 2000.

Table 4.22 The *PS* of Protective device in OC2

Protective device	*Maximum Load Current (A)*	PS^{min} *1.5 Load (A)*	PS^{max} *2 Load (A)*
R1	56.7	85.0	113.3
R2	17.5	26.2	35.0
R3	30.4	45.6	60.8
RDG	32.5	48.75	65
Rec6	27.5	-	55.0
Rec9	8.8	-	17.7
Rec11	19.6	-	39.3

Table 4.23 The lateral fuse parameter

Lateral Fuse	*F constant*	*G constant*	Lateral Fuse	*F constant*	*G constant*
LF5	-1.8	4.7683	LF12	-1.8	4.6860
LF7	-1.8	4.7937	LF13	-1.8	4.4818
LF8	-1.8	4.7785	LF14	-1.8	4.7072
LF10	-1.8	4.7886	LF15	-1.8	4.7978

Other parameter of ROMI-PSO technique is use a default parameter follow in MATLAB environment. In this system, the proposed technique provides the optimal result consist of The OFSS of AOCR, TMS fast-mode and slow mode of recloser, while another parameter of protective device is predetermined. the optimal results of this test system are shown in Table 4.26, 4.28. The operating time of each protective device is illustrated in Table 4.27, 4.29. From the optimal results in Table 4.26 shown that the *CS* obtained by ROMI-PSO technique is EI and STI curve. The *TMS* fast-mode of recloser completely converge to lower bound. The optimal results with 30 trials test show that the *OF (best), OF (avg.), STD* and *Range* of the proposed technique is more superior than the ICGA method.

Table 4.24 The coordination scheme in OC1

Fault Point	Primary	Backup	Primary	Backup
	RP	RB	RP	RB
F2	R1	-	R2	RDG
	1149.5	-	-	-
F3	R2	R1	RDG	-
	910.7	910.7	-	-
F4	R3	R2	R3	RDG
	788	788	-	-
F5	LF5	R3	-	-
	655.1	655.1	-	-
F6	Rec6	R1	Rec6	R2
	777.1	777.1	-	-
F7	LF7	Rec6	-	-
	676.7	676.7	-	-
F8	LF8	Rec6	-	-
	663.7	663.7	-	-
F9	Rec9	R1	Rec9	R2
	837.7	837.7	-	-
F10	LF10	Rec9	-	-
	672.3	672.3	-	-
F11	Rec11	R2	Rec11	RDG
	715.9	715.9	-	-
F12	LF12	Rec11	-	-
	545.7	545.7	-	-
F13	LF13	LF12	-	-
	454.1	454.1	-	-
F14	LF14	R3	-	-
	605.8	605.8	-	-
F15	LF15	R3	-	-
	680.3	680.3	-	-

Table 4.25 The coordination scheme in OC2

Fault Point	Primary	Backup	Primary	Backup
	RP	RB	RP	RB
F2	R1	-	R2	RDG
	1149.5	-	366.7	366.7
F3	R2	R1	RDG	-
	910.7	910.7	685.9	-
F4	R3	R2	R3	RDG
	751.4	751.4	751.4	312
F5	LF5	R3	-	-
	840.6	840.6	-	-
F6	Rec6	R1	Rec6	R2
	939.3	702	939.3	227.7
F7	LF7	Rec6	-	-
	797.5	797.5	-	-
F8	LF8	Rec6	-	-
	779.5	779.5	-	-
F9	Rec9	R1	Rec9	R2
	1028.3	769.5	1028.3	249.2
F10	LF10	Rec9	-	-
	791.4	791.4	-	-
F11	Rec11	R2	Rec11	RDG
	944.5	650.6	944.5	326.3
F12	LF12	Rec11	-	-
	674.3	674.3	-	-
F13	LF13	LF12	-	-
	541.6	541.6	-	-
F14	LF14	R3	-	-
	763.1	763.1	-	-
F15	LF15	R3	-	-
	881.2	881.2	-	-

Table 4.26 Optimal result of each protective device in OC1

Relay	ROMI-PSO			ICGA		
	TMS_i	*PS_i*	*CS_i*	*TMS_i*	*PS_i*	*CS_i*
R1	5.137	163.88	IEEE-STI	0.831392	172.20	IEEE-EI
R2	2.013	91.38	IEEE-EI	0.731097	98.406	IEC-EI
R3	2.067	47.20	IEC-EI	4.411129	50.1	IEEE-EI
RDG	-	-	-	-	-	-
Rec6 (Fast)	0.05	55.7	IEEE-EI	0.0504	55.7	IEEE-EI
Rec6 (Slow)	3.514	55.7	IEEE-EI	3.5138	18.1	IEEE-EI
Rec9 (Fast)	0.05	18.1	IEEE-EI	0.0502	39.8	IEEE-EI
Rec9 (Slow)	9.597	18.1	IEEE-EI	9.600	55.7	IEEE-EI
Rec11 (Fast)	0.05	39.8	IEEE-EI	0.0510	18.1	IEEE-EI
Rec11 (Slow)	4.4993	39.8	IEEE-EI	4.994	39.8	IEEE-EI
*OF (best) **	21.081			21.211		
*OF (avg.) **	21.56			21.573		
*STD **	0.299			0.409		
*Range **	1.05			1.78		

**The 30-trial test raw data are provided in*
https://drive.google.com/drive/folders/1ilbjHjng2TQb2Mw3t21qsxHfWte7Pn7c?usp=sharing

Table 4.27 The operating time of each AOCR in OC1

Fault Point	$t_{j,k}$ (sec.)		$t_{j,k}$ (sec.)	
	RP	RB	RP	RB
F2	R1	-	R2	RDG
	0.66	-	-	-
F3	R2	R1	RDG	-
	0.691	0.991	-	-
F4	R3	R2	R3	RDG
	0.6265	0.9266	-	-
F5	LF5	R3	-	-
	0.5000	0.8535	-	-
F6	Rec6	R1	Rec6	R2
	0.1291 0.6353	1.3324	-	-

Table 4.28 The operating time of each AOCR in OC1 (continuous).

Fault Point	$t_{j,k}$ (sec.)	$t_{j,k}$ (sec.)	Fault Point	$t_{j,k}$ (sec.)
	RP	RB		RP
F7	LF7	Rec6	-	-
	0.5000	0.1314 0.8	-	-
F8	LF8	Rec6	-	-
	0.5000	0.1318 0.8271	-	-
F9	Rec9	R1	Rec9	R2
	0.1252 0.8000	1.156	-	-
F10	LF10	Rec9	-	-
	0.5000	0.1252 0.8000	-	-
F11	Rec11	R2	Rec11	RDG
	0.1262 0.5583	1.1264	-	-
F12	LF12	Rec11	-	-
	0.5748	0.1294 0.8748	-	-
F13	LF13	LF12	-	-
	0.5000	0.8	-	-
F14	LF14	R3	-	-
	0.5000	0.9783	-	-
F15	LF15	R3	-	-
	0.5000	0.8000	-	-

From Table 4.27, the operating time of protective devices are illustrated. We can observe that when the fault occurs in this system, the protective sequence between AOCR-AOCR, AOCR-Recloser, Recloser-Fuse, and Fuse-Fuse are correct sequence and the *CTI* margin between primary and backup protective device is not exceeded 0.3 sec.

Table 4.29 Optimal result of each protective device in OC2

Relay	ROMI-PSO			ICGA		
	TMS_i	PS_i	CS_i	TMS_i	PS_i	CS_i
R1	2.348	98.21	IEC-STI	4.325	86.43	IEEE-VI
R2	0.731	26.25	IEEE-I	0.749	26.39	IEEE-I
R3	2.290	46.02	IEEE-VI	2.022	49.08	IEEE-VI
RDG	1.79	56.0	IEEE-EI	2.38	48.81	IEEE-EI
Rec6 (Fast)	0.050	55.7	IEEE-EI	0.052	55.7	IEEE-EI
Rec6 (Slow)	4.084	55.7	IEEE-EI	4.090	18.1	IEEE-EI
Rec9 (Fast)	0.050	18.1	IEEE-EI	0.058	39.8	IEEE-EI
Rec9 (Slow)	7.798	18.1	IEEE-EI	7.818183	55.7	IEEE-EI
Rec11 (Fast)	0.05	39.8	IEEE-EI	0.053558	18.1	IEEE-EI
Rec11 (Slow)	5.971	39.8	IEEE-EI	5.980745	39.8	IEEE-EI
OF (best) *	28.144			28.613		
OF (avg.) *	29.293			31.303		
STD *	0.653			1.6263		
Range *	2.181			5.6483		

**The 30-trial test raw data are provided in https://drive.google.com/drive/folders/1ilbjHjng2TQb2Mw3t21qsxHfWte7Pn7c?usp=sharing*

Table 4.30 The operating time of each AOCR in OC2

Fault Point	$t_{j,k}$ (sec.)		$t_{j,k}$ (sec.)	
	RP	RB	RP	RB
F2	R1	-	R2	RDG
	1.1354	-	1.0295	1.3295
F3	R2	R1	RDG	-
	0.9601	1.2601	0.4611	-
F4	R3	R2	R3	RDG
	0.6601	0.9601	-	1.8055
F5	LF5	R3	-	-
	0.3192	0.6260	-	-
F6	Rec6	R1	Rec6	R2
	0.1266 0.5179	1.4344	0.1266 0.5179	1.2567

Table 4.31 The operating time of each AOCR in OC2 (continuous).

Fault Point	$t_{j,k}$ (sec.)	$t_{j,k}$ (sec.)	Fault Point	$t_{j,k}$ (sec.)
	RP	RB		RP
F7	**LF7**	**Rec6**	**-**	**-**
	0.3720	0.1284 0.6720	-	-
F8	**LF8**	**Rec6**	**-**	**-**
	0.3743	0.1288 0.6979	-	-
F9	**Rec9**	**R1**	**Rec9**	**R2**
	0.1252 0.6728	1.3679	0.1252 0.6728	1.1944
F10	**LF10**	**Rec9**	**-**	**-**
	0.3728	0.1252 0.6728	-	-
F11	**Rec11**	**R2**	**Rec11**	**RDG**
	0.1252 0.5437	0.9601	0.1252 0.5437	1.6568
F12	**LF12**	**Rec11**	**-**	**-**
	0.3927	0.1265 0.6927	-	-
F13	**LF13**	**LF12**	**-**	**-**
	0.3641	0.5826	-	-
F14	**LF14**	**R3**	**-**	**-**
	0.33	0.6549	-	-
F15	**LF15**	**R3**	**-**	**-**
	0.3138	0.6138	-	-

In the OC2, the optimal results will be changed caused the fault current flowing through the relay was changed. The *CS* of AOCR obtained by the proposed technique is IEEE-VI, IEEE-I, and IEEE-STI as shown in Table 4.28. The operating time of each protective device shows that the *CTI* margin between primary and backup is not exceeded 0.3 sec. and it's not exceeded 0.2 sec for lateral fuse as shown in Table 4.29.

Figure 4.12 shows the objective function of each trial, we can see that OC1 has a lower STD than OC2 caused by the coordination scheme being more complex. Table 4.13 shows that both methods converge to minimum results of around 10 iterations. The typical coordination curve of the protective devices are shown in Figure 4.14-4.17.

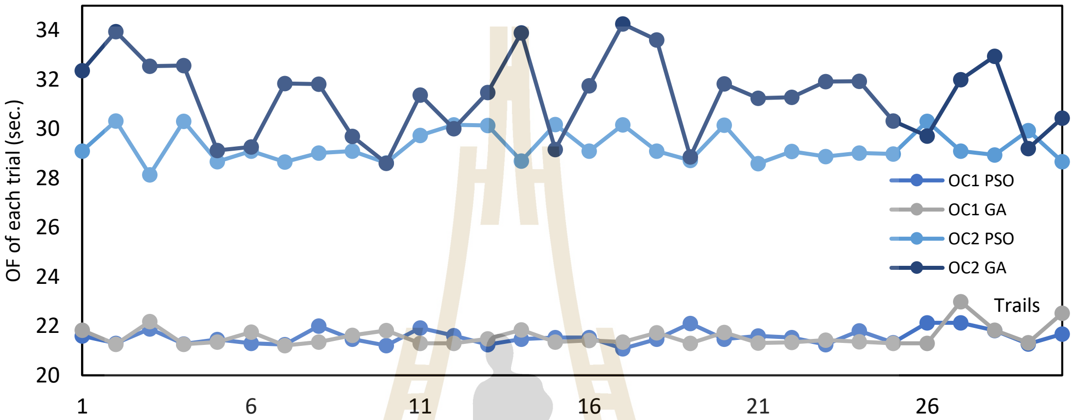

Figure 4.12 The objective function value of each trial

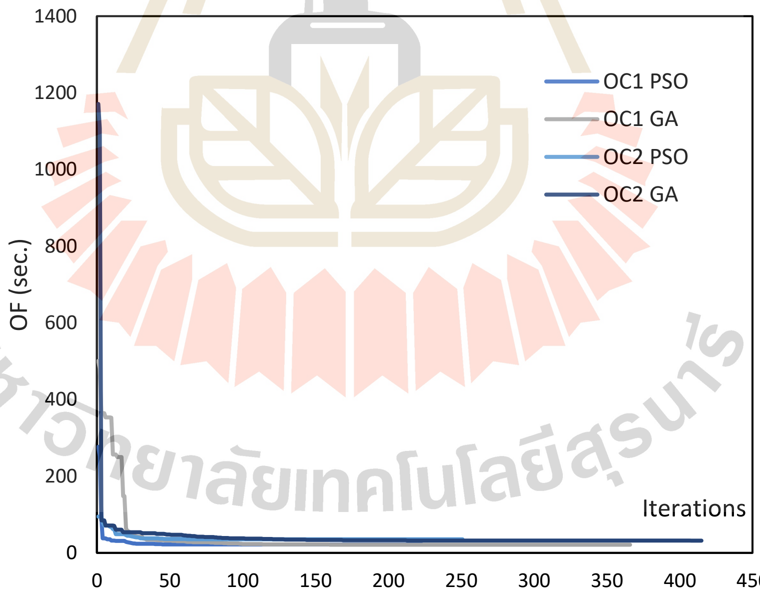

Figure 4.13 The convergence of both method

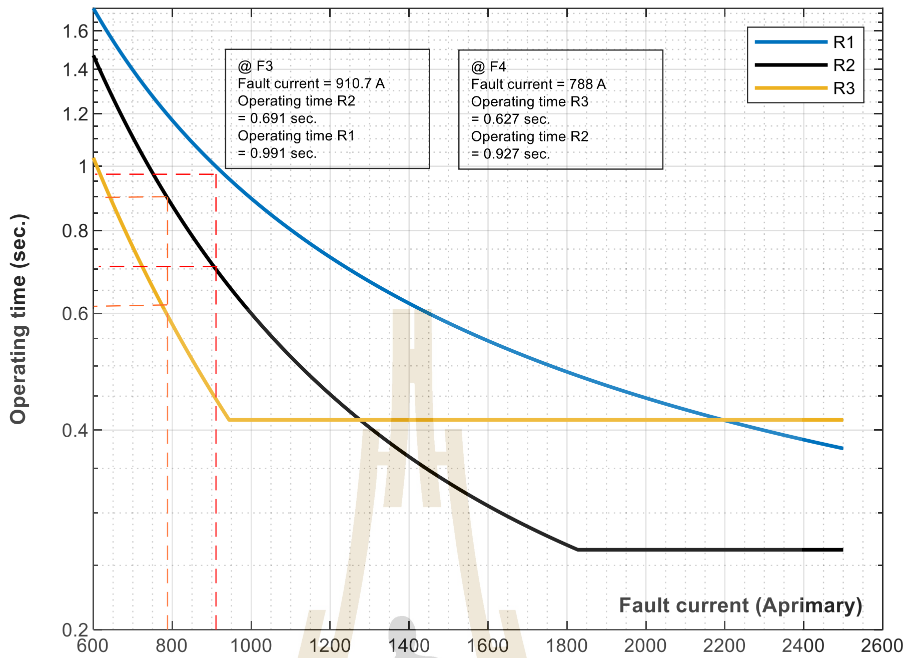

Figure 4.14 The typical coordination curve of AOCR in OC1

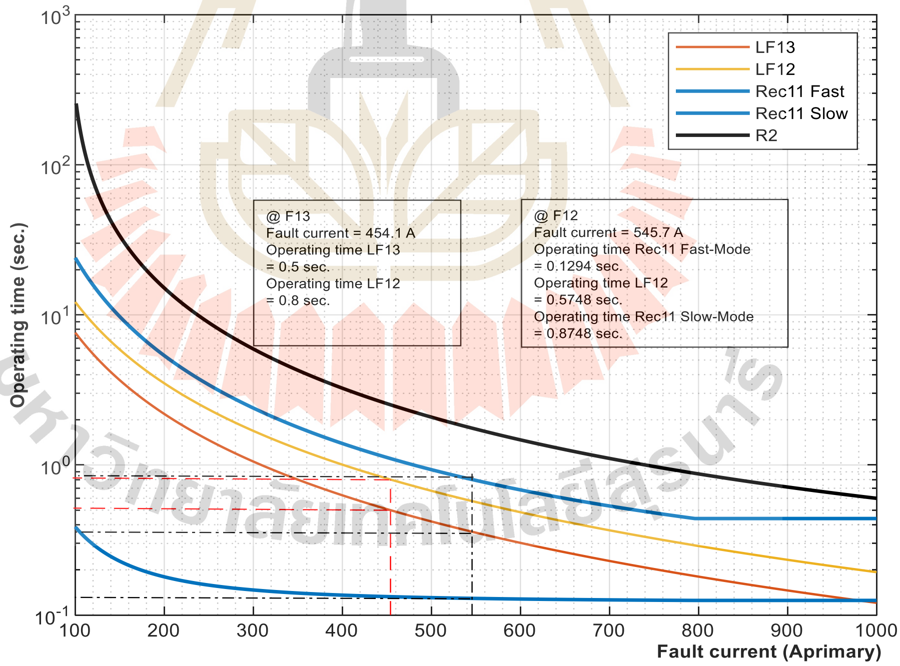

Figure 4.15 The typical coordination curve of protective device in OC1

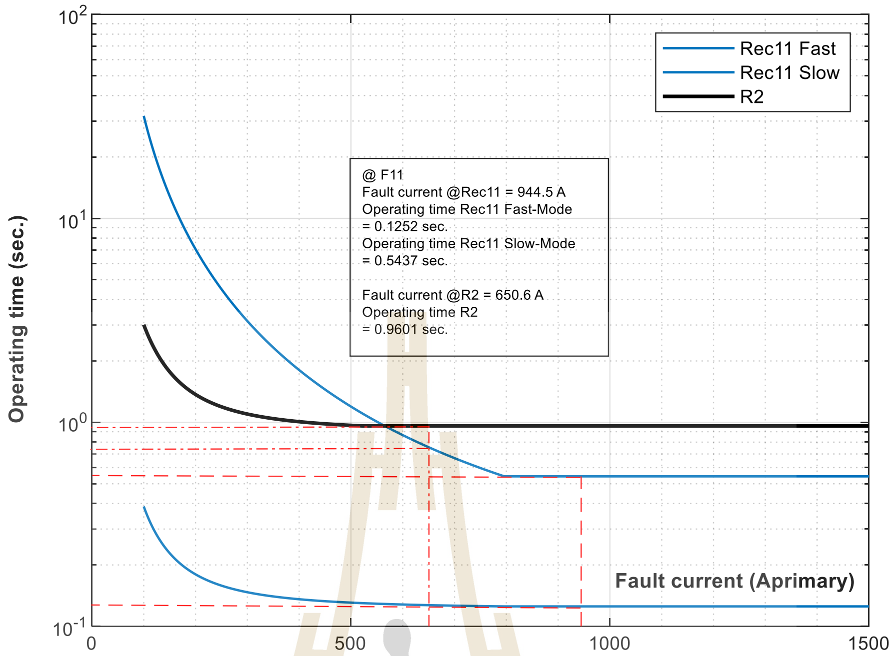

Figure 4.16 The typical coordination curve of Rec11 and R2 in OC2

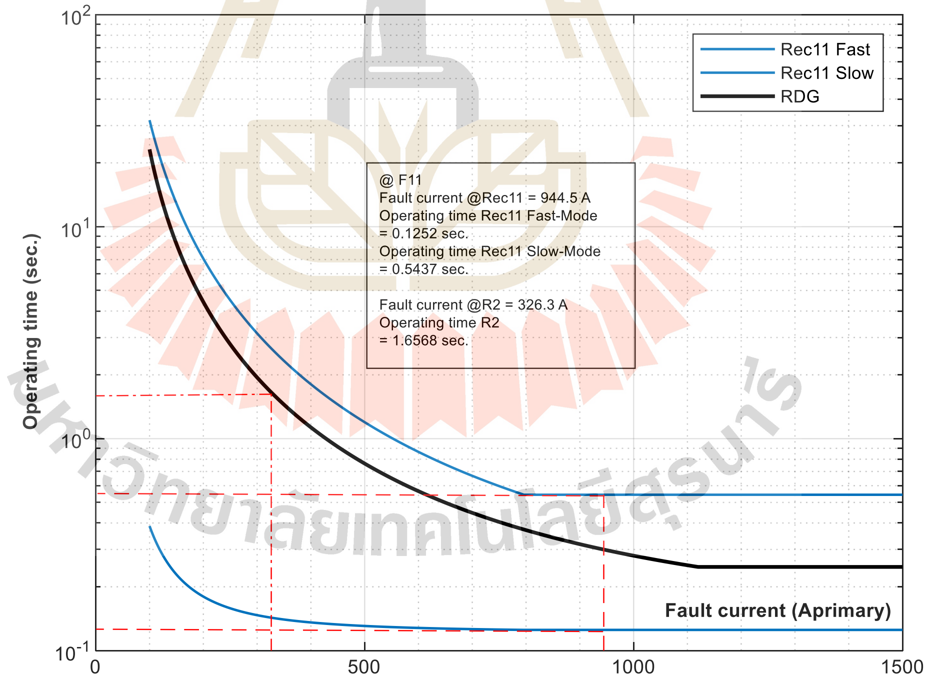

Figure 4.17 The typical coordination curve of Rec11 and RDG in OC2

4.5 Chapter Summary

The ROMI-PSO technique is used, in this section, for obtaining the OFSS of AOCR coordination with several test case. From the simulation results in this section, we can firm that the proposed technique can absolutely decrease the total operating time of the protective devices, usefulness and low computational time. In the other hand the optimal result provides the answer with fairly high STD.

CHAPTER 5
AOCR COORDINATION USING HYBRID PSO-MLIP TECHNIQUE[3]

5.1 Chapter Overview

This chapter investigates a novel approach for effectively solving the optimal coordination of AOCR problem in MILP formulation type, there are including a novel problem formulation and a new technique for obtain an optimal result.

5.2 Mathematical Formulation

This chapter proposes an approach for optimal AOCR coordination considering multiple *CS*, that consider *TMS* and *CS* as decision variables while *PS* is predetermined. Therefore, the formulation of this paper is MILP optimization. As a novelty, this paper represents a novel problem formulation by dividing *CS* into multiple sections depending on the number of *CS* types that are considered, instead of using a single integer variable of each OCR for representing *CS* as in recent existing section. The mathematical formulation can be expressed as follow,

$$\text{Minimize: } OF = \sum_{k=1}^{NF} \sum_{j=1}^{NR} (C_{SI,j} T_{SI,j,k} + C_{VI,j} T_{VI,j,k} + C_{EI,j} T_{EI,j,k}), \tag{5.1}$$

where,

$$T_{SI,j,k} = \frac{0.14\ TMS_j}{\left(PSM_{jk}\right)^{0.02} - 1}, \tag{5.2}$$

---

[3] *Part of this chapter was published in the International Journal of Intelligent Engineering and Systems (IJIES), 2022.*

$$T_{VI,j,k} = \frac{13.5\ TMS_j}{\left(PSM_{jk}\right)^1 - 1}, \tag{5.3}$$

$$T_{EI,j,k} = \frac{80\ TMS_j}{\left(PSM_{jk}\right)^2 - 1}, \tag{5.4}$$

$$PSM_{jk} = \frac{I_{jk}}{\left(PS_j CTR_j\right)} . \tag{5.5}$$

Subjected to: the standard curve selection constraint,

$$C_{SI,j}, C_{VI,j}, C_{EI,j} \in \{0,1\},\ j = 1,\ldots,NR\ , \tag{5.6}$$

$$C_{SI,j} = \begin{cases} 0, \text{ if the relay is not SI curve} \\ 1, \text{ if the relay is SI curve} \end{cases}, \tag{5.7}$$

$$C_{VI,j} = \begin{cases} 0, \text{ if the relay is not VI curve} \\ 1, \text{ if the relay is VI curve} \end{cases}, \tag{5.8}$$

$$C_{EI,j} = \begin{cases} 0, \text{ if the relay is not EI curve} \\ 1, \text{ if the relay is EI curve} \end{cases}, \tag{5.9}$$

$$C_{SI,j} + C_{VI,j} + C_{EI,j} = 1\ ,\ j = 1,\ldots,NR\ , \tag{5.10}$$

Subjected to: Eq 2.16, Eq 2.19-2.21.

Decision variable: *TMS*, C_{SI}, C_{VI}, C_{EI}.

Where, $T_{SI,j,k}$ is the operating time of relay *j* with standard inverse curve type when the fault occur at point *k*, $T_{VI,j,k}$ is the operating time of relay *j* with very inverse curve type when the fault occur at point *k*, $T_{EI,j,k}$ is the operating time of relay *j* with extremely inverse curve type when the fault occurs at point *k*, By Eq. 5.6-5.10, the OCR standard *CS* of each relay can be chosen only one from *SI*, *VI*, or *EI*.

5.3 Hybrid PSO-MILP Technique

The *TMS* of each OCR is a continuous variable while the C_{SI}, C_{VI}, and C_{EI} are a binary integer variable. Thus, the mathematical formulation of this problem is adapted to the mixed-integer nonlinear optimization problem. Meanwhile, traditional particle swarm optimization (PSO) can only solve problems with continuous variables. Hence, the PSO-MILP technique is implemented to solve this problem. The proposed method including two computational phases consist of a main loop and subroutines. A main loop is used the PSO technique to find the optimal *TMS* of each OCR. A subroutine is used the MILP technique to obtain the optimal C_{SI}, C_{VI}, and C_{EI}. The proposed technique computation of each population is shown step by step as bellow.

Step 1: Random initial position of the population matrix ($\mathbf{X}_{\mathrm{TMS}}$) within the TMS limited boundary in Eq. 2.16,

$$\mathbf{X}_{\mathrm{TMS}} = [TMS_i, \ldots, TMS_{NR}]. \tag{5.11}$$

$$TMS_i = rand(TMS_i^{\min}, TMS_i^{\max}),\ i = 1, \ldots., NR, \tag{5.12}$$

Step 2: Calculate $T_{SI,j,k}$, $T_{VI,j,k}$, and $T_{EI,j,k}$ value in Eq. 5.2-5.5 by substitute $\mathbf{X}_{\mathrm{TMS}}$ from Eq. 5.11 to Eq. 5.2-5.5. Then, the *OFnew* will be integer programming optimization with binary integer decision variables (C_{SI}, C_{VI}, and C_{EI}) of each OCR.

$$OF_{new} = OF_{old}\left(\text{subtitute } TMS \text{ to Eq. 5.1}\right) \tag{5.13}$$

Step 3: Solve MILP subroutines with objective function form Eq. 5.13 subjected to constraints in Eq. 5.6-5.10, and Eq 2.19-2.21. to obtain optimal C_{SI}, C_{VI}, and C_{EI} of each population matrix.

Minimize the objective function subroutine in: Eq. 5.13

Subjected to: Eq. 5.6-5.10, Eq 2.19-2.21.

Decision variable: C_{SI}, C_{VI}, C_{EI}.

$$\text{Obtain: } X_{CS} = \begin{bmatrix} C_{SI,i},\ldots,C_{SI,NR} \\ C_{VI,i},\ldots,C_{VI,NR} \\ C_{EI,i},\ldots,C_{EI,NR} \end{bmatrix}, \ i=1,\ldots.,NR. \tag{5.14}$$

Step 4: Find the *pbest* and *gbest* of each population matrix form Eq. 5.13-5.14.

Step 5: Update velocity and position of each population matrix from Eq. 5.12 by Eq. 5.15-5.18.

$$V^{k+1} = wV^k + c_1 r_1 \left(pbest_i^k - X^k\right) + c_2 r_2 (gbest^k - X^k), \tag{5.15}$$

$$V_i^k = [V_1^k,\ldots,V_{3NR}^k], \tag{5.16}$$

$$X_i^{k+1} = X^k + V^{k+1}, \tag{5.17}$$

$$X_{TMS}^{new} = X_i^{k+1}, \tag{5.18}$$

Step 6: Repeat step 2-5 until the maximum iteration.

5.4 Optimal results

The proposed approach was investigated on the IEC benchmark microgrid test system with various OC. In this system, the OC is considered into two conditions only (OC1 and OC2). The limit boundary of decision variables and the constant parameters of every constraint utilized are the same as in (Saldarriaga-Zuluaga, 2020) for compare the optimal solutions. Therefore, the TMS_j limit was set between TMS_j^{min} and TMS_j^{max}, with TMS_j^{min} at 0.05 and TMS_j^{max} at 15. PSM_j has a range of 1.1 PSM to 100 PSM as its limit. $T_{j,k}$ has a range of 0.01 to 2 seconds, and the *CTI* utilized is 0.3 seconds. As a result, a variety of optimal solutions are accessible. Five hundred swarm sizes are used to find the closest global optimum solution. To reduce variation, The 30 trials test is used. In this paper c_1 and c_2 are 1.49. Table 5.1 provides the optimal results of the proposed approach for each AOCR. Table 5.2 shows the operating time of each relay when a fault occurs.

Table 5.1 The optimal results for OC1

Relay	Proposed Approach				
	TMS	C_{SI}	C_{VI}	C_{EI}	*CS*
R1	-	-	-	-	-
R2	0.05	0	0	1	IEC-EI
R3	-	-	-	-	-
R4	1.3262	0	0	1	IEC-EI
R5	-	-	-	-	-
R6	3.7897	0	0	1	IEC-EI
R7	0.1339	1	0	0	IEC-SI
R8	-	-	-	-	-
R9	-	-	-	-	-
R10	0.05	0	0	1	IEC-EI
R11	-	-	-	-	-
R12	0.0821	0	0	1	IEC-EI
R13	-	-	-	-	-
R14	-	-	-	-	-
R15	-	-	-	-	-

Table 5.2 The operating times of OCRs for OC1

Fault Point	Relay	(Saldarriaga-Zuluaga, 2020)		Proposed	
		$t_{j,k}$	*CTI*	$t_{j,k}$	*CTI*
F1	R2	0.0118	0.30	0.0118	0.30
	R4	0.3118		0.3118	
F2	R4	0.2976	0.30	0.1615	0.30
	R6	0.5976		0.4615	
F3	R6	0.5976	0.34	0.173	0.3
	R7	0.9372		0.473	
F4	R12	0.01	1.00	0.01	0.6257
	R7	1.01		0.6357	
F5	R10	0.0118	0.604	0.0118	0.879
	R6	0.6159		0.8908	
OF (sec.)		4.19	2.544	3.14	2.405

Table 5.3 The optimal results for OC2

Relay	Proposed Approach				
	TMS	C_{SI}	C_{VI}	C_{EI}	*CS*
R1	0.2475	0	0	1	IEC-EI
R2	0.0674	0	0	1	IEC-EI
R3	0.05	0	0	1	IEC-EI
R4	2.089	0	0	1	IEC-EI
R5	0.1967	0	0	1	IEC-EI
R6	3.9472	0	0	1	IEC-EI
R7	0.1266	1	0	0	IEC-SI
R8	0.1135	0	0	1	IEC-EI
R9	0.05	0	0	1	IEC-EI
R10	0.0753	0	0	1	IEC-EI
R11	0.1428	0	1	0	IEC-VI
R12	0.1123	0	0	1	IEC-EI
R13	0.1625	0	1	0	IEC-VI
R14	0.0978	0	1	0	IEC-VI
R15	0.0885	1	0	0	IEC-SI

The proposed algorithm provides the results with several types of *CS*, not a single type of curve. The *CSs* obtained by the proposed method are mostly IEC-EI, because it provides the minimum operating time than other curves. Meanwhile, the trend of *TMSs* are converge to the lower bound, but they can slightly increase to avoid the constraint violation. The proposed method improves the objective function by around 34% from the previous paper (Saldarriaga-Zuluaga, 2020) while the total *CTI* of the system is slightly decrease from (Saldarriaga-Zuluaga, 2020). The coordination curve of each AOCR for the proposed approach are shown in Fig. 5.1 From Table 5.3, the *CS* were provided by the proposed algorithm are mostly IEC EI, similar to OC1, the trend of *TMS* still converged as close as possible to lower bound. The proposed algorithm results to the best objective function value, around 44% lower than (Saldarriaga-Zuluaga, 2020). The results also shown that the proposed algorithm can effectively improve the system reliability from (Saldarriaga-Zuluaga, 2020) as illustrated in Table 5.4. The coordination curve of each OCR for the proposed approach can be seen in Fig. 5.2.

With the proposed method, the total operating time of the OCR protection for the IEC benchmark microgrid has decrease over time, by enhancing the constraint and demonstrating the ability of the proposed technique on the OCR’s parameters setting.

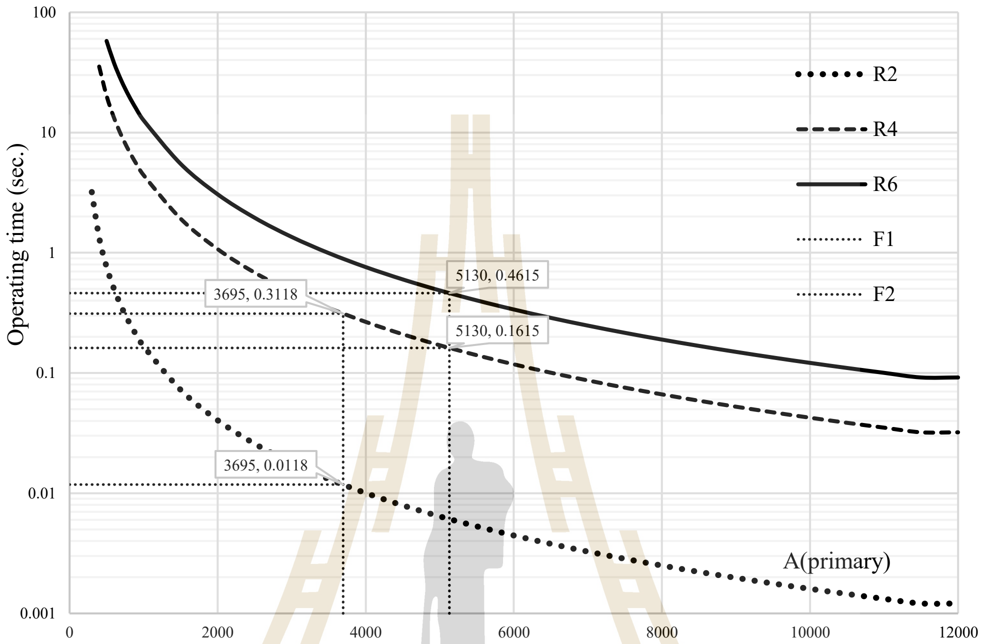

Figure 5.1 The coordination curve of OCR in OC1

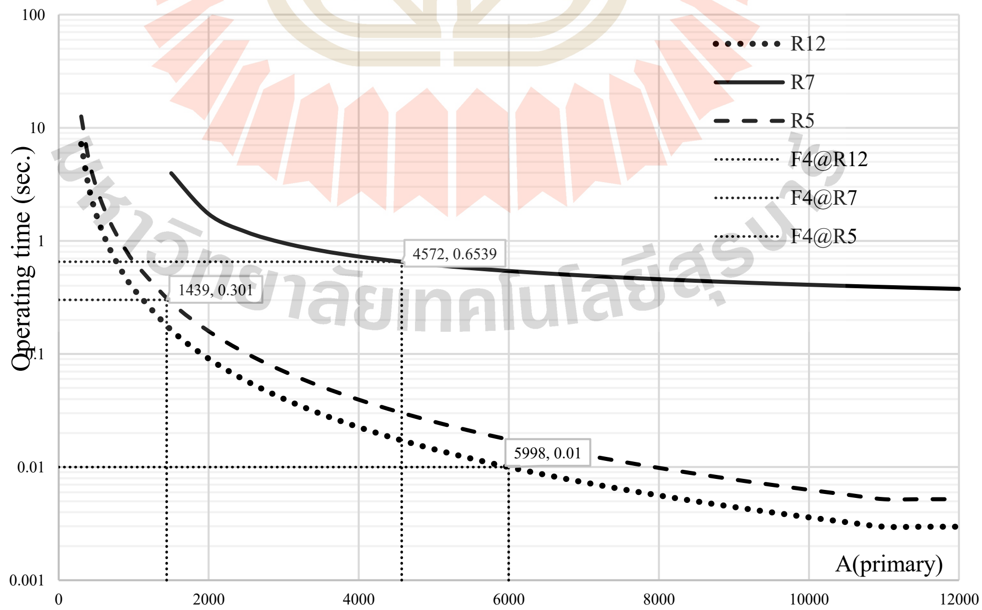

Figure 5.2 The coordination curve of OCR in OC2

Table 5.4 The operating times of OCRs for OC2

<table>
<tr><th rowspan="2">Fault Point</th><th rowspan="2">Relay</th><th colspan="2">(Saldarriaga-Zuluaga, 2020)</th><th colspan="2">Proposed</th></tr>
<tr><th>$t_{j,k}$</th><th>CTI</th><th>$t_{j,k}$</th><th>CTI</th></tr>
<tr><td rowspan="4">F1</td><td>R2</td><td>0.0405</td><td rowspan="2">0.3</td><td>0.01</td><td rowspan="2">0.3</td></tr>
<tr><td>R4</td><td>0.3405</td><td>0.31</td></tr>
<tr><td>R1</td><td>0.2858</td><td rowspan="2">0.3</td><td>0.2959</td><td rowspan="2">0.3</td></tr>
<tr><td>R13</td><td>0.5858</td><td>0.5959</td></tr>
<tr><td rowspan="5">F2</td><td>R4</td><td>0.3405</td><td rowspan="3">0.625</td><td>0.1269</td><td rowspan="3">0.6</td></tr>
<tr><td>R6</td><td>0.6629</td><td>0.4269</td></tr>
<tr><td>R15</td><td>0.6406</td><td>0.4269</td></tr>
<tr><td>R3</td><td>0.0302</td><td rowspan="2">0.3</td><td>0.0759</td><td rowspan="2">0.3</td></tr>
<tr><td>R1</td><td>0.3301</td><td>0.3759</td></tr>
<tr><td rowspan="5">F3</td><td>R6</td><td>0.6629</td><td rowspan="3">0.6</td><td>0.1475</td><td rowspan="3">0.6</td></tr>
<tr><td>R7</td><td>0.9628</td><td>0.4475</td></tr>
<tr><td>R8</td><td>0.9629</td><td>0.4475</td></tr>
<tr><td>R5</td><td>0.186</td><td rowspan="2">0.553</td><td>0.0911</td><td rowspan="2">0.415</td></tr>
<tr><td>R15</td><td>0.7386</td><td>0.5063</td></tr>
<tr><td rowspan="5">F4</td><td>R12</td><td>0.0405</td><td rowspan="3">1.66</td><td>0.01</td><td rowspan="3">0.944</td></tr>
<tr><td>R7</td><td>1.4</td><td>0.6539</td></tr>
<tr><td>R5</td><td>0.3405</td><td>0.301</td></tr>
<tr><td>R8</td><td>0.8467</td><td rowspan="2">0.3</td><td>0.3857</td><td rowspan="2">0.3</td></tr>
<tr><td>R11</td><td>1.14</td><td>0.6857</td></tr>
<tr><td rowspan="5">F5</td><td>R10</td><td>0.0405</td><td rowspan="3">1.157</td><td>0.01</td><td rowspan="3">1.701</td></tr>
<tr><td>R6</td><td>0.3405</td><td>1.0861</td></tr>
<tr><td>R15</td><td>0.8976</td><td>0.6353</td></tr>
<tr><td>R9</td><td>0.1792</td><td rowspan="2">0.3</td><td>0.1698</td><td rowspan="2">0.3</td></tr>
<tr><td>R14</td><td>0.4792</td><td>0.4698</td></tr>
<tr><td>OF (sec.)</td><td></td><td>12.48</td><td>6.09</td><td>8.701</td><td>5.76</td></tr>
</table>

In comparison to existing works, the proposed technique is successfully reduced the total operating time and total *CTI* of the AOCR as shown in Table 5.5. The proposed algorithm has been tested with 30 trials to verify the optimal results. Table 5.6 shows the best, mean, worst, range, and standard deviation (*STD*) of the optimal results. From Table 5.6, it is clear that the biggest advantage of the proposed technique is that it provides the optimal results with significantly low *STD*. Hence, the proposed hybrid PSO-MILP technique is suitable for finding the global minimum objective function value of the overcurrent relay coordination. The convergence plot of the proposed method is shown in Fig. 5.3

Table 5.5 A comparative study with previous works

Operating mode	OC1	OC2	Total time (sec.)	Total *CTI* (sec.)
(Saad, 2019)	7.53	19.18	26.71	9.08
(El-Naily N, 2019)	6.64	17.48	24.12	8.93
(Muñoz-Galeano N, 2020)	4.99	13.66	18.65	8.56
(Saldarriaga-Zuluaga, 2020)	4.19	12.48	16.67	8.29
Proposed	3.14	8.701	11.84	8.165

Table 5.6 The results of 30 trials test

Operating mode	OC1	OC2
*Best**	3.14	8.701
*Mean**	3.14	8.847
*Worst**	3.14	8.984
*STD**	10^{-8}	0.111
*Range**	10^{-8}	0.283

**The 30-trial test raw data are provided in*
https://drive.google.com/drive/folders/1ilbjHjng2TQb2Mw3t21qsxHfWte7Pn7c?usp=sharing

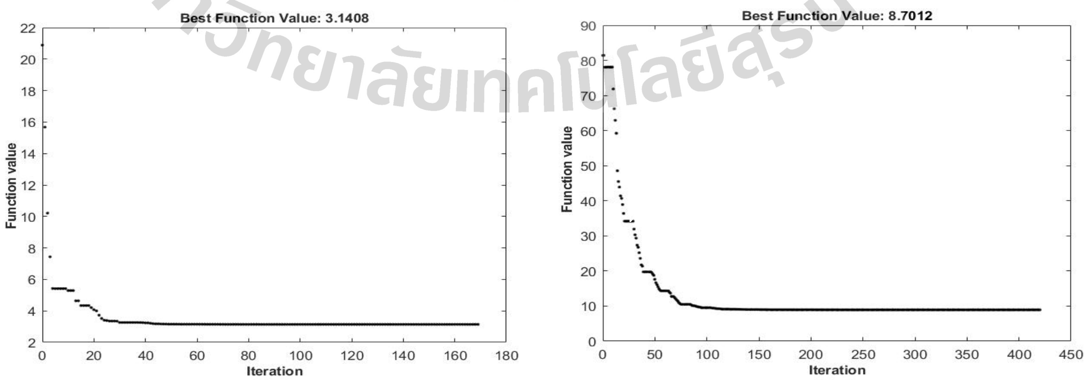

(a) OC1 (b) OC2

Figure 5.3 Convergences plots of the proposed method

5.5 Study on Transferring mode

This section provides further investigation on the advantage of AOCR by considering the emergency case that the optimal setting scheme was not adapted itself when the operating conditions changed.

Table 5.7 The setting group of OC1 when operated in OC2

Fault Point	The setting group of OC1 when operated in OC1				
	Primary	Backup		Primary	Backup
	RP1.1	RB1.1	RB1.2	RP2.1	RB2.1
F1	R2	R4	-	R1	R13
	0.0118	0.3118		-	-
F2	R4	R6	R15	R3	R1
	0.1615	0.4615	-	-	-
F3	R6	R7	R8	R5	R15
	0.173	0.473	-	-	-
F4	R12	R7	R5	R8	R11
	0.01	0.636	-	-	-
F5	R10	R6	R15	R9	R14
	0.0118	0.8908	-	-	-
Fault Point	The setting group of OC1 when operated in OC2				
	Primary	Backup		Primary	Backup
	RP1.1	RB1.1	RB1.2	RP2.1	RB2.1
F1	R2	R4	-	R1	R13
	0.007	0.197		N/A	N/A
F2	R4	R6	R15	R3	R1
	0.081	0.230	N/A	N/A	N/A
F3	R6	R7	R8	R5	R15
	0.142	0.449	N/A	N/A	N/A
F4	R12	R7	R5	R8	R11
	0.007	0.573	N/A	N/A	N/A
F5	R10	R6	R15	R9	R14
	0.007	0.503	N/A	N/A	N/A

** N/A is relay has to operate but it does not.*

From Table 5.7, when the operating condition of network topology changed but the setting scheme of AOCR is still stuck in the previous mode (OC1), we can see that when F1 and F2 have occurred, the relay operating time between primary and backup relay operate with lower CTI than standard (0.2 sec.), it can lead to miscoordination. Furthermore, the relay cannot clear revere flow faults by DG's contribution due to reverse protection relays are not required to operate in OC1 but it requires in OC2.

5.6 Chapter Summary

The hybrid PSO-MILP technique is used, in this section, for obtaining the optimal setting parameters of AOCR coordination with a novel AOCR problem formulation. From the simulation results in this section, we can firm that the proposed technique can absolutely decrease the total operating time of the AOCR by around 34 percent for OC1 and around 44 percent for OC2 when compared with previous research. Therefore, the significant advantage of this technique is providing the optimal results with the lowest *STD* that are suitable for comparing the optimal answer and finding the global optimal results.

CHAPTER 6

CONCLUSSION AND RECOMENDATION

6.1 Chapter Overview

This chapter provides a conclusion on each section and overall, the advantage and disadvantages of this research are obtained in the recommendation.

6.2 Conclusion

Chapter I provide the problem statement of the distribution system with DER penetration and the impact on traditional protection strategy. Therefore, the objective, limitation, and scope of this research are obtained.

In Chapter II, we can conclude that the adaptive protection technology plays an important role to handle this problem by applying the protection setting scheme of OCR with the multi-operating condition of the system to them. In another way, to find the effectiveness's protection setting schemes of OCR, we have reviewed several types of research on the OCR coordination problem.

In Chapter III, we have compared several types of the OCR coordination problem by testing with a modified four bus test system, to find the most effective OCR coordination problem types. Found that the MINLP formulation type with OFSS is the most powerful.

In Chapter IV, we implemented the ROMI-PSO technique to solve OFSS of AOCR coordination with IEC benchmark test system and IEEE 15 bus radial system. Form the optimal results we can conclude that the proposed technique is more suitable than previous existing technique by it can significantly decrease the total operating time while the reliability of system maintained.

In Chapter V, we implemented the novel formulation and new hybrid technique for solving the MILP coordination of AOCR. The optimal results show that the proposed technique can absolutely decrease the total operating time of the relay and provided the results with low STD.

In this research, we proposed several strategies for obtaining the optimal setting scheme of the AOCR coordination problem response to the DG penetration. The ROMI-PSO technique and the hybrid PSO-MILP technique were implemented to find the optimal results. Several tests were carried out using the modified 4 bus radial test system, the IEC benchmark microgrid test system, and the IEEE 15 bus radial system. The optimal results show that the proposed OFSS of AOCR coordination can absolutely address the DG penetration while improving the fast, selective, reliability of the modern OCR protection system.

6.3 Recommendation

The advantage of the proposed OFSS approach is effectively decreasing the total operating time of the adaptive overcurrent relay in the system while maintaining the coordination sequence of the protective device. However, the proposed approach can be guaranteeing only the coordination sequence when a maximum fault occurred because only the maximum fault currents are considered on the objective function.

The advantage of the ROMI-PSO technique is simple, useful, less time-consuming but there are provides optimal results with fairly high STD. Consequently, we can decrease the STD by increasing the swarm size but its effects on computational time increase.

The advantage of the hybrid PSO-MILP technique is obtaining closely global optimum results with fairly low STD. However, this technique used high computational time and there can solve with the mixed integer linear problem only. the OFSS coordination with MINLP type cannot be used

REFFERENCE

REFFERENCE

Abdul Wadood, Chang-Hwan Kim, Saeid Gholami Farkoush, Kumail Hassan Kharal, Sang-Bong Rhee Tahir Khurshaid. (2018). A Protective Optimal Coordination Scheme for Directional Overcurrent Relays Using Modified Seeker Algorithm. **International Conference on Computing, Power and Communication Technologies (GUCON) Galgotias University, Greater Noida, UP, India.**

Abdul Wadood, Chang-Hwan Kim, Saeid Gholami Farkoush, Kumail Hassan Kharal, Sang-Bong Rhee Tahir Khurshaid. (2019). An Improved Optimal Solution for the Directional Overcurrent Relays Coordination Using Hybridized Whale Optimization Algorithm in Complex Power Systems. **IEEE Access, Volume 7.**

Adhishree, Ram Krishan Jyant Mani Tripathi. (2014). Optimal coordination of overcurrent relays using gravitational search algorithm with DG penetration. **6th IEEE Power India International Conference (PIICON), Delhi, India.**

Alnufaie Lafi A. Y. Hatata. (2018). Ant Lion Optimizer for Optimal Coordination of DOC Relays in Distribution Systems Containing DGs. **IEEE Access, Volume 6.**

Amany. M. El Zonkoly, Hamdy. A. Ashour Ayatte. I. Atteya. (2017). Optimal Relay Coordination of an Adaptive Protection Scheme using Modified PSO Algorithm. **Nineteenth International Middle East Power Systems Conference (MEPCON), Menoufia University, Egypt.**

Amol A Kalage Sumit U Pathade. (2017). Optimum Coordination of Directional Overcurrent Relay using Genetic Algorithm Technique. **International Conference on Current Trends in Computer, Electrical, Electronics and Communication (ICCTCEEC-2017), Mysore, India, 278-283.**

Asim Datta, Priyanath Das Debasree Saha. (2015). Optimal coordination of directional overcurrent relays in power systems using Symbiotic Organism Search Optimisation technique. **IET Generation Transmission & Distribution, Volume 10, Issue 11, 2681 – 2688.**

B.K. panigrahi, Rohan Mukherjee Manohar Singh. (2012). Optimum Coordination of Overcurrent Relays Using CMA-ES Algorithm. **IEEE International Conference on Power Electronics, Drives and Energy Systems December16-19, Bengaluru, India,.**

Browh Serge Tekpeti, Xiaoning Kang Mostafa Kheshti. (2016). The Optimal Coordination of Over-current Relay Protection in Radial Network Based on Particle Swarm Optimization. **IEEE PES Asia-Pacific Power and Energy Conference, Xi'an, China.**

Dimas O. Anggriawan, Alfa K. Faizin, Ardyono Priyadi, Margo Pujiantara , Taufik Taufik, Mauridhi Hery Purnomo Anang Tjahjono. (2017). Adaptive modified firefly algorithm for optimal coordination of overcurrent relays. **IET Generation Transmission & Distribution.**

George N. Korres, Nikos D. Hatziargyriou Vasileios A. Papaspiliotopoulos. (2015). Protection Coordination in Modern Distribution Grids Integrating Optimization Techniques with Adaptive Relay Setting. **IEEE Eindhoven PowerTech, Eindhoven, Netherlands.**

Hadi Saadat. (1999). Power system analysis. McGrew-Hill Series in Electrical Engineering and Computer engineering, **University of Michigan**.

Isa Hafidz, Arif Setiawan, Ardyono Priyadi, Mauridhi Hery Purnomo, Dimas Okky Anggriawan, Anang Tjahjono Margo Pujiantara. (2016). Optimization technique based adaptive overcurrent protection in radial system with DG using genetic algorithm. **International Seminar on Intelligent Technology and Its Applications (ISITIA), Lombok, Indonesia.**

Jayant Mani Tripathi, and Soumya R Mohanty Adhishree. (2014). A Simulation Based Comparative Study of Optimization Techniques for Relay Coordination with Distributed Generation. **IEEE Students Conference on Engineering and Systems.**

Jinka Rohit, and O. V. Gnana Swathika A. V. K. Chaitanya. (2017). Optimum Coordination of Overcurrent Relays in Distribution Systems using Differential Evolution and Dual Simplex Methods. **IEEE International Conference on Computing Methodologies and Communication (ICCMC), 212-215.**

Jose Vicente Rodríguez Elmer Sorrentino. (2020). Effects of the curve type of overcurrent functions and the location of analyzed faults on the optimal coordination of directional overcurrent protections. **Computers & Electrical Engineering, Volume 88.**

López-Lezama J.M, Muñoz-Galeano N Saldarriaga-Zuluaga S.D. (2021). Optimal coordination of over-current relays in microgrids considering multiple characteristic curves. **Alexandria Engineering Journal, 2093-2113.**

M.s. Sachdev and T.s. Sidhu Bijoy Chattopahyay. (1996). An on-line relay coordination algorithm for adaptive protection using linear programming technique. **IEEE Transaction on Power Delivery, vol.11, no.1, 165-173.**

Mahamad Nabab Alam. (2019). Overcurrent protection of AC microgrids using mixed characteristic curves of relays. **Computers & Electrical Engineering, Volume 74, 74-88.**

Manohar Singh. (2013). Protection Coordination in Grid Connected & Islanded Modes of Micro-Grid Operations. **IEEE Innovative Smart Grid Technologies-Asia (ISGT Asia).**

Naser El Naily, Jamal Wafi, T. Hussein, Faisal A. Mohame Saad. M. Saad. (2018). An Optimized Proactive Over-Current Protection Scheme for Modern Distribution Grids Integrated with Distributed Generation Units. **The 9th International Renewable Energy Congress (IREC).**

National Energy Policy Council. (2015). Thailand Power Development Plan 2015-2036 (PDP2015).

O.V Gnana Swathika Kevin Isaac Tharakan. (2017). Optimum Coordination of using Overcurrent Relay using Firefly and Ant Colony Optimization Algorithm. **IEEE International Conference on Computing Methodologies and Communication (ICCMC), 617-621.**

O.V. Gnana Swathika, and Dr. S. Hemamalini Anjali Gupta. (2015). Optimum Coordination of Overcurrent Relays in Distribution Systems using Big-M and Dual Simplex Methods. **International Conference on Computational Intelligence and Communication Networks, 1540-1544.**

P. N. Korde P. P. Bedekar. (2016). Optimum Coordination of Overcurrent Relays Using the Modified Jaya Algorithm. **IEEE Uttar Pradesh Section International Conference on Electrical, Computer and Electronics Engineering (UPCON) Indian Institute of Technology (Banaras Hindu University) Varanasi, India, 249-284.**

P. N. Korde P. P. Bedekar. (2017). Determining Optimum Time Multiplier Setting of Overcurrent Relays Using Modified Jaya Algorithm. **International Conference on Innovations in Power and Advanced Computing Technologies (i-PACT2017), 1-6.**

P. P. Bedekar P. N. Korde. (2016). Optimal Overcurrent Relay Coordination in Distribution System using Nonlinear Programming Method. **International Conference on Electrical Power and Energy Systems (ICEPES) Maulana Azad National Institute of Technology, Bhopal, India, 372-376.**

Power System Relaying Committee of the IEEE Power Engineering Society. (1996). IEEE Standard Inverse-Time Characteristic Equations for Overcurrent Relays. Inc. 345 East 47th Street, New York, NY 10017-2394: **The Institute of Electrical and Electronics Engineers.**

R.K. Nema D. Vijayakumar. (2008). Superiority of PSO Relay Coordination Algorithm over Non-Linear Programming: A Comparison Review and Verification. **International Conference on Power System Technology and IEEE Power India Conference.**

R.W. De Mello P.P. Barker. (2000). Determining the Impact of Distributed Generation on Power Systems: Part 1 - Radial Distribution Systems. **Power Engineering Society Summer Meeting, Seattle, WA, USA, 1645-1656.**

Ron Allan, Peter Crossley, Daniel Kirschen, Goran Strba Nick Jenkins. (2000). Embedded Generation Hand book. London, United Kingdom: **The Institution of Engineering and Technology (IET Power and Energy series 31).**

S. Madhu, M. V. G. Raju, and O.V. Gnana Swathika A.M.S. Deepak. (2017). Optimum Coordination of Overcurrent Relays in Distribution Systems using Big-M and Revised Simplex Methods. **IEEE International Conference on Computing Methodologies and Communication (ICCMC), 613-616.**

S.M, El-Naily N, and Mohamed F.A Saad. (2019). A new constraint considering maximum PSM of industrial over-current relays to enhance the performance of the optimization techniques for microgrid protection schemes. **Sustain. Cities Soc., 445–457.**

Saad S.M, Hussein T, Mohamed F.A El-Naily N. (2019). A novel constraint and non-standard characteristics for optimal over-current relays coordination to enhance microgrid protection scheme. **IET Gener. Transm. Distrib., 780–793.**

Saldarriaga-Zuluaga S.D, López-Lezama J.M, Muñoz-Galeano N. (2020). Optimal Coordination of Overcurrent Relays in Microgrids Considering a Non-Standard Characteristic. **Energies.**

Saldarriaga-Zuluaga S.D, Muñoz-Galeano N López-Lezama J.M. (2021). adaptive protection coordination scheme in microgrids using directional over-current relays with non-standard characteristics. **Heliyon Volume 7, Issue 4.**

Sergio D., López-Lezama, Jesús M., Muñoz-Galeano, Nicolás Saldarriaga-Zuluaga. (2020). An Approach for Optimal Coordination of Over-Current Relays in Microgrids with Distributed Generation. **Electronics, Volume 9.**

Shruti Khatri Pushpa Bhatiya. (2017). Optimum values of TMS and PS of Overcurrent Relays using Amalgam of GA-NLP Methods. **International Conference on Information, Communication, Instrumentation and Control (ICICIC), Indore, India.**

Sudhir R. Bhide, and Vijay S. Kale Prashant P. Bedekar. (2009). Optimum coordination of overcurrent relays in distribution system using dual simplex method. **International Conference on Emerging Trends in Engineering and Technology (ICETET-09), pp.555-55.**

Sudhir R. Bhide, and Vijay S. Kale Prashant P. Bedekar. (2009). Optimum coordination of overcurrent relays in distribution system using genetic algorithm. **Third International Conference on Power Systems, Kharagpur, INDIA December 27-29 ICPS – 247.**

Sudhir Ramkrishna Bhide Prashant Prabhakar Bedekar. (2011). Optimum Coordination of Directional Overcurrent Relays Using the Hybrid GA-NLP Approach. **IEEE Transactions on Power Delivery, Volume 26, Issue 1.**

Susmita Kar. (2017). A comprehensive protection scheme for micro-grid using fuzzy rule base approach. **Energy Systems.**

T.A. Kurashvili, G.N. Korres V.A. Papaspiliotopoulos. (2014). Optimal coordination of directional overcurrent relays in distribution systems with distributed generation based on a hybrid PSO-LP algorithm. **MedPower, Athens.**

Tanuja N. Date Sahebrao V. Chakor. (2016). Optimum Coordination of Directional Overcurrent Relay in presence of Distributed Generation Using Genetic Algorithm. **10th International Conference on Intelligent Systems and Control (ISCO), Coimbatore, India.**

Turaj Amraee. (2012). Coordination of Directional Overcurrent Relays Using Seeker Algorithm. **IEEE Transactions on Power Delivery, Volume 27, Issue 3.**

Vasileios Papaspiliotopoulos, George Korres, Nikos Hatziargyriou Vasilis Kleftakis. (2018). Adaptive Protection in Distribution power networks. **NTUA, Athens.**

W. El-Khattam, M. ElMesallamy, and H.A. Talaat A.M. Ibrahima. (2015). Adaptive protection coordination scheme for distribution network with distributed generation using ABC. **International Journal of Electrical Systems and Information Technology.**

APPENDIX

APPENDIX A

PARAMETER OF THE TEST SYSTEM

A.1 The modified 4-bus radial distribution system

Table A.1 Parameter of the system

No.	Particular	Ratings
1	Line	0+j1.0331 p.u
2	Generator	100 MVA ,22 kV, X'd = 1.00 p.u
3	DG	0.5+j0.5 MVA ,22 kV, X'd = 1.20 p.u

A.2 The IEC benchmark microgrid

The base power has been chosen as 10 MVA. The details of the studied IEC microgrid are given as follows,

1) Utility: rated short-circuit MVA = 1000, f = 60 Hz, rated kV = 120, Vbase = 120 kV.

2) DGs: 1) DG1, DG2: synchronous generator with rated MVA = 9, f = 60 Hz, rated kV = 2.4, Inertia constant H = 1.07 s., friction factor F = 0.1 pu, Rs = 0.0036 pu, Xd = 1.56 pu, Xd' = 0.296 pu, Xd'' = 0.177 pu, Xq= 1.06 pu, Xq'' = 0.177 pu, Xl= 0.052 pu, Td' = 3.7 s, Td'' = 0.05 s, Tqo''= 0.05 s.

2) DG3: (inverter base DG) Wind farm consisting of three 2 MVA wind turbines (6 MVA, pf = 0.9), f = 60 Hz, rated kV = 575 V, inertia constant H = 0.62 s, friction factor F = 0.1 pu, Rs = 0.006 pu, Xd = 1.305 pu, Xd' = 0.296 pu, Xd''= 0.252 pu, Xq= 0.474 pu, Xq'' = 0.243 pu, Xl= 0.18 pu, T do'= 4.49 s, T do''= 0.0681 s, T q''= 0.0513 s. 575 V, 60 Hz. The synchronous generator with inverter interface to main grid has been considered for the proposed study (Type-4 detailed model in MATLAB/SIMULINK).

3) DG4: DFIG-based wind farm consisting of six 1.5-MVA wind turbines (9 MVA, pf = 0.9), f = 60 Hz, rated kV = 575 V, Inertia constant H = 0.685 s, friction factor F = 0.01 pu, Rs = 0.023 pu, Lls = 0.18 pu, Rr' = 0.016 pu, Llr' = 0.16 pu, Lm = 2.9 pu.

3) Transformer (TRs): 1) TR1: rated MVA = 15, f = 60 Hz, rated kV = 120/25, Vbase = 25 kV, R1 = 0.00375 pu, X1 = 0.1 pu, Rm = 500 pu, Xm = 500 pu. 2) TR2, TR3: rated MVA = 12, f = 60 Hz, rated kV = 2.4 kV/25 kV, Vbase = 25 kV, R1 = 0.00375 pu, X1 = 0.1 pu, Rm = 500 pu, Xm = 500 pu. 3) TR4: rated MVA = 10, f = 60 Hz, rated kV = 575 V/25 kV, Vbase = 25 kV, R1 = 0.00375 pu, X1 = 0.1 pu, Rm = 500 pu, Xm = 500 pu.

4) Distribution lines (DL): DL1, DL2, DL3, DL4, and DL5: PI-Section, 30 km each, Vbase = 25 kV, R0 = 0.1153 Ω/km, R1 = 0.413 Ω/km, L0 = 1.05 e − 3 H/km, L1 = 3.32 e − 3 H/km, C0 = 11.33 e − 9 F/km, X1 = 5.01 e − 9 F/km.

5) Total loading (sum of L1 to L6) considered: 22 MW, 10 MVAR.

A.3 The modified IEEE 15 bus radial test system

Utility: MVA base= 30, f = 50 Hz, rated kV = 11, Vbase = 11 kV. X'd =1 pu

DG : 500 kW, 500 kVar, X'd = 4 pu.

Table A.2 Branch Data

From	To	Resistance (ohms)	Inductance (ohm)
1	2	1.35309	1.32349
2	3	1.17024	1.14464
3	4	0.84111	0.82271
4	5	1.52348	1.0276
2	9	2.01317	1.3579
9	10	1.68671	1.1377
2	6	2.55727	1.7249
6	7	1.0882	0.734
6	8	1.25143	0.8441
3	11	1.79553	1.2111
11	12	2.44845	1.6515
12	13	2.01317	1.3579
4	14	2.23081	1.5047

Table A.3 Load Data

BUS	Bustype	kW	kVAR	kVA	PF
1	1	0	0	0	0.7
2	3	44.1	44.982	63	0.7
3	3	70	71.4	100	0.7
4	3	140	142.8	200	0.7
5	3	44.1	44.982	63	0.7
6	3	140	142.8	200	0.7
7	3	140	142.8	200	0.7
8	3	70	71.4	100	0.7
9	3	70	71.4	100	0.7
10	3	44.1	44.982	63	0.7
11	3	140	142.8	200	0.7
12	3	70	71.4	100	0.7
13	3	44.1	44.982	63	0.7
14	3	70	71.4	100	0.7
15	3	140	142.8	200	0.7

Table A.4 Load flow results data

	V (pu.)	Del (theta)	V (pu.)	Del (theta)
1	1	0	9	0.967974
2	0.971286	0.000555	10	0.9669
3	0.956674	0.000857	11	0.949957
4	0.95091	0.000981	12	0.945834
5	0.949923	0.001194	13	0.944523
6	0.958235	0.003301	14	0.948613
7	0.956012	0.003776	15	0.948445
8	0.956958	0.003574		

Table A.5 Line flow results data

From	To	Line flow (pu.)
1	2	0.0429393723127171 + 0.0436071145925537i
2	3	0.0245160697557872 + 0.0249463259332516i
3	4	0.0132414467725690 + 0.0134948034297432i
4	5	0.00147184563466518 + 0.00150064489601526i
2	9	0.00382104200591827 + 0.00389134464774518i
9	10	0.00147197225376856 + 0.00150073030165897i
2	6	0.0118757755395348 + 0.0120410456834065i
6	7	0.00467978403017981 + 0.00476884777138287i
6	8	0.00233709712168832 + 0.00238253870672004i
3	11	0.00856504539673790 + 0.00870350891490922i
11	12	0.00382584985446584 + 0.00389458758179599i
12	13	0.00147246684351908 + 0.00150106390658209i
4	14	0.00234016126261751 + 0.00238460549539984i
4	15	0.00468132694173302 + 0.00476988847812777i

Table A.6 Line loses flow results data

From	To	Power loss (pu.)
1	2	0.00125648501147557 + 0.00122899832815097i
2	3	0.000376244253147133 + 0.000368013588599208i
3	4	8.14462668852906e-05 + 7.96645601992569e-05i
4	5	1.84563466472452e-06 + 1.24489601535378e-06i
2	9	1.57364188165671e-05 + 1.06143460865283e-05i
9	10	1.97225376838287e-06 + 1.33030165961473e-06i
2	6	0.000192227720999796 + 0.000129659205305872i
6	7	1.31173635136905e-05 + 8.84777138306266e-06i
6	8	3.76378835534969e-06 + 2.53870672011197e-06i
3	11	7.25288756051479e-05 + 4.89213331135614e-05i
11	12	2.00496776128810e-05 + 1.35236752139816e-05i
12	13	2.46684351871409e-06 + 1.66390658218720e-06i
4	14	6.82792928379840e-06 + 4.60549540002610e-06i
4	15	1.46602750664450e-05 + 9.88847812789014e-06i

Table A.7 Three phase fault flow data

Bus fault	From	To	IA	PA	IB	PB	IC	PC
1	1	2	0.0	135.6	0.0	15.6	0.0	255.6
1	2	3	0.0	135.6	0.0	15.6	0.0	255.6
1	3	4	0.0	-44.4	0.0	-164.4	0.0	75.6
1	4	5	0.0	0.0	0.0	-120.0	0.0	120.0
1	2	9	0.0	146.0	0.0	26.0	0.0	266.0
1	9	10	0.0	146.0	0.0	26.0	0.0	266.0
1	2	6	0.0	146.0	0.0	26.0	0.0	266.0
1	6	7	0.0	-34.0	0.0	-154.0	0.0	86.0
1	6	8	0.0	-34.0	0.0	-154.0	0.0	86.0
1	3	11	0.0	-34.0	0.0	-154.0	0.0	86.0
1	11	12	0.0	-34.0	0.0	-154.0	0.0	86.0
1	12	13	0.0	146.0	0.0	26.0	0.0	266.0
1	4	14	0.0	146.0	0.0	26.0	0.0	266.0
1	4	15	0.0	146.0	0.0	26.0	0.0	266.0
2	1	2	1149.5	-44.4	1149.5	-164.4	1149.5	75.6
2	2	3	0.0	135.6	0.0	15.6	0.0	255.6
2	3	4	0.0	-44.4	0.0	-164.4	0.0	75.6
2	4	5	0.0	0.0	0.0	-120.0	0.0	120.0
2	2	9	0.0	146.0	0.0	26.0	0.0	266.0
2	9	10	0.0	146.0	0.0	26.0	0.0	266.0
2	2	6	0.0	146.0	0.0	26.0	0.0	266.0
2	6	7	0.0	-34.0	0.0	-154.0	0.0	86.0
2	6	8	0.0	-34.0	0.0	-154.0	0.0	86.0
2	3	11	0.0	-34.0	0.0	-154.0	0.0	86.0
2	11	12	0.0	-34.0	0.0	-154.0	0.0	86.0
2	12	13	0.0	146.0	0.0	26.0	0.0	266.0
2	4	14	0.0	146.0	0.0	26.0	0.0	266.0
2	4	15	0.0	146.0	0.0	26.0	0.0	266.0
3	1	2	910.7	-44.4	910.7	-164.4	910.7	75.6
3	2	3	910.7	-44.4	910.7	-164.4	910.7	75.6
3	3	4	0.0	135.6	0.0	15.6	0.0	255.6
3	4	5	0.0	0.0	0.0	-120.0	0.0	120.0

Table A.8 Three phase fault flow data (cont.)

Bus fault	From	To	IA	PA	IB	PB	IC	PC
3	2	9	0.0	-34.0	0.0	-154.0	0.0	86.0
3	9	10	0.0	-34.0	0.0	-154.0	0.0	86.0
3	2	6	0.0	-34.0	0.0	-154.0	0.0	86.0
3	6	7	0.0	146.0	0.0	26.0	0.0	266.0
3	6	8	0.0	-34.0	0.0	-154.0	0.0	86.0
3	3	11	0.0	146.0	0.0	26.0	0.0	266.0
3	11	12	0.0	146.0	0.0	26.0	0.0	266.0
3	12	13	0.0	146.0	0.0	26.0	0.0	266.0
3	4	14	0.0	-34.0	0.0	-154.0	0.0	86.0
3	4	15	0.0	-34.0	0.0	-154.0	0.0	86.0
4	1	2	788.0	-44.4	788.0	-164.4	788.0	75.6
4	2	3	788.0	-44.4	788.0	-164.4	788.0	75.6
4	3	4	788.0	-44.4	788.0	-164.4	788.0	75.6
4	4	5	0.0	0.0	0.0	-120.0	0.0	120.0
4	2	9	0.0	-34.0	0.0	-154.0	0.0	86.0
4	9	10	0.0	-34.0	0.0	-154.0	0.0	86.0
4	2	6	0.0	-34.0	0.0	-154.0	0.0	86.0
4	6	7	0.0	146.0	0.0	26.0	0.0	266.0
4	6	8	0.0	0.0	0.0	-120.0	0.0	120.0
4	3	11	0.0	-34.0	0.0	-154.0	0.0	86.0
4	11	12	0.0	-34.0	0.0	-154.0	0.0	86.0
4	12	13	0.0	-34.0	0.0	-154.0	0.0	86.0
4	4	14	0.0	146.0	0.0	26.0	0.0	266.0
4	4	15	0.0	0.0	0.0	-120.0	0.0	120.0
5	1	2	655.1	-44.4	655.1	-164.4	655.1	75.6
5	2	3	653.7	-44.4	653.7	-164.4	653.7	75.6
5	3	4	649.7	-44.4	649.7	-164.4	649.7	75.6
5	4	5	656.3	-34.0	656.3	-154.0	656.3	86.0
5	2	9	0.0	-34.0	0.0	-154.0	0.0	86.0
5	9	10	0.0	-34.0	0.0	-154.0	0.0	86.0
5	2	6	0.0	-34.0	0.0	-154.0	0.0	86.0
5	6	7	0.0	146.0	0.0	26.0	0.0	266.0

Table A.9 Three phase fault flow data (cont.)

Bus fault	From	To	IA	PA	IB	PB	IC	PC
5	6	8	0.0	-34.0	0.0	-154.0	0.0	86.0
5	3	11	0.0	0.0	0.0	-120.0	0.0	120.0
5	11	12	0.0	0.0	0.0	-120.0	0.0	120.0
5	12	13	0.0	-34.0	0.0	-154.0	0.0	86.0
5	4	14	0.0	-34.0	0.0	-154.0	0.0	86.0
5	4	15	0.0	-34.0	0.0	-154.0	0.0	86.0
6	1	2	777.1	-44.4	777.1	-164.4	777.1	75.6
6	2	3	0.0	-44.4	0.0	-164.4	0.0	75.6
6	3	4	0.0	135.6	0.0	15.6	0.0	255.6
6	4	5	0.0	-34.0	0.0	-154.0	0.0	86.0
6	2	9	0.0	-34.0	0.0	-154.0	0.0	86.0
6	9	10	0.0	-34.0	0.0	-154.0	0.0	86.0
6	2	6	785.1	-34.0	785.1	-154.0	785.1	86.0
6	6	7	0.0	146.0	0.0	26.0	0.0	266.0
6	6	8	0.0	-34.0	0.0	-154.0	0.0	86.0
6	3	11	0.0	146.0	0.0	26.0	0.0	266.0
6	11	12	0.0	-34.0	0.0	-154.0	0.0	86.0
6	12	13	0.0	146.0	0.0	26.0	0.0	266.0
6	4	14	0.0	-34.0	0.0	-154.0	0.0	86.0
6	4	15	0.0	-34.0	0.0	-154.0	0.0	86.0
7	1	2	676.7	-44.4	676.7	-164.4	676.7	75.6
7	2	3	0.0	-44.4	0.0	-164.4	0.0	75.6
7	3	4	0.0	135.6	0.0	15.6	0.0	255.6
7	4	5	0.0	0.0	0.0	-120.0	0.0	120.0
7	2	9	0.0	-34.0	0.0	-154.0	0.0	86.0
7	9	10	0.0	-34.0	0.0	-154.0	0.0	86.0
7	2	6	684.5	-34.0	684.5	-154.0	684.5	86.0
7	6	7	684.5	-34.0	684.5	-154.0	684.5	86.0
7	6	8	0.0	0.0	0.0	-120.0	0.0	120.0
7	3	11	0.0	146.0	0.0	26.0	0.0	266.0
7	11	12	0.0	-34.0	0.0	-154.0	0.0	86.0
7	12	13	0.0	-34.0	0.0	-154.0	0.0	86.0

Table A.10 Three phase fault flow data (cont.)

Bus fault	From	To	IA	PA	IB	PB	IC	PC
7	4	14	0.0	0.0	0.0	-120.0	0.0	120.0
7	4	15	0.0	-34.0	0.0	-154.0	0.0	86.0
8	1	2	663.7	-44.4	663.7	-164.4	663.7	75.6
8	2	3	0.0	135.6	0.0	15.6	0.0	255.6
8	3	4	0.0	135.6	0.0	15.6	0.0	255.6
8	4	5	0.0	-34.0	0.0	-154.0	0.0	86.0
8	2	9	0.0	-34.0	0.0	-154.0	0.0	86.0
8	9	10	0.0	-34.0	0.0	-154.0	0.0	86.0
8	2	6	671.4	-34.0	671.4	-154.0	671.4	86.0
8	6	7	0.0	146.0	0.0	26.0	0.0	266.0
8	6	8	671.4	-34.0	671.4	-154.0	671.4	86.0
8	3	11	0.0	146.0	0.0	26.0	0.0	266.0
8	11	12	0.0	-34.0	0.0	-154.0	0.0	86.0
8	12	13	0.0	-34.0	0.0	-154.0	0.0	86.0
8	4	14	0.0	-34.0	0.0	-154.0	0.0	86.0
8	4	15	0.0	-34.0	0.0	-154.0	0.0	86.0
9	1	2	837.7	-44.4	837.7	-164.4	837.7	75.6
9	2	3	0.0	135.6	0.0	15.6	0.0	255.6
9	3	4	0.0	135.6	0.0	15.6	0.0	255.6
9	4	5	0.0	-34.0	0.0	-154.0	0.0	86.0
9	2	9	845.5	-34.0	845.5	-154.0	845.5	86.0
9	9	10	0.0	146.0	0.0	26.0	0.0	266.0
9	2	6	0.0	-34.0	0.0	-154.0	0.0	86.0
9	6	7	0.0	146.0	0.0	26.0	0.0	266.0
9	6	8	0.0	0.0	0.0	-120.0	0.0	120.0
9	3	11	0.0	-34.0	0.0	-154.0	0.0	86.0
9	11	12	0.0	-34.0	0.0	-154.0	0.0	86.0
9	12	13	0.0	-34.0	0.0	-154.0	0.0	86.0
9	4	14	0.0	0.0	0.0	-120.0	0.0	120.0
9	4	15	0.0	-34.0	0.0	-154.0	0.0	86.0
10	1	2	672.3	-44.4	672.3	-164.4	672.3	75.6
10	2	3	0.0	135.6	0.0	15.6	0.0	255.6

Table A.11 Three phase fault flow data (cont.)

Bus fault	From	To	IA	PA	IB	PB	IC	PC
10	3	4	0.0	135.6	0.0	15.6	0.0	255.6
10	4	5	0.0	-34.0	0.0	-154.0	0.0	86.0
10	2	9	680.1	-34.0	680.1	-154.0	680.1	86.0
10	9	10	680.1	-34.0	680.1	-154.0	680.1	86.0
10	2	6	0.0	-34.0	0.0	-154.0	0.0	86.0
10	6	7	0.0	146.0	0.0	26.0	0.0	266.0
10	6	8	0.0	-34.0	0.0	-154.0	0.0	86.0
10	3	11	0.0	-34.0	0.0	-154.0	0.0	86.0
10	11	12	0.0	-34.0	0.0	-154.0	0.0	86.0
10	12	13	0.0	-34.0	0.0	-154.0	0.0	86.0
10	4	14	0.0	0.0	0.0	-120.0	0.0	120.0
10	4	15	0.0	0.0	0.0	-120.0	0.0	120.0
11	1	2	715.9	-44.4	715.9	-164.4	715.9	75.6
11	2	3	711.8	-44.4	711.8	-164.4	711.8	75.6
11	3	4	0.0	135.6	0.0	15.6	0.0	255.6
11	4	5	0.0	-34.0	0.0	-154.0	0.0	86.0
11	2	9	0.0	-34.0	0.0	-154.0	0.0	86.0
11	9	10	0.0	-34.0	0.0	-154.0	0.0	86.0
11	2	6	0.0	-34.0	0.0	-154.0	0.0	86.0
11	6	7	0.0	0.0	0.0	-120.0	0.0	120.0
11	6	8	0.0	0.0	0.0	-120.0	0.0	120.0
11	3	11	718.5	-34.0	718.5	-154.0	718.5	86.0
11	11	12	0.0	146.0	0.0	26.0	0.0	266.0
11	12	13	0.0	146.0	0.0	26.0	0.0	266.0
11	4	14	0.0	-34.0	0.0	-154.0	0.0	86.0
11	4	15	0.0	-34.0	0.0	-154.0	0.0	86.0
12	1	2	545.7	-44.4	545.7	-164.4	545.7	75.6
12	2	3	542.9	-44.4	542.9	-164.4	542.9	75.6
12	3	4	0.0	135.6	0.0	15.6	0.0	255.6
12	4	5	0.0	-34.0	0.0	-154.0	0.0	86.0
12	2	9	0.0	-34.0	0.0	-154.0	0.0	86.0
12	9	10	0.0	-34.0	0.0	-154.0	0.0	86.0

Table A.12 Three phase fault flow data (cont.)

Bus fault	From	To	IA	PA	IB	PB	IC	PC
12	2	6	0.0	-34.0	0.0	-154.0	0.0	86.0
12	6	7	0.0	0.0	0.0	-120.0	0.0	120.0
12	6	8	0.0	-34.0	0.0	-154.0	0.0	86.0
12	3	11	549.7	-34.0	549.7	-154.0	549.7	86.0
12	11	12	549.7	-34.0	549.7	-154.0	549.7	86.0
12	12	13	0.0	146.0	0.0	26.0	0.0	266.0
12	4	14	0.0	-34.0	0.0	-154.0	0.0	86.0
12	4	15	0.0	-34.0	0.0	-154.0	0.0	86.0
13	1	2	454.1	-44.4	454.1	-164.4	454.1	75.6
13	2	3	452.1	-44.4	452.1	-164.4	452.1	75.6
13	3	4	0.0	135.6	0.0	15.6	0.0	255.6
13	4	5	0.0	0.0	0.0	-120.0	0.0	120.0
13	2	9	0.0	-34.0	0.0	-154.0	0.0	86.0
13	9	10	0.0	0.0	0.0	-120.0	0.0	120.0
13	2	6	0.0	-34.0	0.0	-154.0	0.0	86.0
13	6	7	0.0	146.0	0.0	26.0	0.0	266.0
13	6	8	0.0	0.0	0.0	-120.0	0.0	120.0
13	3	11	458.3	-34.0	458.3	-154.0	458.3	86.0
13	11	12	458.3	-34.0	458.3	-154.0	458.3	86.0
13	12	13	458.3	-34.0	458.3	-154.0	458.3	86.0
13	4	14	0.0	0.0	0.0	-120.0	0.0	120.0
13	4	15	0.0	0.0	0.0	-120.0	0.0	120.0
14	1	2	605.8	-44.4	605.8	-164.4	605.8	75.6
14	2	3	604.2	-44.4	604.2	-164.4	604.2	75.6
14	3	4	600.7	-44.4	600.7	-164.4	600.7	75.6
14	4	5	0.0	0.0	0.0	-120.0	0.0	120.0
14	2	9	0.0	-34.0	0.0	-154.0	0.0	86.0
14	9	10	0.0	-34.0	0.0	-154.0	0.0	86.0
14	2	6	0.0	0.0	0.0	-120.0	0.0	120.0
14	6	7	0.0	0.0	0.0	-120.0	0.0	120.0
14	6	8	0.0	0.0	0.0	-120.0	0.0	120.0
14	3	11	0.0	0.0	0.0	-120.0	0.0	120.0

Table A.13 Three phase fault flow data (cont.)

Bus fault	From	To	IA	PA	IB	PB	IC	PC
14	11	12	0.0	146.0	0.0	26.0	0.0	266.0
14	12	13	0.0	-34.0	0.0	-154.0	0.0	86.0
14	4	14	607.6	-34.0	607.6	-154.0	607.6	86.0
14	4	15	0.0	-34.0	0.0	-154.0	0.0	86.0
15	1	2	680.3	-44.4	680.3	-164.4	680.3	75.6
15	2	3	679.1	-44.4	679.1	-164.4	679.1	75.6
15	3	4	675.0	-44.4	675.0	-164.4	675.0	75.6
15	4	5	0.0	0.0	0.0	-120.0	0.0	120.0
15	2	9	0.0	-34.0	0.0	-154.0	0.0	86.0
15	9	10	0.0	0.0	0.0	-120.0	0.0	120.0
15	2	6	0.0	-34.0	0.0	-154.0	0.0	86.0
15	6	7	0.0	146.0	0.0	26.0	0.0	266.0
15	6	8	0.0	0.0	0.0	-120.0	0.0	120.0
15	3	11	0.0	0.0	0.0	-120.0	0.0	120.0
15	11	12	0.0	-34.0	0.0	-154.0	0.0	86.0
15	12	13	0.0	-34.0	0.0	-154.0	0.0	86.0
15	4	14	0.0	-34.0	0.0	-154.0	0.0	86.0
15	4	15	681.2	-34.0	681.2	-154.0	681.2	86.0

APPENDIX B
LIST OF PUBLICATION

C. Plongkrathok and K. Chayakulkheeree (2020), A Comparative Study on Scenario Based Optimal Overcurrent Relay Coordination for Distribution System with Distributed Generator Using Linear Programing, The 43rd Electrical Engineering Conference (EECON-43), Phitsanulok, Thailand.

C. Plongkrathok and K. Chayakulkheeree (2022), Optimal Overcurrent Relay Coordination Considering Multiple Characteristic Curve for Microgrid Protection Using Hybrid PSO-MILP Technique, International Journal of Intelligent Engineering and Systems, pp 329-337.

A Comparative Study on Scenario Based Optimal Overcurrent Relay Coordination for Distribution System with Distributed Generator Using Linear Programing

Chakit Plongkrathok and Keerati Chayakulkheeree

School of Electrical Engineering, Institute of Engineering
Suranaree University of Technology, Thailand, keerati.ch@sut.ac.th

Abstract

This paper presents the optimal coordination of overcurrent relay (OCR) with the presence of distributed energy resources (DER) using linear programming techniques. In addition, a comparative scenario-based between non-adaptive relay settings and adaptive relay settings has been investigated. A four bus radial distribution system is used to test the proposed method. The simulation prosperously has shown that the linear programing can successfully solve for optimal OCR coordination. Meanwhile, an adaptive relay setting can handle the overcoming distribution network problem more efficiently than a non-adaptive relay setting.

Keywords: adaptive protection, optimal coordination of overcurrent relay, linear programing (LP).

1. Introduction

Modern distribution systems consist of various distributed generators (DG) to make reliable power systems [1] and commonly used to supply the local loads [2]. The penetration of distributed generation leads to violating the overcurrent relay (OCR) coordination in the distribution network [2]. The effects of DG on the distribution system is the loss of coordination of distribution system protection. This is because the fault current can be higher when the short circuit location is near to the generator. The impact of DG on OCR coordination effects on both current setting and the operating time of OCR. The coordination time interval (CTI) associated with primary and backup relay pairs is getting violated due to changes in the fault current level [2]. Thus, conventional coordination between primary and backup relays usually fails in the presence of DG. Hence, the interconnection of DG in the distribution system causes an adverse impact on protection coordination. Meanwhile, relay coordination problem has many constraints due to coordination criteria [2]. Therefore, coordination of overcurrent relays with DG is a big challenge for protection engineers.

Several methods to find the optimal value for the coordination of OCR are illustrated in the available literature. Linear programming technique is a powerful scheme for obtaining a basic feasible solution [3]. Big-M and dual simplex methods are used to find the optimum values of time multiplier settings (*TMS*) [4]. With the optimum values for both pick-up current (I_p) and *TMS* nonlinear programming problem (NLP) is a grateful method [5]. Particle swarm optimization (PSO) is a metaheuristic method that follows the social behavior of animals such as bird flocking and is very efficient [6]. A genetic algorithm (GA) is also proposed to find the optimum solution for relay settings in [2]. The latest optimization technique Gravitational Search Algorithm (GSA) is a new technique based on newton's laws of attraction to find the optimum solution for relay setting [1]. Meanwhile, a comparative study of optimization techniques for OCR coordination with DG is mentioned in [7].

However, most researches on optimal OCR coordination concern only non-adaptive OCR, without comparing to adaptive OCR coordination. The investigation on the advantage of emerging adaptive OCR is a benefit to the system. Consequently, the motivation of this paper is to find the optimum values of the OCR setting by used linear programming techniques and comparing the results between using conventional setting and adaptive setting of OCR.

This paper was arranged into four sections as follows. Section 2 represents the problem formulation limit constraint and determined all of the variables. Section 3 indicates the result and discussion form the four bus radial distribution test system. Finally, section 4 provides the conclusion.

2. Problem Formulation

In the general form, the objective function of OCR coordination is a non-linear optimization problem.to optimize both *TMS* and I_p. However, solving nonlinear optimization problem methods are complex as well as time-consuming [2]. To avert complexity, this problem commonly formulated as a linear programming problem (LP) by predetermined I_p based on minimum fault current for relay. In this case study, linear programming is adapted to find optimal *TMS* only. The objective function of the problem is the total operating time of all the relays present in the system [7]. The function is to be minimized so that each relay operates in minimum time and reliability of the system is maintained [7]. The formulated objective function is,

$$\text{minimize } Y = \sum_{i=1}^{NR} t_i, \tag{1}$$

where,

$$t_i = A_i TMS_i, i = 1, \ldots, NR, \tag{2}$$

$$A_i = \frac{K_i}{\left(\frac{I_{Ri}}{I_{Pi}}\right)^{n_i} - 1}, i = 1, \ldots, NR, \tag{3}$$

subjected to the coordination constraint,

$$t^k_{b,i} - t^k_{m,i} \geq \Delta t_i, i = 1,...,NC, \quad (4)$$

relay operating time constraint,

$$t_i \geq t_i^{\min}, i = 1,...,NR, \quad (5)$$

and the time multiplier limit constraint,

$$TMS_i^{\min} \leq TMS_i \leq TMS_i^{\max}, i = 1,...,NR. \quad (6)$$

Where,

Y is the total relay operating time (s),

t_i is the operating time of relay i for main fault (s) ,

$t_i^{\min}$ is the minimum operating time of relay i,

A_i is the constant predetermined for different zones of protection of relay i,

TMS_i is the time multiplier of relay i,

$TMS_i^{\max}$ is the maximum time multiplier of relay i,

$TMS_i^{\min}$ is the minimum time multiplier of relay i,

K_i is the constant characteristic of relay i,

n_i is the constant characteristic of relay i,

I_{Ri} is the current flowing through relay i (A),

I_{Pi} is the pick-up current setting of relay i (A),

$t^k_{b,i}$ is the operating time of backup relay i for fault in zone k (s),

$t^k_{m,i}$ is the operating time of primary relay i for fault in same zone (s),

Δt_i is the coordination time interval (CTI) (s),

NR is the total number of relay, and

NC is total number of relay for primary and backup coordination.

3. Results and Discussion

According to the problem formulation the main target is to find the *TMS* of all relay and comparative total operating time of relay between non-adaptive relay setting approach and adaptive relay setting approach, so *TMS* is variable here and the total operating time of all the relays for fault in main zone is taken as the objective function which is to be minimized. The objective function is found by integrating the relay characteristic constraint (equations 2 and 3). The other inequality constraints are included in the algorithm. In this paper, the OCR used is IEC Standard Inverse Curve (SI). Therefore, the constraint K = 0.14 and n =0.02, in equation (3). CTI = 0.3 s, in equation (4). The $t^{\min}$ normally used = 0.1 s, in equation (5), and the *TMS* limit in the range is 0.1-1, in equation (6).

3.1 Test Case

A single source four bus radial system with the presence of DG at bus 1. In order to prevent faults in all areas of the system, use five OCR (R_{Gr}, R_{DG}, R_1, R_2 and R_3) installed at the upstream of each transmission line.

The multi-scenario of OCR setting is categorized into;

Case I: Grid connected without DG

Case II: Grid connected with DG

Case III: Islanding mode with DG.

As shown in Fig. 1. The fault is created at each bus and fault current is found by relay. Table 2, 3, and 4 gives the fault current seen by each relay for all case.

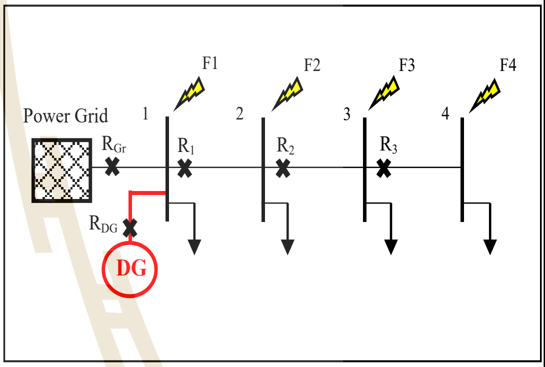

Fig. 1 Four buses radial test system

Table 1 Parameter of the system

No.	Particular	Ratings
1	Line	0+j1.0331 p.u
2	Generator	100 MVA ,22 kV , X'd = 1.00 p.u
3	DG	0.5+j0.5 MVA ,22 kV, X'd = 1.20 p.u

Table 2 Fault current of case I

Fault Point	Fault Current (A)	R_{Gr}	R_{DG}	R_1	R_2	R_3
Bus1	Max	2624.3	-	-	-	-
	Min	2272.7	-	-	-	-
Bus2	Max	1290.8	-	1290.8	-	-
	Min	1117.9	-	1117.9	-	-
Bus3	Max	855.9	-	855.9	855.9	-
	Min	741.2	-	741.2	741.2	-
Bus4	Max	640.2	-	640.2	640.2	640.2
	Min	554.4	-	554.4	554.4	554.4

Note: '-'indicates that the fault is not seen by the relay

Table 3 Fault current of case II

Fault Point	Fault Current (A)	R_{Gr}	R_{DG}	R_1	R_2	R_3
Bus1	Max	2624.3	2186.9	-	-	-
	Min	2272.7	1893.9	-	-	-
Bus2	Max	906.8	755.7	1662.5	-	-
	Min	785.3	654.4	1439.8	-	-
Bus3	Max	548.1	456.8	1004.9	1004.9	-
	Min	474.6	395.6	870.2	870.2	-
Bus4	Max	392.7	327.3	720.0	720.0	720.0
	Min	340.1	283.4	623.5	623.5	623.5

Table 4 Fault current of case III

The procedure of this paper starts from reading the system data, find the short circuit current flowing through each relay, predetermined I_p, and calculate the *TMS* using LP as shown in Fig.2

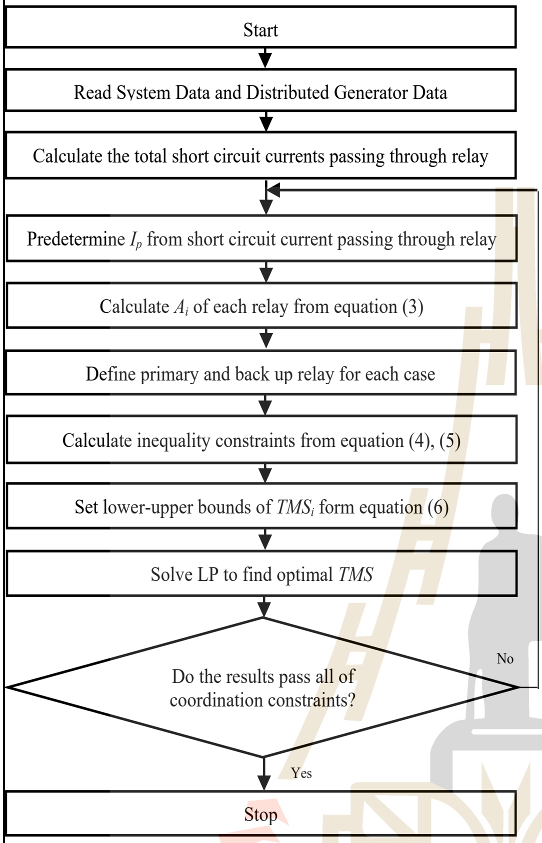

Fig. 2 Computational procedure

3.2 Non-adaptive relay setting

In this non-adaptive relay setting case, the relay will be set I_p and *TMS* only once for all situations, and must be set to cover all of the fault cases that can occur in the system (Cases I-III). I_p is predetermined by the smallest fault current flowing through the relays of the three cases divided by three. The predetermined of I_p as shown in Table 5 and the selection of the primary relays and backup relays for coordination as shown in Table 6.

Table 5 Pick-up current for each relay with non-adaptive relay

Relay	I_p (A)
R_{Gr}	261.76
R_{DG}	218.13
R_1	231.93
R_2	176.20
R_3	176.20

Table 6 Primary and backup relay with non-adaptive relay

Fault Point	Primary	Backup
Bus1	R_{Gr}, R_{DG}	-
Bus2	R_1	R_{Gr}, R_{DG}
Bus3	R_2	R_1
Bus4	R_3	R_2

In this non-adaptive relay setting case has three difference objective function for comparative three difference case The value of A_i shown in Table 7 and the optimal *TMS* result shown in Table 8.

Table 7 Constant A_i with non-adaptive relay

	Case I	Case II	Case III
A_1	2.967	2.967	0
A_2	0	2.967	2.967
A_3	4.008	3.484	4.244
A_4	4.359	3.951	4.544
A_5	3.536	4.903	5.564

Table 8 The optimal *TMS* results with non-adaptive relay

	Non-adaptive relay setting		
	Case I	Case II	Case III
TMS_{Gr}	0.2544	0.2544	0.2544
TMS_{DG}	0.2802	0.2802	0.2802
TMS_1	0.1991	0.1991	0.1991
TMS_2	0.1612	0.1612	0.1612
TMS_3	0.1	0.1	0.1
Y (s)	2.791	3.4068	2.9652

3.3 Adaptive relay setting

In adaptive relay setting case, the relay can be set I_p and *TMS* multiple times depending on where the system is working at that time. So, I_p can be predetermined appropriately in each case. The predetermined of I_p for each system case as shown in Table 9, the selection of the primary relays and backup relays for coordination as shown in Table 10, the value of A_i shown in the Table 11, and the optimal *TMS* result shown in Table 12.

Table 9 Pick-up current for each relay with adaptive relay

Relay	I_p (A)		
	Case I	Case II	Case III
R_{Gr}	372.63	261.76	-
R_{DG}	-	218.13	339.26
R_1	247.06	290.06	231.93
R_2	184.8	207.83	176.2
R_3	184.8	207.83	176.2

Table 10 Primary and backup relay with adaptive relay

Fault Point	Case I		Case II		Case III	
	Primary	Backup	Primary	Backup	Primary	Backup
Bus1	R_{Gr}	-	R_{Gr} R_{DG}	-	R_{DG}	-
Bus2	R_1	R_{Gr}	R_1	R_{Gr} R_{DG}	R_1	R_{DG}
Bus3	R_2	R_1	R_2	R_1	R_2	R_1
Bus4	R_3	R_2	R_3	R_2	R_3	R_2

Table 11 Constant A_i for with adaptive relay

	Case I	Case II	Case III
A_1	3.517	2.967	0
A_2	0	2.967	3.687
A_3	4.164	3.939	4.244
A_4	4.497	4.372	4.544
A_5	5.564	5.564	5.564

Table 12 The optimal *TMS* results with adaptive relay

	Adaptive relay setting		
	Case I	Case II	Case III
TMS_{Gr}	0.1874	0.1777	-
TMS_{DG}	-	0.1777	0.1909
TMS_1	0.1783	0.1749	0.1796
TMS_2	0.1539	0.1539	0.1539
TMS_3	0.1	0.1	0.1
Y (s)	2.6501	2.9726	2.722

3.4 Discussion

Table 13 Comparative non-adaptive and adaptive relay

	Case I		Case II		Case III	
	Non-adaptive	Adaptive	Non-adaptive	Adaptive	Non-adaptive	Adaptive
TMS_{Gr}	0.2544	0.1874	0.2544	0.1777	0.2544	-
TMS_{DG}	0.2802	-	0.2802	0.1777	0.2802	0.1909
TMS_1	0.1991	0.1783	0.1991	0.1749	0.1991	0.1796
TMS_2	0.1612	0.1539	0.1612	0.1539	0.1612	0.1539
TMS_3	0.1	0.1	0.1	0.1	0.1	0.1
Y (s)	2.791	2.6501	3.4068	2.9726	2.9652	2.722

From the simulation results, the DG penetration at bus 1 when considering the system operation (Cases I-III). However, the short circuit current of the three cases will flow in the same direction. The primary and backup relay assignments for coordination are still similar in all three cases. In case II the level of short circuit current is significantly increased. but still, it is possible to use a non-adaptive relay setting method and find the optimal *TMS* to decrease the total relay operating time as in the table and can be seen that the non-adaptive relay setting method there will be only one optimal *TMS* scenario which is used to protect all of the system operations. However, comparing to the adaptive relay setting method, it can be seen that the optimal *TMS* is appropriate for each system operation. Resulting in the total relay operating time of the system is significantly reduced, as shown in the table.The reduction of fault clearing time is leading to system reliability enhancement.

4. Conclusion

The linear programing optimization technique is used in this paper to find the optimal *TMS* of five OCR relays so that their operating time can be minimized. The objective function is formulated for three cases. Further, it is minimized by maintaining the range of *TMS* of each relay as 0.1-1 and CTI as 0.3 s. The range of I_p determined for each relay is based on minimum fault current flowing through a relay. A comparative study between the adaptive relay setting and non-adaptive relay setting for every case of the system was mentioned in this paper. From the simulation results, it was found that the adaptive relay setting method results in the total operating time of all relay faster than the non-adaptive relay setting method. Therefore, it can be concluded that the adaptive relay setting method is more suitable for distribution systems with the presence of DG.

References

[1] Adhishree Srivastava, Jayant Mani Tripathi and Jayant Mani Tripathi "Optimal Coordination of Overcurrent Relays Using Gravitational Search Algorithm With DG Penetration" *IEEE Transactions on Industry Applications*, vol. 54, no. 2, pp. 1155-1165, 2018.

[2] Mr. Sahebrao V. Chakor, Prof. Mrs. Tanuja N. Date "Optimum Coordination of Directional Overcurrent Relay in presence of Distributed Generation Using Genetic Algorithm" *10th International Conference on Intelligent Systems and Control (ISCO)* , 2016.

[3] Bijoy Chattopahyay, M.S. Sachdev and T.S. Sidhu "An on -line relay coordination algorithm for adaptive protection using linear programing technique" *IEEE Transactions on Power Delivery,* vol. 11, no. 1, pp.165-173, 1996.

[4] Anjali Gupta, O.V. Gnana Swathika, and Dr. S. Hemamalini "Optimum Coordination of Overcurrent Relays in Distribution Systems using Big-M and Dual Simplex Methods" *International Conference on Computational Intelligence and Communication Networks,* pp.1540-1543, 2015.

[5] Pragati N. Korde, Prashant. P. Bedekar "Optimal Overcurrent Relay Coordination in Distribution System using Nonlinear Programming Method" *International Conference on Electrical Power and Energy Systems (ICEPES)* , pp. 372-376, 2016.

[6] Ayatte. I. Atteya, Amany. M. El Zonkoly and Hamdy. A. Ashour "Optimal Relay Coordination of an Adaptive Protection Scheme using Modified PSO Algorithm" *Nineteenth International Middle East Power Systems Conference (MEPCON), Menoufia University, Egypt,* pp. 689-694, 2017.

[7] Adhishree, Jayant Mani Tripathi, Soumya R Mohanty and Nand Kishor "A Simulation Based Comparative Study of Optimization Techniques for Relay Coordination with Distributed Generation" *IEEE Students Conference on Engineering and Systems,* 2014.

Biography

Chakit Plongkrathok received his B. Eng. i EE from Suranaree University of Technolog in 2020. He is currently a graduate student i power system program at Suranare University of Technology (SUT). His curre interests are in power system optimizatio algorithms and power system protections.

Keerati Chayakulkheeree received his E Eng. in EE from KMITL in 1995, M. Eng. an D. Eng. degree in Electric Power Syste Management from AIT, in 1999 and 200 respectively. He is currently an associat professor at School of Electrical Engineerin Institute of Engineering, Suranare University of Technology, Thailand.

International Journal of
Intelligent Engineering & Systems

http://www.inass.org/

Optimal Overcurrent Relay Coordination Considering Multiple Characteristic Curve for Microgrid Protection Using Hybrid PSO-MILP Technique

Chakit Plongkrathok **Keerati Chayakulkheeree***

School of Electrical Engineering, Suranaree University of Technology, Thailand

* Corresponding author's Email: keerati.ch@sut.ac.th

Abstract: This paper proposes an approach for the optimal setting parameters of overcurrent relay (OCR) coordination considering multiple characteristic curves. The proposed approach considers time multiplier setting (TMS) and the relay characteristic curve setting (CS) as decision variables. As an inventiveness, the CS of OCR can be chosen as decision variables, instead of fixing a single type of curve for all relays that used in many existing works. The proposed approach allows three different curve types of IEC standard characteristic curves for combination results in the optimal protection coordination, including the standard inverse (SI) curve, very inverse (VI) curve, and extremely inverse (EI) curve. The proposed technique for solving this problem is hybrid particle swarm mixed integer linear programming (PSO-MILP). To show the effectiveness of the proposed approach, several tests were carried out using the standard IEC benchmark microgrid system. A comparison with previous existing methods illustrated that the proposed technique can absolutely decrease the total operating time of the OCR by around 34 percent for OM1, around 44 percent for OM2, and slightly decrease the total CTI of the test system. Therefore, the proposed approach is outstanding in finding lower the operating times and provides suitable operation of microgrid protections under different fault allocation and operating conditions.

Keywords: Optimal overcurrent relay coordination, Microgrid protection, Artificial intelligence

1. Introduction

One of the most appealing features of microgrid systems is that the power delivered to consumers who prefer an uninterruptible power resource with reliable and high quality. Furthermore, there are savings in power generation costs through the implementation of photovoltaic (PV), wind turbine (WT), distributed generator (DG), and energy storage systems (ESS) into micro-networks. Nevertheless, the penetration of DG plays a role in significantly contributing fault current into the system [1]. Therefore, the protection strategy of microgrids is a new challenge for protection engineers.

An overcurrent relays (OCR) can extensively be applied as the primary protection strategy in distribution systems, sub-transmission systems, and microgrid systems or as backup protection in transmission systems. In order to improve the fast and reliability of the protection strategy, OCRs must be operated with minimum time and able to coordinate with another relay to improve the system reliability. Consequently, the OCR can adjust the operating point by adjusting the setting parameters, including the pickup current setting (*PS*), the time multiplier setting (*TMS*), and characteristic curve settings (*CS*). Hence, OCRs coordination can be variously formulated in optimization problems. The coordination between primary and backup relay leading highly non-linear inequality constraints to this problem.

In order to obtain better results, numerous approaches and techniques for solving the optimal setting parameter of OCR was published. In the earliest era, the *PS* has been predetermined, and *CS* of each relay have been set to specific characteristic curve, hence this problem has been formulated as a linear optimization. The minimum total operating time of the primary relay is the objective function subjected to the coordination constraint. As a result, dual simplex approach [3], the Big-M strategy [4], and the reverse simplex method by [5], and artificial bee colony [6] have all been proposed as solutions to these problems. Subsequently, the problem was improved to the nonlinear optimization by considering the *PS* and the *TMS* as a decision variable, whereas the *CS* has remained unchanged. The objective function was minimized by avoiding the limit boundary of *TMS* and *PS*, the coordination constraint, and the minimum operating time. In order to solve this issue, several artificial intelligence techniques were proposed. For example, Adaptive modified fly fire algorithm (AMFA) was introduced in [7]. The seeker optimization (SOA), the gravitational search method (GSA), and the hybrid genetic algorithm-nonlinear programming approach (GA-NLP) were proposed in [8], [9], and [10], respectively. Meanwhile, [11] developed the symbiotic organism search algorithm (SOS). Afterward, the researchers proposed that the *PS* could be considered to be the step/discrete variable instead of the continuous variable to illustrate the realized industrial OCR. The problem was transformed into a mixed-integer nonlinear optimization problem (MINLP). Numerous techniques were proposed to solve this problem, for example, modified seeker algorithm (MSA) [12], hybrid whale optimization (HWOA) [13], ant lion optimization (ALO), and the artificial immune system (AIS) [14], hybrid GA-LP [15]. In recent years, various novel constraints were implemented for representing the practical industrial OCR such as the plug setting multiplier (*PSM*) constraint to be within the range of 1.1 times to 20 times [16], and the range of 1.1 times to 100 times [17]. Then, researchers have focused on the maximum *PSM* as a decision variable that can reduce the total operating time and total *CTI* of the relay [18], considering the transient stability constraint to ensure the network transient stability in [14]. In another way, the researcher demonstrated that various types of *CS* have an impact on the relay's operating time. According to the results, the mixed *CS* type solutions outperformed the fixed *CS* type solution [19]. Consequently, the researcher proposed that the *CS* and *TMS* are decision variables by fixed one integer variable of each OCR for represented the *CS*, while the *PS* is predefined. Then the problem became mixed-integer linear programming (MILP). The problem was solved by integer code genetic algorithm (ICGA) subjected to coordination constraint, operating time constraint, and *PSM* constraint. The results show that this method is the most effective in decreasing the total operating time of the relay [20].

As a result, this paper proposes an approach for optimal OCR coordination considering multiple *CS*, that consider *TMS* and *CS* as decision variables. The formulation of this paper is MILP optimization. As a novelty, this paper represents a novel problem formulation by dividing *CS* into multiple sections depending on the number of *CS* types that are considered, instead of using a single integer variable of each OCR for representing *CS* as in recent existing work [20]. The hybrid PSO-MILP technique was developed to solve this problem. The coordination constraint, the operating time constraint, and the *PSM* constraint were considered in this paper. To show the capability of the proposed technique, the result was compared with those previous papers [16-18],[20], in the same test system.

The following are the five sections of this paper. The formulation of the objective function, the determination of all variables, the limit boundary, and all of the constraints in this problem are all represented in Section 2. The procedure of proposed technique is obtained in Section 3. The optimal results and discussions of the proposed technique on the IEC benchmark microgrid test system is presented in Section 4. The conclusion is contained in Section 5.

1. Mathematical Formulation

The IEC standard OCR has inverse time-current characteristics. The operating time of OCR is depending on short circuit current flowing through relay and setting parameters include *TMS*, *PS*, and *CS*. In this paper, the decision variables are *TMS* and *CS*, while *PS* is predetermined of each OCR. The objective function (*OF*) of this problem is to minimize the total operating time of all the OCRs present in the system. The function is to be minimized so that each relay operates in minimum time and the reliability of the system is maintained by the constraints. The mathematical formulation can be expressed as follow.

Minimize,

$$OF = \sum_{k=1}^{NF}\sum_{j=1}^{NR}(C_{SI,j}T_{SI,j,k} + C_{VI,j}T_{VI,j,k} + C_{EI,j}T_{EI,j,k}), \quad (1)$$

where,

$$T_{SI,j,k} = \frac{0.14\ TMS_j}{\left(PSM_{jk}\right)^{0.02} - 1}, \quad (2)$$

$$T_{VI,j,k} = \frac{13.5\ TMS_j}{\left(PSM_{jk}\right)^1 - 1}, \quad (3)$$

$$T_{EI,j,k} = \frac{80\ TMS_j}{\left(PSM_{jk}\right)^2 - 1}, \quad (4)$$

$$PSM_{jk} = \frac{I_{jk}}{\left(PS_j CTR_j\right)} . \quad (5)$$

Subjected to the standard curve selection constraint,

$$C_{SI,j}, C_{VI,j}, C_{EI,j} \in \{0,1\},\ j = 1,...,NR , \quad (6)$$

$$C_{SI,j} = \begin{cases} 0, \text{ if the relay is not SI curve} \\ 1, \text{ if the relay is SI curve} \end{cases} , \quad (7)$$

$$C_{VI,j} = \begin{cases} 0, \text{ if the relay is not VI curve} \\ 1, \text{ if the relay is VI curve} \end{cases} , \quad (8)$$

$$C_{EI,j} = \begin{cases} 0, \text{ if the relay is not EI curve} \\ 1, \text{ if the relay is EI curve} \end{cases} , \quad (9)$$

$$C_{SI,j} + C_{VI,j} + C_{EI,j} = 1 ,\ j = 1,...,NR , \quad (10)$$

the time multiplier limit boundary,

$$TMS_j^{\min} \le TMS_j \le TMS_j^{\max},\ j = 1,...,NR , \quad (11)$$

the plug setting multiplier constraint,

$$PSM_j^{\min} \le PSM_j \le PSM_j^{\max},\ j = 1,...,NR , \quad (12)$$

the coordination constraint,

$$T_{b,k} - T_{p,k} \ge CTI,\ k = 1,...,NF , \quad (13)$$

the operating time constraint,

$$T_{j,k}^{\max} \ge T_{j,k} \ge T_{j,k}^{\min},\ j = 1,...,NR . \quad (14)$$

Where,

$T_{SI,j,k}$ is the operating time of relay *j* with standard inverse curve type when the fault occurs at point *k*,
$T_{VI,j,k}$ is the operating time of relay *j* with very inverse curve type when the fault occurs at point *k*,
$T_{EI,j,k}$ is the operating time of relay *j* with extremely inverse curve type when the fault occurs at point *k*,
TMS_j is the time multiplier setting of relays *j*,
TMS_j^{max} is the maximum time multiplier of relay *j*,
TMS_j^{min} is the minimum time multiplier of relay *j*,
PSM_j is the plug setting multiplier of relay *j*,
PSM_j^{max} is the maximum plug setting multiplier of relay *j*,
PSM_j^{min} is the minimum plug setting multiplier of relay *j*,
$T_{b,k}$ is the operation time of the backup relay *b* when fault *k* occurs,
$T_{p,k}$ is the operation time of the primary relay *p*, for the same fault,
CTI is the coordination time interval,
$T_{j,k}^{min}$ is the minimum operating of each relay *j* when fault *k* occurs,
$T_{j,k}^{max}$ is the maximum operating of each relay *j* when fault *k* occurs.
I_{jk} is the short-circuit current flowing through relay *j* when fault at *k* is occurred (A),
PS_j is the pickup setting of relay *j* (A),
CTR_j is the CT ratio of relay *j*,
NF is a number of faults that can be take place in the system,
NR is a number of the operating relays when fault occur at point *k*.

By Eq. (6-10), the OCR standard *CS* of each relay can be chosen only one from SI, VI, or EI.

1. PSO-MILP Technique

The *TMS* of each OCR is a continuous variable while the CS_I, C_{VI}, and C_{EI} are a binary integer variable. Thus, the mathematical formulation of this problem is adapted to the mixed-integer nonlinear optimization. Meanwhile, traditional particle swarm optimization (PSO) can only solve problems with continuous variables [21]. Hence, the PSO-MILP technique is implemented to solve this problem. The proposed method including two computational phases consist of a main loop and subroutines. A main loop is used the PSO technique to find the optimal *TMS* of each OCR. A subroutine is used the MILP technique to obtain the optimal CS_I, C_{VI}, and C_{EI}. The proposed technique computation of each population is shown step by step as bellow.

Step 1: Random initial position of the population matrix ($\mathbf{X_{TMS}}$) within the *TMS* limited boundary in Eq. (11),

$$\mathbf{X_{TMS}} = [TMS_i, ..., TMS_{NR}]. \quad (15)$$

$$TMS_i = rand(TMS_i^{\min}, TMS_i^{\max}),\ i = 1,....,NR, \quad (16)$$

Step 2: Calculate $T_{SI,j,k}$, $T_{VI,j,k}$, and $T_{EI,j,k}$ value in Eq. 1 by substitute $\mathbf{X}_{\mathbf{TMS}}$ from Eq. (16) to Eq. (2-5). Then, the OF_{new} will be integer programming optimization with binary integer decision variables (CS_I, C_{VI}, and C_{EI}) of each OCR.

$$OF_{new} = OF_{old}\left(\text{subtitute } TMS \text{ in Eq.(1-5)}\right) \quad (17)$$

Step 3: Solve MILP with objective function form Eq. (17) subjected to constraints in Eq. (6-10), and Eq. (12-14) to obtain optimal CS_I, C_{VI}, and C_{EI} of each population matrix.

Minimize the objective function in: Eq. (17)
Subjected to: Eq. (6-10), and Eq. (12-14)

$$\text{Obtain: } \mathbf{X}_{\mathbf{CS}} = \begin{bmatrix} C_{SI,i},...,C_{SI,NR} \\ C_{VI,i},...,C_{VI,NR} \\ C_{EI,i},...,C_{EI,NR} \end{bmatrix},\ i = 1,....,NR. \quad (18)$$

Step 4: Find the *pbest* and *gbest* of each population matrix form Eq. (17-18).

Step 5: Update velocity and position of each population matrix from Eq. (16) by Eq. (19-22).

$$\mathbf{V}^{\mathbf{k+1}} = w\mathbf{V}^{\mathbf{k}} + A_1 + A_2, \quad (19)$$

$$A_1 = c_1 r_1\left(pbest_i^{\,k} - \mathbf{X}^{\mathbf{k}}\right), \quad (20)$$

$$A_2 = c_2 r_2 (gbest^k - \mathbf{X}^{\mathbf{k}}), \quad (21)$$

$$\mathbf{V}_{\mathbf{i}}^{\mathbf{k}} = [V_1^k,...,V_{3NR}^k], \quad (22)$$

$$\mathbf{X}_{\mathbf{i}}^{\mathbf{k+1}} = \mathbf{X}^{\mathbf{k}} + \mathbf{V}^{\mathbf{k+1}}, \quad (23)$$

$$\mathbf{X}_{\mathbf{TMS}}^{\mathbf{new}} = \mathbf{X}_{\mathbf{i}}^{\mathbf{k+1}}, \quad (24)$$

where, k indicates the iteration, w is the inertia weight, v^i_k is the i particle's velocity vector, x^i_k is the i particle's vector, $gbest^k$ is the historically best position of the entire swarm, $pbest_i^k$ is the historically best position of particle i, $c_1$and c_2 are the personal and global learning coefficients, respectively, while r_1 and r_2 are uniformly distributed random numbers in the range [0,1].

Step 6: Repeat step 2-5 until the maximum iteration.

1. Results and Discussions

4.1 Test Case

The proposed approach was investigated on the IEC benchmark microgrid test system [16-18,20] with various operating modes (OMs) as shown in Fig. 1. In this system, the OM can be classified into two conditions (OM1 and OM2) depend on the circuit breaker status as show in Table 1. The IEC benchmark microgrid consist of main six buses, six constant power loads, two distributed synchronous generators (DG1 and DG3), two wind turbines generator (DG-2 and DG-4), and five distribution lines (DL-1, DL-2,..., DL-5). The three-phase faults occur in the middle point of each distribution line (F1-F5).

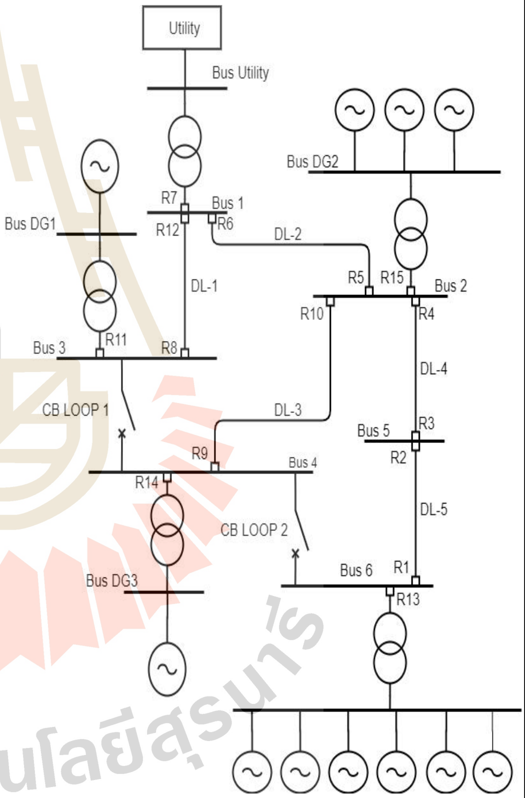

Figure. 1 an IEC benchmark micro-grid test system [20]

Table 1. The circuit breaker status of each OM

OM	Utility	DG1	DG2	DG3	DG4
OM1	on	off	off	off	off
OM2	on	on	on	on	on

Therefore, F1 denote the fault on distribution line DL-5. F2, F3, and F4 represents the fault on distribution lines DL-4, DL-2, and DL-1, respectively. F5 indicates the fault on lines DL-3. The fault level on each distribution line within various OMs can be seen in Fig. 2. To address these faults that can be occurred in this system, the relay was established at every end of the distribution line and the common coupling point of each DG (R1-R15). The parameters and fault levels of the system are referred to [22-23]. To avoid the complexity of the system, CB LOOP 1 and CB LOOP 2 are considered in open circuit status on any OM.

4.2 Simulation Setup

The limit boundary of decision variables and the constant parameters of every constraint utilized are the same as in [20] for compare the optimal solutions. Therefore, the TMS_j limit was set between TMS_j^{min} and TMS_j^{max}, with TMS_j^{min} at 0.05 and TMS_j^{max} at 15. Table 2 shows the CT ratio and *PS* of each OCR. PSM_j has a range of 1.1 *PSM* to 100 *PSM* as its limit. $T_{j,k}$ has a range of 0.01 to 2 seconds, and the *CTI* utilized is 0.3 seconds. As a result, a variety of optimal solutions are accessible. Five hundred swarm sizes are used to find the closest global optimum solution. To reduce variation, The 30 trials test is used. In this paper c_1 and c_2 are 1.49.

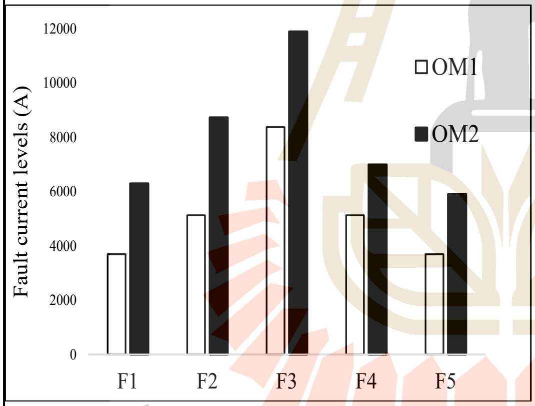

Figure. 2 Fault current level of both OM [21]

Table 2. The CT ratio and *PS* of each OCR

Relay	CT ratio	*PS*	Relay	CT ratio	*PS*
R1	400	0.50	R9	400	0.50
R2	400	0.50	R10	400	0.50
R3	400	0.50	R11	400	0.65
R4	400	0.50	R12	400	0.50
R5	400	0.50	R13	400	0.88
R6	400	0.50	R14	400	0.65
R7	1200	1.00	R15	400	0.65
R8	400	0.50			

4.3 Simulation Results

4.3.1. OM1 Results: In OM1, the test system which is connected to the utility, but all of DG is not energized. As a result, the power flow and the short circuit flow are in the same direction. Current flows from the utility to the load point or fault location. As a result, under this operational mode, just six relays are desired to detect (R2, R4, R6, R7, R10, R12). Table 3 demonstrates the coordination schemes and short circuit current passing through each OCR in this operating mode. Table 4 provides the optimal results of the proposed approach for each OCR. Table 5 shows the operating time of each relay when a fault occurs.

Table 3. The coordination schemes of OM1 [16]

Fault Point	RP1	RB1.1	RB1.2	RP2	RB2.1
F1	R2 3695	R4 3695	-	R1 -	R13 -
F2	R4 5130	R6 5130	R15 -	R3 -	R1 -
F3	R6 8375	R7 8375	R8 -	R5 -	R15 -
F4	R12 5130	R7 5130	R5 -	R8 -	R11 -
F5	R10 3695	R6 3695	R15 -	R9 -	R14 -

Table 4. The optimal results for OM1

Relay	Proposed Approach				
	TMS	CS_I	C_{VI}	C_{EI}	*CS*
R1	-	-	-	-	-
R2	0.05	0	0	1	IEC-EI
R3	-	-	-	-	-
R4	1.3262	0	0	1	IEC-EI
R5	-	-	-	-	-
R6	3.7897	0	0	1	IEC-EI
R7	0.1339	1	0	0	IEC-SI
R8	-	-	-	-	-
R9	-	-	-	-	-
R10	0.05	0	0	1	IEC-EI
R11	-	-	-	-	-
R12	0.0821	0	0	1	IEC-EI
R13	-	-	-	-	-
R14	-	-	-	-	-
R15	-	-	-	-	-

Table 3. shows that the primary and backup relay can see the same magnitude fault current for a one fault source because this operating condition has a radial topology. Thus, the fault current level is increase when the fault point near the fault source and decrease when fault point far from fault source. From

The proposed algorithm provides the results with several types of *CS*, not a single type of curve. The *CS*s obtained by the proposed method are mostly IEC-EI, because it provides the minimum operating time than other curves. Meanwhile, the trend of *TMSs* are converge to the lower bound, but they can slightly increase to avoid the constraint violation. The proposed method improves the objective function by around 34% from the previous paper [20] while the total *CTI* of the system is slightly decrease from [20]. The coordination curve of each OCR for the proposed approach are shown in Fig. 3.

Table 5. The operating times of OCRs for OM1

Fault Point	Relay	ICGA [20]		Proposed	
		$T_{j,k}$	CTI	$T_{j,k}$	CTI
F1	R2	0.0118	0.30	0.0118	0.30
	R4	0.3118		0.3118	
F2	R4	0.2976	0.30	0.1615	0.30
	R6	0.5976		0.4615	
F3	R6	0.5976	0.34	0.173	0.3
	R7	0.9372		0.473	
F4	R12	0.01	1.00	0.01	0.6257
	R7	1.01		0.6357	
F5	R10	0.0118	0.604	0.0118	0.879
	R6	0.6159		0.8908	
Total		4.19	2.544	3.14	2.405

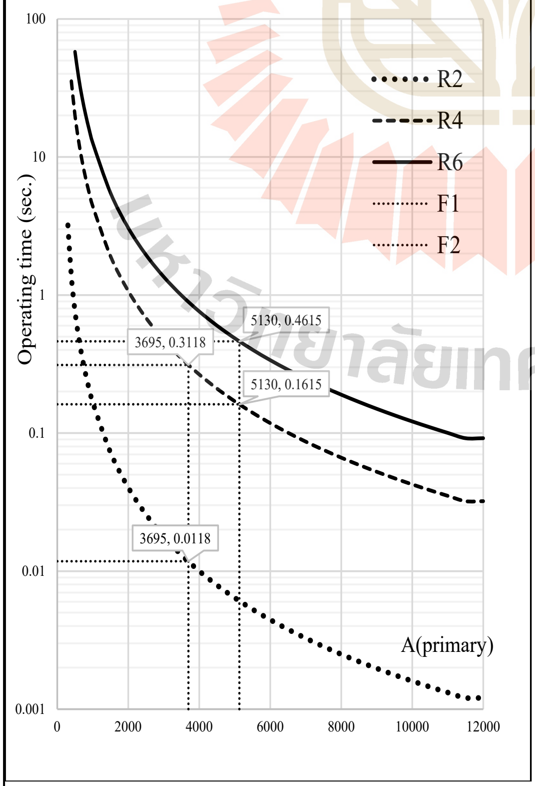

Figure. 3 The coordination curve of OCR in OM1

4.3.2. OM2 Results: In the OM2, the test system is connected to the utility and all of DG are energized. The power flow and the short circuit current flow can be in bi-direction and complex. The direction of current flow is from utility and DGs to load point or fault point. All relays are required to protect the system under this operating condition. The coordination schemes and short circuit current flowing through each relay of this operating mode are shown in Table 6. Table 7 provides the optimal results of the proposed approach for each OCR. Table 8 shows the operating time of each relay when fault occurs

Table 6. The coordination schemes of OM2 [16]

Fault Point	RP1	RB1.1	RB1.2	RP2	RB2.1
F1	R2 4648	R4 4648	-	R1 1648	R13 1648
F2	R4 7260	R6 5443	R15 920	R3 1465	R1 1465
F3	R6 9256	R7 8375	R8 923	R5 2635	R15 737
F4	R12 5998	R7 4572	R5 1439	R8 991	R11 991
F5	R10 4913	R6 3416	R15 578	R9 991	R14 991

Table 7. The optimal results for OM2

Relay	Proposed Approach				
	TMS	CS_I	C_{VI}	C_{EI}	*CS*
R1	0.2475	0	0	1	IEC-EI
R2	0.0674	0	0	1	IEC-EI
R3	0.05	0	0	1	IEC-EI
R4	2.089	0	0	1	IEC-EI
R5	0.1967	0	0	1	IEC-EI
R6	3.9472	0	0	1	IEC-EI
R7	0.1266	1	0	0	IEC-SI
R8	0.1135	0	0	1	IEC-EI
R9	0.05	0	0	1	IEC-EI
R10	0.0753	0	0	1	IEC-EI
R11	0.1428	0	1	0	IEC-VI
R12	0.1123	0	0	1	IEC-EI
R13	0.1625	0	1	0	IEC-VI
R14	0.0978	0	1	0	IEC-VI
R15	0.0885	1	0	0	IEC-SI

Table 6 shows that when F1 occurs, the fault flows current from DG4 is detected by relays R1 and R13. The fault current flows in a different direction from and R15. As a result, when F3 occurs, R5 and R15 will operate to clear the fault from downstream DG (DG2, DG3, DG4). For this fault from the utility and DG1, R6, R7, and R8 must be operational. As a result, when fault F4 occurs, R8 and R11 from DG1 are required to operate for this fault. R12, R7, and R5 are required to operate for this fault from the utility and downstream DGs. On the other hand, R9 and R14 are required to operate for this fault from DG3 when F5 occurs. In the meantime, R10, R6, and R15 must operate for this fault from a different fault source. As a consequence, when the number of fault sources increases, the coordination schemes must become more sophisticated in order to preserve system reliability.

Table 8. The operating times of OCRs for OM2

Fault Point	Relay	ICGA [20] $T_{j,k}$	ICGA [20] CTI	Proposed $T_{j,k}$	Proposed CTI
F1	R2	0.0405	0.3	0.01	0.3
	R4	0.3405		0.31	
	R1	0.2858	0.3	0.2959	0.3
	R13	0.5858		0.5959	
F2	R4	0.3405	0.625	0.1269	0.6
	R6	0.6629		0.4269	
	R15	0.6406		0.4269	
	R3	0.0302	0.3	0.0759	0.3
	R1	0.3301		0.3759	
F3	R6	0.6629	0.6	0.1475	0.6
	R7	0.9628		0.4475	
	R8	0.9629		0.4475	
	R5	0.186	0.553	0.0911	0.415
	R15	0.7386		0.5063	
F4	R12	0.0405	1.66	0.01	0.944
	R7	1.4		0.6539	
	R5	0.3405		0.301	
	R8	0.8467	0.3	0.3857	0.3
	R11	1.14		0.6857	
F5	R10	0.0405	1.157	0.01	1.701
	R6	0.3405		1.0861	
	R15	0.8976		0.6353	
	R9	0.1792	0.3	0.1698	0.3
	R14	0.4792		0.4698	
Total		12.48	6.09	8.701	5.76

From Table 7, the *CS* were provided by the proposed algorithm are mostly IEC EI, similar to OM1, the trend of *TMS* still converged as close as possible to lower bound. The proposed algorithm results to the best objective function value, around 44% lower than [20]. The results also shown that the proposed algorithm can effectively improve the system reliability from [20] as illustrated in Table 8. The coordination curve of each OCR for the proposed approach can be seen in Fig. 4.

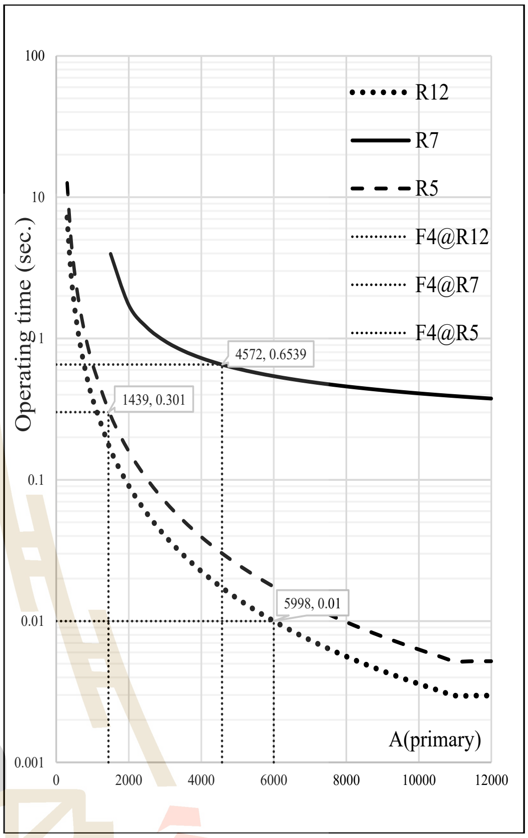

Figure. 4 The coordination curve of OCR in OM2

4.3.3. The summary results of the proposed technique: With the proposed method, the total operating time of the OCR protection for the IEC benchmark microgrid has decrease over time, by enhancing the constraint and demonstrating the ability of the proposed technique on the OCR's parameters setting.

Table 9. A comparative study with previous works

Operating modes	[16]	[17]	[18]	[20]	Proposed
OM1	7.53	6.64	4.99	4.19	3.09
OM2	19.18	17.48	13.66	12.48	8.77
Total time	26.71	24.12	18.65	16.67	11.84
Total CTI	9.08	8.93	8.56	8.29	8.165

Table 10. The results of 30 trials test

Operating mode	OM1	OM2
Best	3.14	8.701
Mean	3.14	8.847
Worst	3.14	8.984
STD	10^{-8}	0.111

In comparison to existing works, the proposed technique is successfully reduced the total operating time and total *CTI* of the OCR as shown in Table 9. The proposed algorithm has been tested with 30 trials to verify the optimal results. Table 10 shows the best, mean, worst, range, and standard deviation (STD) of the optimal results. From Table 10, it is clear that the biggest advantage of the proposed technique is that it provides the optimal results with significantly low STD. Hence, the proposed hybrid PSO-MILP technique is suitable for finding the global minimum objective function value of the overcurrent relay coordination. The convergence plot of the proposed method is shown in Fig. 5.

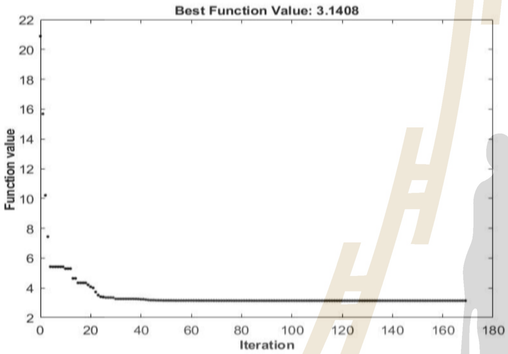

(a) OM1

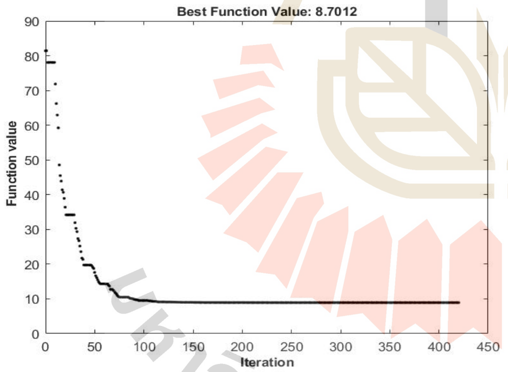

(b) OM2

Figure. 5 Convergences plots of the proposed method

1. Conclusion

The PSO-MILP technique is used, in this paper, for obtaining the optimal setting parameters of OCR coordination, which are *TMS* and *CS*. The total operating time of the relay in the system is minimized by maintaining the reliability of the system through the coordination constraint. As a results, the proposed technique provides the results with multiple curve types instead of single curve types. When compared to previous researches, the proposed technique can absolutely decrease the total operating time of the OCR by around 34 percent for OM1 and around 44 percent for OM2. Therefore, it can be concluded that the proposed method is suitable for the microgrid protection strategy. To demonstrate the usefulness of the proposed technique, the larger system, and other *CS* types can be considered in further work.

2. Conflicts of Interest

The authors declare no conflict of interest.

3. Author Contributions

Conceptualization, methodology, validation, formal analysis, and investigation, C. Plongkrathok and K. Chayakulkheeree; writing original draft preparation, visualization, C. Plongkrathok; writing-review and editing, supervision, K. Chayakulkheeree.

References

[1] V. A. Papaspiliotopoulos, G. N. Korres, V. A. Kleftakis, and N. D. Hatziargyriou, “Hardware-In-the-Loop Design and Optimal Setting of Adaptive Protection Schemes for Distribution Systems With Distributed Generation”, *IEEE Transactions on Power Delivery*, Vol. 32, No. 1, pp. 393-400, 2017.

[2] B. Chattopadhyay, M. S. Sachdev, and T. S. Sidhu, “An on-line relay coordination algorithm for adaptive protection using linear programming technique”, *IEEE Transactions on Power Delivery*, Vol. 11, No. 1, pp. 165-173, 1996.

[3] P. P. Bedekar, S. R. Bhide, and V. S. Kale, “Optimum Coordination of Overcurrent Relays in Distribution System Using Dual Simplex Method”, *2009 Second International Conference on Emerging Trends in Engineering & Technology*, pp. 555-559, 2009.

[4] A. Gupta, O. V. G. Swathika, and S. Hemamalini, “Optimum Coordination of Overcurrent Relays in Distribution Systems Using Big-M and Dual Simplex Methods”, *2015 International Conference on Computational Intelligence and Communication Networks (CICN)*, pp. 1540-1543, 2015.

[5] A. M. S. Deepak, S. Madhu, M. V. G. Raju, and O. V. G. Swathika, “Optimum coordination of overcurrent relays in distribution systems using big-m and revised simplex methods”, *2017 International Conference on Computing Methodologies and Communication (ICCMC)*, pp. 613-616, 2017.

[1] A.M. Ibrahim, W. El-Khattam, M. ElMesallamy, and H.A. Talaat, "Adaptive protection coordination scheme for distribution network with distributed generation using ABC", *Journal of Electrical Systems and Information Technology,* Vol. 3, Issue 2, pp. 320-332, 2016.

[2] A. Tjahjono, D. Anggriawan, A. Faizin, A. Priyadi, M. Pujiantara, T. Taufik, and M. Purnomo, "Adaptive modified firefly algorithm for optimal coordination of overcurrent relays", *IET Generation Transmission & Distribution*, Vol.11, Issue 10, pp.2575-2585, 2017.

[3] T. Amraee, "Coordination of Directional Overcurrent Relays Using Seeker Algorithm", *IEEE Transactions on Power Delivery*, Vol. 27, No. 3, pp. 1415-1422, 2012.

[4] A. Srivastava, J. M. Tripathi, R. Krishan, and S. K. Parida, "Optimal Coordination of Overcurrent Relays Using Gravitational Search Algorithm With DG Penetration", *IEEE Transactions on Industry Applications*, Vol. 54, No. 2, pp. 1155-1165, 2018.

[5] P. P. Bedekar and S. R. Bhide, "Optimum Coordination of Directional Overcurrent Relays Using the Hybrid GA-NLP Approach", *IEEE Transactions on Power Delivery*, Vol. 26, No. 1, pp. 109-119, 2011.

[6] D. Saha, A. Datta, and P. Das, "Optimal coordination of directional overcurrent relays in power systems using Symbiotic Organism Search Optimisation technique", *IET Generation Transmission & Distribution*, Vol. 10, Issue 11, pp. 2681-2688, 2015.

[7] A. S. Noghabi, J. Sadeh, and H. R. Mashhadi, "Considering Different Network Topologies in Optimal Overcurrent Relay Coordination Using a Hybrid GA", *IEEE Transactions on Power Delivery*, Vol. 24, No. 4, pp. 1857-1863, 2009.

[8] T. Khurshaid, A. Wadood, C. Kim, S. G. Farkoush, K. Hassan Kharal, and S. Rhee, "A Protective Optimal Coordination Scheme for Directional Overcurrent Relays Using Modified Seeker Algorithm", *2018 International Conference on Computing, Power and Communication Technologies (GUCON)*, pp. 535-539, 2018.

[9] T. Khurshaid, A. Wadood, S. Gholami Farkoush, J. Yu, C. Kim, and S. Rhee, "An Improved Optimal Solution for the Directional Overcurrent Relays Coordination Using Hybridized Whale Optimization Algorithm in Complex Power Systems", *IEEE Access*, Vol. 7, pp. 90418-90435, 2019.

[10] A. Y. Hatata and A. Lafi, "Ant Lion Optimizer for Optimal Coordination of DOC Relays in Distribution Systems Containing DGs", *IEEE Access*, Vol. 6, pp. 72241-72252, 2018.

[11] S. M. Saad, N. El-Naily, F. A. Mohamed, "A new constraint considering maximum PSM of industrial over-current relays to enhance the performance of the optimization techniques for microgrid protection schemes", *Sustainable Cities and Society*, Vol. 44, pp. 445-457, 2019.

[12] N. El-Naily, S. M. Saad, T. Hussein, F.A. Mohamed, "A novel constraint and non-standard characteristics for optimal over-current relays coordination to enhance microgrid protection scheme", *IET Generation Transmission & Distribution*, Vol. 13, Issue 6, pp. 780–793, 2019.

[13] S. D. Saldarriaga-Zuluaga, J. M. López-Lezama, and N. Muñoz-Galeano, "Optimal Coordination of Overcurrent Relays in Microgrids Considering a Non-Standard Characteristic", *Energies*, Vol. 13, Issue 4, 2020.

[14] M. N. Alam, "Overcurrent protection of AC microgrids using mixed characteristic curves of relays", *Computers & Electrical Engineering*, Vol. 74, pp. 74-88, 2019.

[15] S. D. Saldarriaga-Zuluaga, J. M. López-Lezama, and N. Muñoz-Galeano, "An Approach for Optimal Coordination of Over-Current Relays in Microgrids with Distributed Generation", *Electronics*, Vol. 9, Issue 10, 2020.

[16] J. Kennedy, R. Eberhart, "Particle swarm optimization", *Proceedings of ICNN'95 - International Conference on Neural Networks*, Vol. 4, pp. 1942–1948, 1995.

[17] S. Kar, "A comprehensive protection scheme for micro-grid using fuzzy rule base approach", *Energy Systems*, Vol. 8, pp. 449-464, 2017.

[18] S. Kar, S. R. Samantaray, and M. D. Zadeh, "Data-Mining Model Based Intelligent Differential Microgrid Protection Scheme", *IEEE Systems Journal*, Vol. 11, No. 2, pp. 1161-1169, 2017.

VITAE

Chakit Plongkrathok received his B. Eng. in EE from Suranaree University of Technology in 2020. He is currently a graduate student in power system program at Suranaree University of Technology (SUT). His current interests are in power system optimization algorithms, power system protections, and Artificial intelligence.

When I was studying for my bachelor's degree at Suranaree University of Technology, I interned at CPT Drive and Power Company. I have experience in many powers electrical systems,

After I graduated with a bachelor's degree, I immediately studied for a master's degree at Suranaree University of Technology. I am so proud of my teacher assistant position duty to teach laboratory for students. I also accepted paper and participated in EE-Conference 41, and accept journal in international journal of intelligent and systems (IJIES) about protection system research.

Moreover, I have experience in consult assistance of PV power plant, my duty is analyzing and energy management systems for the installation of PV power plants in power system.

Finally, I have experience as a project engineer for induction motor work at Suranaree University of Technology. This work helps me develop my electrical engineering skills.